MARINE INFLUENCE ON CHEMICAL COMPOSITION OF AEROSOL IN THAILAND

Miss Jariya Kayee

จุฬาลงกรณ์มหาวิทยาลัย
CHULALONGKORN UNIVERSITY

A Dissertation Submitted in Partial Fulfillment of the Requirements

for the Degree of Doctor of Philosophy in Marine Science

Department of Marine Science

FACULTY OF SCIENCE

Chulalongkorn University

Academic Year 2020

อิทธิพลจากทะเลต่อองค์ประกอบทางเคมีของละอองลอยในประเทศไทย

น.ส.จริยา กาหยี

วิทยานิพนธ์นี้เป็นส่วนหนึ่งของการศึกษาตามหลักสูตรปริญญาวิทยาศาสตรดุษฎีบัณฑิต
สาขาวิชาวิทยาศาสตร์ทางทะเล ภาควิชาวิทยาศาสตร์ทางทะเล
คณะวิทยาศาสตร์ จุฬาลงกรณ์มหาวิทยาลัย
ปีการศึกษา 2563

Thesis Title	MARINE INFLUENCE ON CHEMICAL COMPOSITION OF AEROSOL IN THAILAND
By	Miss Jariya Kayee
Field of Study	Marine Science
Thesis Advisor	Assistant Professor PENJAI SOMPONGCHAIYAKUL, Ph.D.
Thesis Co Advisor	SUJAREE BUREEKUL, Ph.D.

Accepted by the FACULTY OF SCIENCE, Chulalongkorn University in Partial Fulfillment of the Requirement for the Doctor of Philosophy

.... Dean of the FACULTY OF SCIENCE
(Professor POLKIT SANGVANICH, Ph.D.)

DISSERTATION COMMITTEE

.... Chairman
(Professor VORANOP VIYAKARN, Ph.D.)

.... Thesis Advisor
(Assistant Professor PENJAI SOMPONGCHAIYAKUL, Ph.D.)

.... Thesis Co-Advisor
(SUJAREE BUREEKUL, Ph.D.)

.... Examiner
(Assistant Professor PATAMA SINGHRUCK, Ph.D.)

.... Examiner
(CHAWALIT CHAROENPONG, Ph.D.)

.... External Examiner
(Assistant Professor Reshmi Das, Ph.D.)

จริยา กาหยี : อิทธิพลจากทะเลต่อองค์ประกอบทางเคมีของละอองลอยในประเทศไทย. (MARINE INFLUENCE ON CHEMICAL COMPOSITION OF AEROSOL IN THAILAND) อ.ที่ปรึกษาหลัก : ผศ. ดร.เพ็ญใจ สมพงษ์ชัยกุล, อ.ที่ปรึกษาร่วม : อ. ดร.สุจารี บุรีกุล

ในการศึกษาละอองลอยในครั้งนี้ ครอบคลุมพื้นที่ทั้งในแผ่นดินและในทะเล ในแผ่นดินเก็บตัวอย่างจากกรุงเทพฯ ชลบุรี และเชียงราย โดย 2 เมืองแรกเป็นเมืองชายฝั่ง เพื่อศึกษาผลกระทบจากความผันแปรตามฤดูกาลและอิทธิพลของ บรรยากาศ-ทะเล-แผ่นดิน ต่อองค์ประกอบทางเคมีของละอองลอยเหนือเมืองชายฝั่งด้วยการวิเคราะห์ทางเคมี (โลหะ ไอโซโทปตะกั่ว และไอออนละลายน้ำ) และวิเคราะห์เส้นทางการเคลื่อนที่ย้อนกลับของมวลอากาศ โดยแบ่งการศึกษาออกเป็น 3 ส่วน ส่วนที่ 1 เก็บตัวอย่างละอองลอยขนาดเล็กกว่าหรือเท่ากับ 2.5 ไมครอน ($PM_{2.5}$) ในกรุงเทพฯ และชลบุรี (มกราคม 2561 ถึง เมษายน 2562) จากการวิเคราะห์โลหะและไอโซโทปตะกั่ว พบว่าทั้งกรุงเทพฯ และชลบุรีมีปริมาณ $PM_{2.5}$ สูงสุดในฤดูลมมรสุมตะวันออกเฉียงเหนือ และต่ำสุดในฤดูลมมรสุมตะวันตกเฉียงใต้ โดยช่วงลมมรสุมตะวันออกเฉียงเหนือ กรุงเทพฯและชลบุรีได้รับอิทธิพลจากการเผาไหม้ถ่านหินจากประเทศจีนและเวียดนาม และฝุ่นจากธรรมชาติ ขณะที่ช่วงลมมรสุมตะวันตกเฉียงใต้จะได้รับอิทธิพลจากละอองลอยทางทะเลที่พามาจากมหาสมุทรอินเดียและอ่าวไทย การเผาไหม้ถ่านหิน กระบวนการผลิตแร่ และมลพิษทางถนน ในช่วงระหว่างมรสุมองค์ประกอบทางเคมีใน $PM_{2.5}$ คล้ายกับในฤดูลมมรสุมตะวันตกเฉียงใต้ ส่วนที่ 2 เก็บตัวอย่างละอองลอยในอ่าวไทย โดยเรือสำรวจ SEAFDEC-2 และในทะเลอันดามัน โดยเรือสำรวจ Dr. Fridtjof Nansen ในช่วงฤดูมรสุมตะวันตกเฉียงใต้ (สิงหาคมถึงตุลาคม 2561) โดยในอ่าวไทยได้เพิ่มการเก็บตัวอย่างละอองลอยขนาด $PM_{10-2.5}$ ผลการศึกษาโลหะและไอออนละลายน้ำ พบว่า ทั้ง $PM_{10-2.5}$ และ $PM_{2.5}$ ในบรรยากาศเหนือทะเล มีองค์ประกอบที่เกิดจากละอองกระเซ็นจากทะเล (sea spray) เป็นหลัก และธาตุที่มาจากทะเลจะพบมากใน $PM_{10-2.5}$ สำหรับตัวอย่างที่ใกล้แผ่นดินพบว่าทั้ง $PM_{10-2.5}$ และ $PM_{2.5}$ จะได้รับอิทธิพลจากละอองลอยจากพื้นทวีป และใน $PM_{2.5}$ ยังมีการปนเปื้อนของโลหะจากกิจกรรมของมนุษย์ที่ถูกพามาจากระยะไกล ในส่วนที่ 3 เก็บตัวอย่าง $PM_{2.5}$ ในเชียงราย และกรุงเทพฯ ในช่วงฤดูการเผาไหม้ (มกราคมถึงเมษายน 2562) พบว่า $PM_{2.5}$ ในเชียงราย มีองค์ประกอบเคมีจากฝุ่นจากภาคพื้นทวีป การเผาไหม้ชีวมวล อุตสาหกรรม การเผาไหม้ขยะ และฝุ่นจากถนน ขณะที่ในกรุงเทพฯ จะได้รับอิทธิพลจากอุตสาหกรรม การเผาไหม้ถ่านหิน มลพิษทางถนน และละอองลอยทางทะเล และยังพบว่าละอองลอยที่เกิดจากการเผาไหม้ที่เชียงรายมีอิทธิพลมาไม่ถึงกรุงเทพฯ

สาขาวิชา	วิทยาศาสตร์ทางทะเล	ลายมือชื่อนิสิต ....
ปีการศึกษา	2563	ลายมือชื่อ อ.ที่ปรึกษาหลัก ....
		ลายมือชื่อ อ.ที่ปรึกษาร่วม ....

5972851823 : MAJOR MARINE SCIENCE

KEYWORD: PM2.5, PM10-2.5, Marine aerosol, Trace metals, Pb isotope ratios, water-soluble ions

Jariya Kayee : MARINE INFLUENCE ON CHEMICAL COMPOSITION OF AEROSOL IN THAILAND. Advisor: Asst. Prof. PENJAI SOMPONGCHAIYAKUL, Ph.D. Co-advisor: SUJAREE BUREEKUL, Ph.D.

This study was focused on atmospheric aerosols covering aerosols over both continent and ocean. Continent's aerosols were collected from two coastal cities, Bangkok and Chonburi, and one in-land city, Chiangrai. To investigate seasonal variation and air-sea-land influences on chemical composition of aerosols, metals, lead isotope and water-soluble inorganic ions were examined coupled with air mass trajectory analysis. The study was divided into 3 parts. The first part, $PM_{2.5}$ samples were collected in Bangkok and Chonburi during January 2018 to April 2019. The results revealed the highest $PM_{2.5}$ concentrations in NE monsoon, and the lowest in SW monsoon. During NE monsoon, Bangkok and Chonburi were influenced by coal combustion emission from China and Vietnam and natural background of crustal soil dust. While long-range transport of marine aerosols from Indian Ocean and the Gulf of Thailand (GoT), as well as coal combustion emission, ore processing and road traffic emission played important roles during SW monsoon winds. The chemical composition of $PM_{2.5}$ during the inter-monsoon winds had similarity with the SW monsoon winds. In the second part, aerosols over Thai waters during SW monsoon (August to October 2018) were collected on board of M.V. SEAFDEC-2 and R.V. Dr. Fridtjof Nansen in the GoT and the Andaman Sea, respectively. For the GoT campaign, $PM_{10-2.5}$ was also collected. The results indicated composition of both $PM_{10-2.5}$ and $PM_{2.5}$ were dominated by sea spray aerosols, especially $PM_{10-2.5}$. Near-shore aerosols, both $PM_{10-2.5}$ and $PM_{2.5}$, have shown signals of the continent sources. Furthermore, these near-shore samples were influenced by anthropogenic activities. For the third part, $PM_{2.5}$ was collected in Bangkok and Chiangrai during the biomass burning season (January to April 2019). The results indicated that the $PM_{2.5}$ in Chiangrai was influenced by crustal dust, biomass burning, industrial source and refuse incineration mixed with road dust. While Bangkok aerosols contained natural background, elements mixed with those from industrial emission, coal combustion, traffic emission and sea spray. No long-range transport from forest fire in the north was found reaching Bangkok.

Field of Study:	Marine Science	Student's Signature ....
Academic Year:	2020	Advisor's Signature ....
		Co-advisor's Signature ....

ACKNOWLEDGEMENTS

TABLE OF CONTENTS

จุฬาลงกรณ์มหาวิทยาลัย
CHULALONGKORN UNIVERSITY

LIST OF TABLES

จุฬาลงกรณ์มหาวิทยาลัย

CHULALONGKORN UNIVERSITY

LIST OF FIGURES

จุฬาลงกรณ์มหาวิทยาลัย
CHULALONGKORN UNIVERSITY

CHAPTER 1

INTRODUCTION

1.1 Overview

In the past, the studies of aerosols did not get as much attention in Thailand, and were mostly based on remote sensing and physical properties. This is most likely due to the complicated sampling and analyses. Currently, it is generally accepted that aerosols play important roles in Earth's atmosphere and climate system. However, comprehensive study on atmospheric aerosol in Thailand is almost still lacking. To better understand the roles of aerosols in Thailand, it is essential to study local aerosols, long distance transport aerosols and marine aerosols.

1.2 Aerosol sources, size fraction and processes

Atmospheric aerosols are suspended particles of liquid or solid in the atmosphere (Saltzman, 2009). These aerosols are emitted from both "anthropogenic" (e.g., sulfates, organic carbon, black carbon, nitrates) and "natural" (e.g., crustal dust, pollen and sea spray) sources.

Atmospheric PMs or aerosols that directly emitted from their sources into the atmosphere are called "primary aerosols", while the "secondary aerosols" are formed by in situ aggregation or nucleation of gaseous molecules of natural or anthropogenic (gas to particle conversion) (Saltzman, 2009). The primary aerosols from anthropogenic sources are commonly generated as black carbon and as heavy organic materials such as polycyclic aromatic hydrocarbons (Bond et al., 2007).

Aerosols have both direct and indirect effects on climate variability. Aerosols affect on earth's radiation budget either through "directs effect" occurring in cloud-free situation (scatter to cooling, and absorb to heating), or "indirect effects" small droplet caused scattering, more droplet caused prolonging cloud lifetime, and heat absorbing caused cloud evaporated (Takemura et al., 2005).

Aerosol particles can be divided by size-fractions into 4 major modes (Figure 1.1); Nucleation, Aitken, Accumulation and Coarse modes. The Nucleation and Aitken modes are ultra-fine particles formed by coagulation and condensate growth of the gaseous molecules. In marine environment, the relatively volatile gases (i.e., nitric acid or sulfuric acid) generated from the ocean's surface will mix with the pre-existing particles (e.g., water vapor) and to form cloud condensation nuclei (CCN). An increasing size of the ultra-fine aerosols to become sub-micron aerosols (fine particles; $PM_{2.5}$), so-called accumulation modes, involves in cloud formation process (water droplets). This process affects indirectly to cool the earth surface. A large portion of $PM_{2.5}$ are generated from anthropogenic sources of high-temperature processes, such as industrial processes, vehicular emission, fossil fuels combustion, biomass burning, and waste incineration. They compose of sulfate, elemental carbon (EC), organic carbon (OC), and trace element (Pósfai et al., 2003). The coarse mode particles ($PM_{10-2.5}$) are those of PMs with diameter ranging from 2.5 to 10 μm. They are generated by different mechanisms, accounting for mostly primary aerosols of natural processes including crustal dust, volcanic debris, biogenic aerosols and sea spray.

The lifetimes in the atmosphere of aerosol particles can range from days to weeks. After emission, aerosols undergo long distance transport and various physical/chemical processes, of which altered size, composition, and structure of the particles. These aerosols are finally removed from the atmosphere via dry (i.e., gravity) and wet (e.g., rain or washout) deposition processes. The atmospheric deposition can be an important source of macro- and micronutrients to the ocean that can impact marine biogeochemistry by enhancing or inhibiting phytoplankton growth rates and thereby modifying plankton community structure.
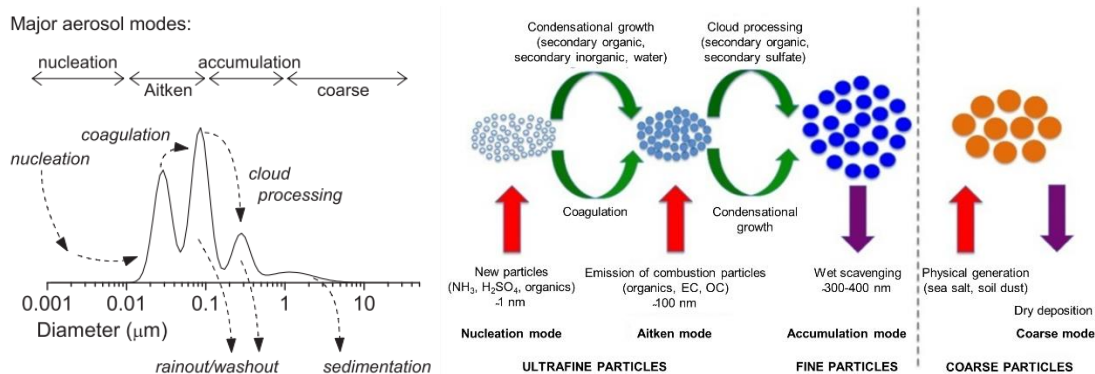
Figure 1.1 Distribution of aerosol size and its mechanisms

(source: Saltzman, 2009 (left) and Griffin, 2013 (right)

1.3 Marine aerosols

Marine aerosols consist of all various types of particles found over the ocean. They can be (i) gas or particles generated at the sea surface, (ii) gas or particles formed chemically by atmospheric reactions after the emission from the sea, and (iii) aerosols from long-range transport. Marine aerosols become increasingly important as they involve in global biogeochemical cycles, ocean acidification, nutrient fluxes, climate change, as well as human health (Saltzman, 2009).

Ocean's surface is the main contributor of the natural source of primary aerosols, as sea salt aerosols. However, ocean is not only a main contributor for sea salt aerosols (sea spray), but also precursor gases from marine productions including biogenic sulfate aerosols (dimethyl sulfide; DMS). The production and emission of such marine aerosols are considerable important and can vary from region to region. In other word, marine aerosols can play significant roles for physical and chemical characteristics of the Earth's atmosphere and climate system.

In the atmosphere, such marine aerosols can be mixed or interacted with land-derived or continental aerosols (mainly contributed from fossil fuels combustion, biomass burning and soil dust). This extensive atmospheric interaction poses an influence on biogeochemistry of the surface ocean through long-range transport and deposition of terrestrial and marine-derived nutrients and trace elements.
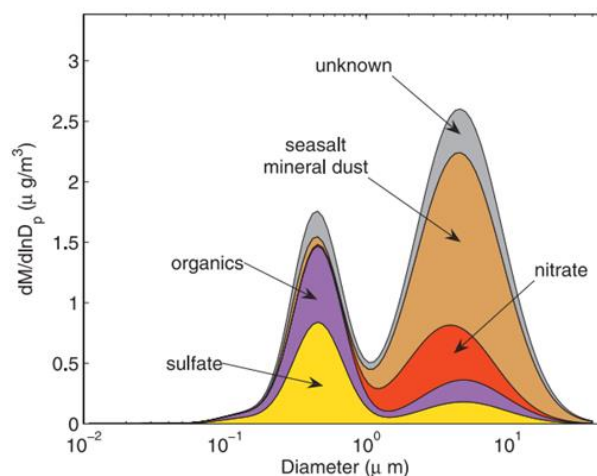
Figure 1.2 Marine aerosol size distribution (source: Saltzman, 2009)

Figure 1.2 demonstrates mass concentration with sized resolved distribution of marine aerosol (Saltzman, 2009). Sulfate aerosol contributed to the third most mass concentration of marine aerosol, following Na^+ and Cl^- ions (in sea salt). Details of interesting chemical composition in aerosols are as following.

1.3.1 Water-soluble inorganic ions

Water soluble inorganic ions (WSIIs) include Na^+, NH_4^+, K^+, Mg^{2+}, Ca^{2+}, Cl^-, NO_3^-, and SO_4^{2-}. Most of the WSIIs are sea spray aerosols, e.g., Na^+, K^+, Mg^{2+}, Ca^{2+}, Cl^- and SO_4^{2-}. However, SO_4^{2-}, K^+, and Ca^{2+} can also be generated from non-marine sources. Thus, SO_4^{2-}, K^+, and Ca^{2+} in the atmosphere are mixtures of those from sea salt and non-sea salt origins. Non-sea salt (nss) components in WSIIs can be estimated by using Na^+ as a sea spray marker as following (Keene et al., 1986),

$$[nss\text{-}SO_4^{2-}] = [SO_4^{2-}] - 0.25 \times [Na^+] \qquad (1\text{-}1)$$

$$[nss\text{-}K^+] = [K^+] - 0.036 \times [Na^+] \qquad (1\text{-}2)$$

$$[nss\text{-}Ca^{2+}] = [Ca^{2+}] - 0.038 \times [Na^+] \qquad (1\text{-}3)$$

For the three species of non-sea salt aerosols in the WSIIs, nss-SO_4^{2-} is a tracer of anthropogenic sources, nss-SO_4^{2-} and nss-K^+ are tracers of biomass burning, while nss-Ca^{2+} is a tracer of crustal dust.

Sulfate aerosols are emitted from both natural and anthropogenic sources. Natural sources of sulfate aerosols are from sea-salt sulfate and biogenic non-sea-salt sulfate aerosols (short-lived and long-lived sulfur emission). If not account for sea-salt, sulfate aerosols are the most abundant WSIIs in the marine atmosphere. Atmospheric sulfur aerosols are those sulfur dioxide (SO_2), sulfuric acid (H_2SO_4), methanesulfonic acid (MSA) and sea-salt sulfate. The SO_2 is a gas that becomes dissolved in water droplets and forms weak H_2SO_4. While MSA are sulfate aerosols derived from biogenic sulfur dimethyl sulfide (DMS). Sea-salt sulfate and DMS are those emitted directly from ocean. Sea salt sulfate can easily be distinguished from non-sea salt sulfate aerosols. The size of sea salt sulfate is generally bigger than non-sea salt sulfate and can commonly be quantified by conservative tracer in seawater (e.g., Na^+). Non-sea salt sulfate, on the other hand, resides mostly in the accumulation mode. The major gas precursors of those non-sea salt sulfate include SO_2 (from volcanic and fossil fuel combustion) and biogenic emission input of DMS (Saltzman, 2009). Figure 1.3 illustrates the size distribution of sulfate aerosols in the marine atmosphere over Atlantic Ocean.

Emissions of sea-salt sulfate aerosols and biogenic derived non-sea salt sulfate aerosols are accounted for 44 and 98 Tg, respectively. While anthropogenic sulfur which mainly originated from industrial processes and fossil fuel combustion, contributes 70 Tg of sulfur per annum (Brimblecombe, 2014). Generally, the highest levels of SO_2 are found near large industrial complexes or at other point sources. After the long-range transport, sulfur is removed from the atmosphere by wet and dry depositions (Figure 1.4).

One of the most direct sulfur emissions from ocean is biogenic DMS, a volatile sulfur compound produced by phytoplankton and bacteria in seawater. The DMS acts as a major gas-phase precursor for secondary aerosols over the oceans. Once emitted to atmosphere, DMS is oxidized to SO_2 and dimethyl sulfoxide (DMSO), leading to the formation of condensable H_2SO_4 and MSA, which react and condensate to form new

particles of sulfate aerosols. This new sulfate aerosol contributes to the increase of CCN which is relevant to the climate indirect effect (Charlson et al., 1987).
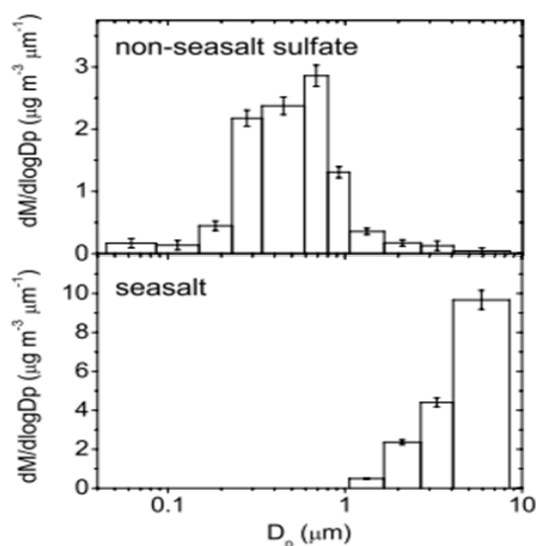
Figure 1.3 Size distribution of sulfate aerosol in the marine atmosphere over Atlantic Ocean (source: Saltzman, 2009)

Concentration of DMS in seawater varies from less than 0.1 to greater than 50 nM depending on season and location. Seasonal variations of DMS have been previously studied based on field measurements and model applications (Dani and Loreto, 2017; Shenoy et al., 2006; Speeckaert et al., 2018). All these studies reported a seasonal cycle in DMS with a maximum in spring followed by a decrease to low winter values. It is recognized that DMS in seawater is controlled mainly by phytoplankton composition rather than by the total algal biomass or production (Liss et al., 1993). Moreover, DMS can be produced by different groups of phytoplankton in the following orders: coccolithophores, phaeocystis, dinoflagellates, and diatoms (Keller, 1989).

DMS, a volatile sulfur compound, in seawater is present in nanomolar concentration, and can easily emit to the atmosphere. Ideally, real-time measurement of DMS with high sensitivity instrument is the best method. When DMS emit to the

atmosphere, it is dominated by non-sea salt sulfate from anthropogenic emissions. Sea salt sulfate aerosols can be segregated from non-sea salt sulfate aerosols by size. Sea salt aerosols are present mostly in $PM_{10-2.5}$ in marine aerosols, while non-sea salt aerosols are present mainly in $PM_{2.5}$ (Hsu et al., 2008). Sulfate in non-sea salt aerosols can be distinguished between continental or anthropogenic origins by mean of elemental ratios.
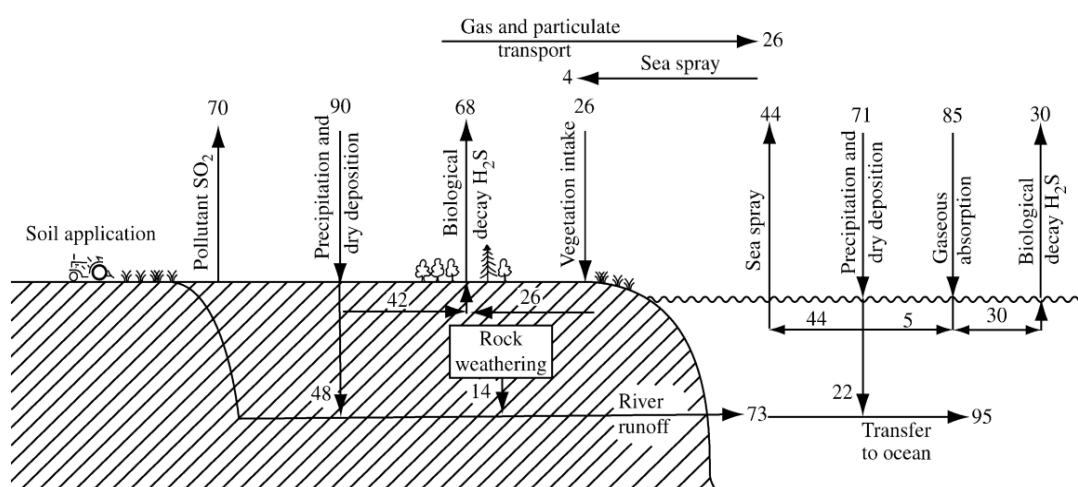
Figure 1.4 Sulfur cycle (source: Brimblecombe, 2014)

1.3.2 Trace metals

Chemical composition of marine aerosol is of importance to the biogeochemical state of the underlying ocean. For example, micronutrients in the ocean are partly provided by the deposition of Fe, Zn, Co, Mn and Cu contained in aerosol dust. However, some metals, i.e. copper, can be toxic at high concentrations to some phytoplankton (Jordi et al., 2012). Jordi et al. (2012) has shown a decline in phytoplankton biomass after the deposition of high Cu concentrations in atmospheric aerosols.

Metal concentrations in $PM_{2.5}$ can originate either from anthropogenic sources (such as industrial process, coal combustion, power plant, fuel oil, and road transport) or from natural sources (such as biomass burning, volcanoes, and sea spray).

Concentration and size resolved distribution on PM$_{2.5}$-bond metal is characterized as unknown group in Figure 1.2 (Jeong et al., 2016). Sources and type of PM$_{2.5}$-bound metal are listed in Table 1.1 (Ismal et al., 2018; Kang et al., 2019).

Chemical composition of PM$_{2.5}$ aerosols can be complex and vary in space and time along with the weather conditions (Hu et al., 2015). To identify sources or origin of aerosols, concentration and metal composition in PM$_{2.5}$ (Table 1.1) can be used as a rough guideline. In addition, metal ratios in PM$_{2.5}$ can reveal air-sea-land influences on chemical composition in marine aerosols (Jeong et al., 2016).

1.4 Aerosol Source identification

As mentioned above, the sea salt component is typically in PM$_{10-2.5}$ and non-sea salt aerosol in PM$_{2.5}$. The following tracers can be used to identify anthropogenic sources of the PM$_{2.5}$ aerosols which are mainly non-sea salt origin.

1.4.1 Elemental ratios

To quantify source apportionment of aerosol, the elemental ratios, either of trace metals as listed in Table 1.1 or conservative elements in seawater, can be used (Buck et al., 2019).

For example, the Cl/Na ratio is a tracer for sea salt aerosols, while the Fe/Al ratio can be used as a tracer for crustal dust and biomass burning, and the V/Ni ratio can be used to identify the type of oil combustion (Table 1.2). These element ratios can be mixed sources that are anthropogenic or natural sources, so additional uses of enrichment factor must be applied assist the source identification.

Table 1.1 Sources and type of PM$_{2.5}$-bound metal (following Kang et al., 2019; Ismal et al., 2018)

Sources	Metals
Sea spray	Ca, Ba, Mg, Fe, Sr, Na
Biomass burning	Cu, K, Zn
Gasoline combustion	Al, Ag, Cd, Cu, Fe, Mg, Mn, Pb, Ti, Zn
Coal combustion	Al, Ba, Co, Cr, Cu, Fe, Mg, Mn, Pb, Ti, Sb, Se, Sr, Zn
Fuel oil combustion	Al, Ba, Co, Fe, Mn, Ni, V
Industrial process	Cu, Ba, Fe, Mn, Ni, V, Pb, Zn

Table 1.2 Elemental ratios in natural or anthropogenic sources

Sources	Zn/Pb	Fe/Al	V/Ni	Cl/Na	References
Soil					
Chinese soil	2.9	0.44	3.1	-	Pan et al. (2013)
Crustal soil	3.3	0.4	2.9	-	Reimann and Caritat (1998)
Coal					
Vietnamese coal	0.7	-	0.55	-	Chifflet et al. (2018)
Chinese coal	2.7	1.1	2.6	-	Pan et al. (2013)
Petroleum fuels					
Gasoil	3869		0.15	-	Chifflet et al. (2018)
Diesel	32		0.09	-	Chifflet et al. (2018)
Traffic	1.7	-	1.49-2.4	-	Thorpe and Harrison (2008)
Industrial activities					
Steel production	0.73	-	-	-	Pacyna and Pacyna (2011)
Steel production	3.5	-	-	-	Oravisjärvi et al. (2003)
Marine aerosol					
Newly formed	-	-	-	1.8	Duce and Hoffman (1976)
Observed form	-	-	-	1.3	Kritz and Rancher (1980)
Seawater	-	-	-	1.16	Chester and Jickells (2012)

1.4.2 Enrichment factor

Enrichment factor (EF) defined as the concentration ratio between interested metals in aerosol sample and in Earth's crust or oceans. Thus, EF of elements in the aerosols can be used to evaluate natural or anthropogenic sources (Ismal et al., 2018; Zhao et al., 2015).

1.4.3 Principal component analysis

Principal component analysis (PCA) is a dimensionality reduction method that is frequently used to reduce the dimensionality of large data sets, by changing a large set of variables into a smaller one that still contains most of the data in the large set. It is often used in environmental studies.

1.4.4 Lead isotopes

Lead in atmosphere is almost entirely anthropogenic in origin. In particular, lead contained in gasoline or coal were focused in the past. Anthropogenic lead in the aerosols can be effectively traced by using lead isotopic compositions (Komárek et al., 2008). ^{204}Pb, ^{206}Pb, ^{207}Pb, and ^{208}Pb are the four naturally occurring stable isotopes of lead. Except for ^{204}Pb radioactive decay of uranium and thorium (^{238}U, ^{235}U, ^{232}Th). Pb isotope compositions are usually reported as ratios. For example, old Pb ores show lower $^{206}Pb/^{207}Pb$ as compared to young Pb ores (Gulson et al., 1981).

The isotopic composition of lead is not affected by chemical or physical fractionation during transport and deposition. Therefore, the isotopic ratio of lead can be used to determine specifically sources (air mass origin) and pathways of atmospheric lead (Bollhöfer and Rosman, 2001). The $^{206}Pb/^{207}Pb$ and $^{208}Pb/^{207}Pb$ ratios in different sources of plausible anthropogenic and natural end members from the region were shown in Table 1.3.

1.4.5 Air mass backward trajectory analysis

Backward trajectory is the retrospective tracking of atmospheric particles. Hybrid Single Particle Lagrangian Integrated Trajectory (HYSPLIT) model provided by NOAA (National Oceanic and Atmospheric Administration) can be used to estimate

origins and sources of atmospheric particles. The trajectory drawing principle is based on integration of particles' position in the air mass, regarding to time, height, temperature, rainfall and relative humidity (Šaulienė and Šukiene, 2006). Air mass trajectory is a helpful tool to confirm transportation route of the aerosols from the source to the sampling site.

1.5 Aerosol study in Thailand

Previously, the studies of aerosols in Thailand are generally focused on PM_{10} using optical properties and remote sensing. Most studies were conducted in the Northern part of Thailand, where forests fire during fire season was most intense as seen in elevated PM_{10}. Although there are reports on the relationship between metals in $PM_{2.5}$ fraction and lung cancer, the study of $PM_{2.5}$ in aerosols and aerosol sources is still lacking. Recent study on sulfate aerosols throughout Thailand was performed by aerosol optical depths (Janjai et al., 2012; Sugimoto et al., 2015). Table 1.4 is a list of optical properties studies for aerosols in Thailand since 2001.

The studies on the chemical compositions of aerosols in Thailand are focused mostly in northern Thailand and Bangkok (Table 1.5). Among these, several publications are based on the chemical composition of the aerosols in the same sample collection during 2012-2015. There are less publications that reported metal composition in $PM_{2.5}$ aerosols in Bangkok, i.e., Rungratanaubon et al. (2008), Pongpiachan and Iijima (2016) and Pongpiachan et al. (2017). However, these three studies used different techniques to quantify metals composition. The data given of many metals, particularly trace metals, were so different by many orders of magnitude. Rungratanaubon et al. (2008) used inductively coupled plasma atomic emission spectrometry (ICP-AES) to determine Al, Cd, Cr, Cu, Fe, K, Mn, Na, Ni, Pb, and Zn after acid digestion. Pongpiachan and Iijima (2016) used inductively coupled plasma mass spectrometry (ICP-MS) after acid digestion to determine Al, Sc, V, Cr, Mn, Co, Ni, Cu, Zn, As, Se, Cd, Sb, Ba, La, Ce and Pb. Pongpiachan et al. (2017) used energy dispersive X-ray fluorescence (ED-XRF) to determine Al, Sc, V, Cr, Mn, Co, Ni, Cu, Zn, As, Se, Cd,

Sb, Ba, La, Ce, Pb, Na, Mg, Si, P, S, Cl, K, Ca, Ti, Fe, Ga, Br, Rb, Sr, Y, Zr, Nb, Mo, Pd, Ag, In, Sn, Cs, Sm, Eu, Tb, Hf, Ta, W, Ir, Au, Hg, Tl, U.

The metal concentrations from ED-XRF were apparently high since this method is not an appropriate technique for aerosol analysis due to its high detection limit compared to the trace amount of many metals therein. While analysis of metal concentrations using ICP after acid digestion is more appropriate, it was noticed that the works of Rungratanaubon et al. (2008) and Pongpiachan and Iijima (2016) were not conducted in clean laboratory. Liang et al. (1990) had proved that metal concentration in the normal laboratory was 3 to 10 times higher than clean laboratory. To date, it is widely except that preparation step prior to instrumental analysis is crucial. The preparation step needs to be conducted in the clean laboratory because the excess metal concentration from contamination will lead to misinterpretation and cause an error in source identification. Not only that the reliable of metals data is in question, but there was no previous work in Thailand using Pb isotope ratios for source apportionment analysis. In addition, there is no work studies on the influences of air-sea-land on chemical composition of the aerosols, particularly coastal cities. Thus, the study on the chemical composition in aerosols over coastal cities is challenging.

Table 1.3 The ^{206}Pb/^{207}Pb and ^{208}Pb/^{207}Pb ratios in different anthropogenic and natural end members

Sources	^{206}Pb/^{207}Pb	^{208}Pb/^{207}Pb	References
Atmospheric aerosol			
Thailand (Bangkok)	1.1210	2.3970	Mukai et al. (1993)
Thailand (Bangkok)	1.1270	2.4040	Bollhöfer and Rosman (2000)
Malaysia (Kuala Lumpur)	1.1410	2.4100	Bollhöfer and Rosman (2000)
Vietnam	1.1610	2.4415	Bollhöfer and Rosman (2000)
Indonesia (Jakarta)	1.1310	2.3950	Bollhöfer and Rosman (2000)
Singapore	1.1470	2.4240	Lee et al. (2014)
Oil combustion			
China (Shanghai)	1.1516	2.4385	Chen et al. (2005) and Zhao et al. (2015)
Vietnam (Haiphong)	1.1530	2.4369	Chifflet et al. (2018)
Taiwan (Taipei)	1.1468	2.4263	Yao et al. (2015)
Coal			
China	1.1926	2.4765	Chifflet et al. (2018)
India	1.2090	2.4943	Das et al. (2018)
Australia	1.2055	2.4866	Diaz-Somoano et al. (2009)
Indonesia	1.1835	2.4770	Diaz-Somoano et al. (2009)
Vietnam	1.1768	2.4695	Chifflet et al. (2018)
River sediment			
Southeast Asia	1.1966	2.4888	Millot et al. (2004)
Sediment			
South China Sea	1.2077	2.4875	Zhu et al. (2002)
Ores			
India	1.0700	2.3471	Sangster et al. (2000)
Australia	1.1120	2.3873	Sangster et al. (2000)
China	1.0823	2.3978	Sangster et al. (2000)

Table 1.4 Studies of aerosols in Thailand (physical analysis)

Region	Study area	Method of study	Composition & type of aerosols	Year of study	References
North	Mainland Southeast Asia	Remote Sensing – MODIS	$PM_{2.5}$ - Active forest fire	2001-2016	Yin et al. (2019)
	Chiangmai	Remote Sensing – MODIS	PM_{10} – Active forest fire	2007	Trang and Tripathi (2014)
	Chiangrai	Remote Sensing – MODIS	PM_{10} – Active forest fire	2007-2010	Sirimongkonlertkul and Phonekeo (2012)
	Chiangmai	Remote Sensing – MODIS	PM_{10} and $PM_{2.5}$ - Active forest fire	2007-2012	Kanabkaew (2013)
	Northern Thailand	Remote Sensing – MODIS	PM and Carbon monoxide – Active forest fire	2008-2010	Sukitpaneenit and Oanh (2013)
	Upper northern Thailand	Remote Sensing – MODIS	PM_{10} and $PM_{2.5}$ – Active forest fire	2009-2010	Phayungwiwatthanakoon et al. (2014)
	Chiangrai	Remote Sensing – MODIS	PM_{10} and $PM_{2.5}$ – Active forest fire	2009-2012	Sirimongkonlertkul et al. (2013)
	Phayao	Remote Sensing – MODIS	PM_{10} and $PM_{2.5}$ – Active forest fire	2011-2017	Pimonsree and Vongruang (2018)
	Chiangmai	Remote Sensing – MODIS	PM_{10} – Active forest fire	2007-2016	Suwanprasit et al. (2018)
	Northern Thailand	Remote Sensing – MODIS	PM_{10} – Active forest fire	2010-2015	(Punsompong and Chantara, 2018)
	Chiangmai	Remote Sensing – MODIS	PM – Active forest fire	2015	Sayer et al. (2016)
Northeast	Nakhonratchasima	Lidar depolarization, sky radiometer	Soil dust, OC, sulfate	2012-2013	Sugimoto et al. (2015)
East	Eastern Thailand	Remote Sensing – GIS, ASR, ASMR	$PM_{2.5}$ – Lung cancer	2010-2013	Zhang and Tripathi (2018)
Thailand	Chiangmai Ubonratchathani Nakhonpathom Songkhla	Remote Sensing – MODIS Sunphotometer	Aerosol optical depth, single scattering albedo, size distribution	2008-2009	Janjai et al. (2012)

Table 1.5 Studies of aerosols in Thailand (Chemical analysis)

Region	Study area	Method of study	Composition & type of aerosols	Year of study	References
North	Chiangmai	Air Volume Sampling 100L/min – Glass fiber filters, continuously	TPS - Element	2003-2004	Tippayawong et al. (2006)
	Chiangmai	Air Volume Sampling 700L/min, 23 h	PM - PAHs	2010	Chuesaard et al. (2014)
	Chiangmai	Air Volume Sampling - Teflon filter, 24h	$PM_{2.5}$ - OC, EC, WSOC and anhydrosugars	2010-2013	Chuang et al. (2016)
	Northern Thailand	Air Volume Sampling 5L/min, 24h	$PM_{2.5}$ – Organic group using FTIR	2012-2013	Pongpiachan et al. (2013)
	Northern Thailand	Air Volume Sampling 5L/min - Quart filter, 24h	$PM_{2.5}$ - PAHs biomass burning	2012-2013	Pongpiachan (2015)
	Northern Thailand	Air Volume Sampling 5L/min - Quart filter, 24h	$PM_{2.5}$ – PAHs-cancer risk	2012-2013	Pongpiachan (2016)
	Northern Thailand	Air Volume Sampling 5L/min - Quart filter, 24h	$PM_{2.5}$ - PAHs biomass burning	2012-2015	Pongpiachan et al. (2017)
East	Rayong	Air Volume Sampling 1.1L/min - Quart microfiber filter, 24 h	PM_{10} – PAHs (shipping emission)	2008-2012	Pongpiachan (2015)
Central	Bangkok	Air Volume Sampling – Glass fiber filters, 24 hr	TSP - Metals and source identification	2006-2007	Rungratanaubon et al. (2008)
	Bangkok	Air Volume Sampling 1.113L/min – Glass fiber filters, 24 hr	PM_{10^-} Metals	2008	Pongpiachan and Iijima (2016)
	Bangkok	Air Volume Sampling 1.113L/min – Glass fiber filters, 24 hr	PM_{10} - carbonaceous	2011-2014	Pongpiachan et al. (2017)
	Bangkok	Air Volume Sampling 5L/min - Quart microfiber filter, 72 hr	$PM_{2.5}$- carbonaceous (vehicle)	2010-2012	Pongpiachan et al. (2015)
	Bangkok	Air Volume Sampling 5L/min, 72 hr	$PM_{2.5}$ – Metals	2010-2011	Pongpiachan et al. (2017)
	Bangkok	Air Volume Sampling, 72 hr	PM_1 and $PM_{2.5}$ - carbonaceous	2016	Vejpongsa et al. (2017)

1.6 Roles of atmospheric circulation on marine and anthropogenic aerosol in Thailand

Thailand is located between Latitudes 5° 36.5´ N to 20° 27.5´ N, and Longitudes 97° 20.4´ E to 105° 38.1´ E. The atmosphere over Thailand is influenced by airmasses to the north from mainland China, to the east from South China Sea, to the west from Indian Ocean, and to the south from the Gulf of Thailand (GoT).

The atmospheric circulation of Thailand is influenced by the monsoon system, namely northeast (NE) monsoon and southwest (SW) monsoon. The NE monsoon (mid-October to mid-February) transports aerosol from mainland China and upper South China Sea toward central Thailand before blowing through the GoT and then southern Thailand. The SW monsoon (mid-May to mid-October) brings the air mass from the Indian Ocean through southern Thailand and the GoT to central Thailand. Inter-monsoon (mid-February to mid-May) is the transition period from NE monsoon to SW monsoon. The inter-monsoon wind originates over the South China Sea and blows towards central Thailand to Andaman Sea (https://www.tmd.go.th/).

Bangkok Metropolis is located on the delta of Chao Phraya River, approximately 40 km north of the GoT. The metropolis is well known for traffic congestion, and marred by air pollution from industrial emission, endless construction activities and traffic emissions. On the other hand, Chonburi is a coastal town, located on the east coast of the GoT, approximately 80 km southeast of Bangkok. Chonburi is a major tourist destination and industrial estates. Oil refineries and deep-sea ports are situated therein. Both Bangkok and Chonburi are affected by marine aerosols especially during SW monsoon, when the air mass flows over the GoT toward these two coastal cities.

Chiangrai is the northernmost province of Thailand sharing borders with Laos and Myanmar. For 9-10 months in a year, Chiangrai has a pristine atmosphere, which drastically changes during the burning season during February to April. Biomass is burnt for harvesting of sugarcane, and clearing land and preparing the fields for the next crop cycle (rice paddy and other crops). Many provinces in northern Thailand have fire-related air pollution peaking in March and April (Pongpiachan et al., 2013). The GoT

has been shown affected by long-range transported aerosols from forest fire in Sumatra during SW monsoon, especially in July to September (Vadrevu et al., 2015), with the highest impact during El Niño year (e.g., 2015 and 2019).

1.7 Rationale and objectives

The study of marine aerosols is very important as it involves in global biogeochemical cycles, ocean acidification, nutrient fluxes, climate change, as well as human health. In the atmosphere, marine aerosols are mixed or interact with landed-derived or "continental" aerosols (contributes from fossil fuels combustion, biomass burning and soil dust). This extensive atmospheric interaction poses the influence on biogeochemistry of surface ocean through long-range transport and deposition of terrestrial and marine-derived nutrients and trace elements.

In addition to very few works on aerosol chemistry and sources apportionment in Thailand, more scarce is the work done in the coastal cities of Thailand. Furthermore, no work has been done over Thai waters. To fill in these gaps, it is essential to investigate aerosol chemistry over the coastal areas and over the sea surface.

The main objective of this work is to investigate the seasonal variation and air-sea-land influence on chemical composition of aerosol over coastal cities (Bangkok and Chonburi). To achieve this objective, studies have been undertaken for one year to cover the monsoon season. The second objective is to understand the distribution and chemical composition of aerosol over Thai waters. To achieve this objective, aerosol samples were collected over Thai waters (Andaman Sea and Gulf of Thailand) during SW monsoon in 2018. The third objective is to verify the trace metal emission during the biomass burning and determine whether burning-related air pollution reached far down to Bangkok. To achieve this objective, aerosol samples were collected over Chiangrai and Bangkok during burning season in 2019.

To better understand the sources of aerosols, air mass trajectories were tracked to determine transportation route. In addition, principal component analysis (PCA), enrichment factor (EF), Pb isotope ratios, elemental ratios and Pearson's correlation

coefficient were used to identify potential sources of the air mass over the sampling sites.

1.8 Scope of the investigation

In this study, the chemical composition of the aerosols was investigated in coastal cities (Bangkok and Chonburi), Thai waters (the Andaman Sea and the Gulf of Thailand), and northern Thailand (Chiangrai).

For the coastal cities, weekly sampling of $PM_{2.5}$ was collected during two monsoon seasons. Trace metal concentrations in conjunction with Pb isotope ratios were analyzed to identify the sources of atmospheric aerosol over coastal cities.

In case of Thai waters, $PM_{2.5}$ was collected on board during southwest monsoon both in the Gulf of Thailand and the Andaman Sea. $PM_{10-2.5}$ was also collected over the Gulf of Thailand. The water-soluble inorganic ions (WSIIs) and metal concentrations were determined to understand the chemical composition and sources of atmospheric aerosol over Thai waters.

The burning-related metal over Chiang Rai were collected compared to the aerosol over Bangkok during burning season. Aerosol samples were collected every week during burning season (January to April) and metal concentration along with Pb isotope ratios were examined and computed to identify the local sources and to determine whether burning-related air pollution reached far down to Bangkok.

1.9 Expected outcome

This study expects to gain a better understanding of distribution, transportation and chemical composition of aerosols over Thailand, and the influences of marine aerosols on the coastal cities.

The thesis contains six chapters and appendices. Introductory material and literature reviews are given in this chapter. Experimental materials and procedures are described in Chapter 2. The main body of scientific research are divided into three chapters according to the objective. Seasonal variation and air-sea-land influence on chemical composition of aerosols over coastal cities was reported and discussed in Chapter 3. Distribution and chemical composition of aerosols over Thai waters are presented and discussed in Chapter 4. Chapter 5 presents the results and discussion of metal emission and transportation related to biomass burning in Chiangrai. Source apportionment of $PM_{2.5}$ in Chiangrai and Bangkok is also discussed in this chapter. A summary and conclusions of the entire work are given in chapter 6.

The results from this research have already been published in 2 journal articles, and one is a draft manuscript for journal submission.

– Chapter 3 is published in "Kayee, J., Bureekul, S., Sompongchaiyakul, P., Wang, X.-F., and Das, R. (2021) Sources of atmospheric lead (Pb) after quarter century of phasing out of leaded gasoline in Bangkok, Thailand. Atmospheric Environment 253, 118355. https://doi.org/https://doi.org/10.1016/j.atmosenv.2021.118355"

– Chapter 4 is a manuscript for journal submission under the tentative topic of "Distribution and chemical composition of atmospheric aerosols over Thai waters during 2018 Southwest monsoon"

– Chapter 5 is published in "Kayee, J., Sompongchaiyakul, P., Sanwlani, N., Bureekul, S., Wang, X., Das, R., 2020. Metal Concentrations and Source Apportionment of PM2.5 in Chiang Rai and Bangkok, Thailand during a Biomass Burning Season. ACS Earth and Space Chemistry 4, 1213–1226. https://doi.org/10.1021/acsearthspacechem.0c00140"

CHAPTER 2

METHODOLOGY

2.1 Study area

Thailand is located between Latitudes 5° 36.5′ N to 20° 27.5′ N, and Longitudes 97° 20.4′ E to 105° 38.1′ E (Figure 2.1). Aerosols from three cities in Thailand, namely Bangkok, Chonburi and Chiangrai, were collected and investigated under different sampling protocols in order to clarify three objectives. Bangkok, the capital of Thailand, is located on the delta of the Chao Phraya River, approx. 40 km north of the Gulf of Thailand (GoT) and approx. 80 km northwest of Chonburi. Chonburi is coastal town, located on the east coast of the GoT. Chiangrai is the northernmost province of Thailand sharing borders with Laos and Myanmar. Aerosols over Thai waters were collected both in the GoT and the Andaman Sea.

Sampling station in Bangkok (13° 44.24′ N, 100° 31.48′ E) was located on the 4th floor terrace of the Department of Marine Science, Chulalongkorn University (approx. 20 m above ground level (AGL)) (Figure 2.2a). Sampling station in Chonburi (13° 20.24′ N, 100° 55.48′ E) was located on the 3rd floor terrace of the Laboratory building in Angsila Marine Animal Research Station of Faculty of Science, Chulalongkorn University (approx. 20 m AGL) (Figure 2.2b). Sampling station in Chiangrai was located at the roof top of a house (19° 51.00′ N, 99° 48.36′ E) in downtown (approx. 9 m AGL) (Figure 2.2c).

To investigate the seasonal variation and air-sea-land influence on chemical composition of aerosols over coastal cities, the aerosol samples were collected in Bangkok and Chonburi during January 2018 and April 2019. The sampling period was covering annual atmospheric circulation of Thailand which is influenced by the monsoon system.

To understand the distribution and chemical composition of aerosol over Thai waters, the aerosols were collected on board of M.V. SEAFDEC-2 (approx. 10 m ASV) in

the GoT (Figure 2.3a) and R.V. Dr.Fridtjof NANSEN in the Andaman Sea (approx. 22 m above sea level (ASV)) (Figure 2.3b) during southwest monsoon in 2018.
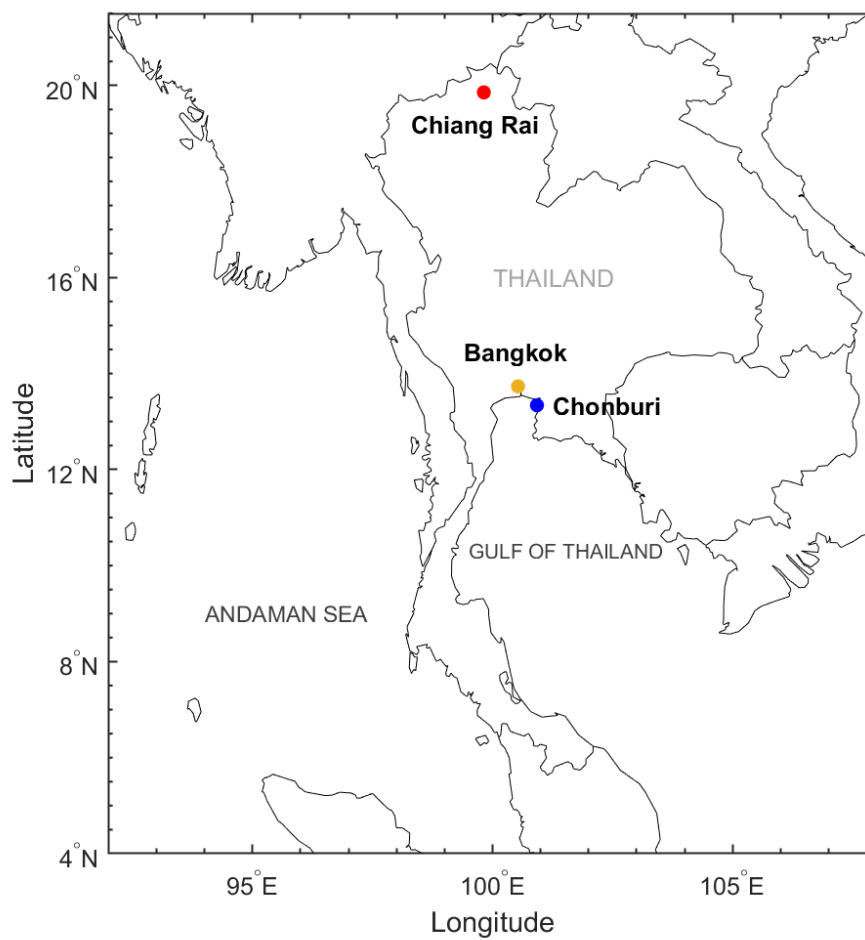
Figure 2.1 The map indicated sampling locations including two coastal cities, Bangkok and Chonburi, and one inland city, Chiangrai

<div align="center">(a)   (b)   (c)</div>

Figure 2.2 Impactor setting for aerosols sampling in (a) Bangkok, (b) Chonburi, and (c) Chiangrai

<table>
<tr><td>(a)</td><td>(b)</td></tr>
</table>

Figure 2.3 Impactor setting for aerosol sampling on board of (a) M.V. SEAFDEC-2 in the Gulf of Thailand, and (b) R.V. Dr.Fridtjof Nansen in the Andaman Sea

To verify trace metal emission during biomass burning and determine whether burning-related air pollution reached far down to Bangkok, the aerosols were collected in Chiangrai during January to April 2019 covering burning season in the northern Thailand to compare with the aerosols of the same period in Bangkok.

2.2 Filter preparation

To avoid metal contamination, PTFE filters (2.0 μm 47 mm, PALL[®]) were precleaned prior to sample collection. The filters were soaked in 1 N HCl at 140°C for a few hours, then rinsed several times with ultrapure water. The acid-cleaned filters were placed to dry at room temperature in a laminar flow cabinet (clean bench) for 2 days (Figure 2.4) and then in an oven for 1 hour. After cooling down for 30 min, the cleaned filters were kept individually in sterile petri dishes and stored in a desiccator until used.

2.3 Sample collection

Aerosols samples were collected on pre-acid cleaned 47 mm PTFE filters with SKC personal modular impactor $PM_{2.5}$ (Figure 2.5a) connected to the sampling pump. The sampling pump using for Bangkok and Chonburi sites was a SKC Deployable

Particulate Sampler (Figure 2.5b), while the pump using for Chiangrai and onboard of the research cruises were Gilian AirCon-2 Area Air Sampling Pumps (Figure 2.5c).

Figure 2.4 Drying precleaned PTFE filters in a laminar flow cabinet

(a)   (b)   (c)
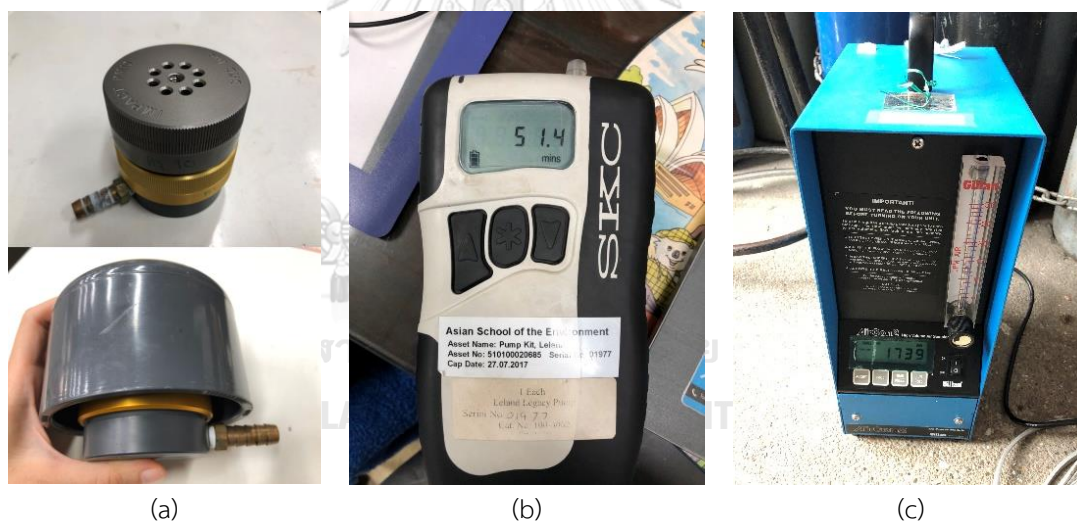
Figure 2.5 Aerosols sampling equipment (a) SKC personal modular impactor and the rain cover, (b) SKC Deployable Particulate Sampler, and (c) Gilian AirCon-2 Area Air Sampling Pump

2.3.1 Aerosols over terrestrial cities

PM$_{2.5}$ aerosols over the terrestrial cities at all sites, each sample was collected at the flow rate of 10 L/min for 24 hours. Most samples were collected weekly, however biweekly interval was performed according to the time available of the equipment or the researcher. The sampling intervals were presented in Table 2.1. For marine aerosols, the flow rate of 15 L/min was used. The marine aerosols were collected only while the ships were sailing at the accumulated time of 20-40 hours for each sample. The filters after terrestrial aerosol sampling were presented in Figure 2.6a.

2.3.2 Marine aerosols over Thai waters

Marine aerosols were collected during southwest monsoon over the GoT by M.V. SEAFDEC-2 during 18th August to 18th October 2018 and over the Andaman Sea by R.V. Dr.Fridtjof NANSEN during 1st to 15th. In the GoT, PM$_{10-2.5}$ and PM$_{2.5}$ were collected, while only PM$_{2.5}$ was collected in the Andaman Sea. The sampling tracks in Thai waters were presented in Figure 2.7. The filters after marine aerosol sampling were presented in Figure 2.6b.

2.4 Chemical Analysis

2.4.1 Analytical equipment and Laboratory

Sample preparation processes for metals and Pb-isotopes analysis was conducted in a Clean Chemistry Laboratory-Class 1000 (Clean Room) of the Earth Observatory of Singapore (EOS), Nanyang Technological University, in Singapore. Ultrapure grade acids from Seastar Chemicals and ultrapure water at 18.2 MΩ.cm resistivity (Super-Q, Merck Millipore) were used throughout the analytical processes. Determination of metals and Pb-isotopes was performed at the EOS using a sector-field inductively coupled plasma mass spectrometer (SF-ICP-MS, an Element 2 from Thermo Fisher Scientific) (Figure 2.8a) and a Multicollector ICP-MS (Neptune Plus from Thermo Fisher Scientific) (Figure 2.8b), respectively.

Table 2.1 Sampling intervals for aerosols collection of the terrestrial sites in 2018-2019

	2018												2019			
	1	2	3	4	5	6	7	8	9	10	11	12	1	2	3	4
Bangkok			–			B	W			–			W			–
Chonburi	D*	–		W		B	W		B		W			–		
Chaingrai						–								W		–

D*   sampling on 22, 24 and 25 June 2018
W   weekly sampling
B   biweekly sampling

(a) (b)
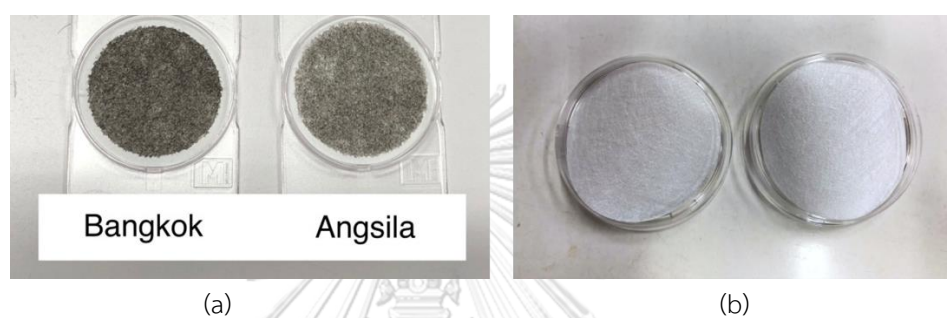
Figure 2.6 PTFE filters after sampling, (a) terrestrial aerosol samples, and (b) marine aerosol samples

(a) (b)
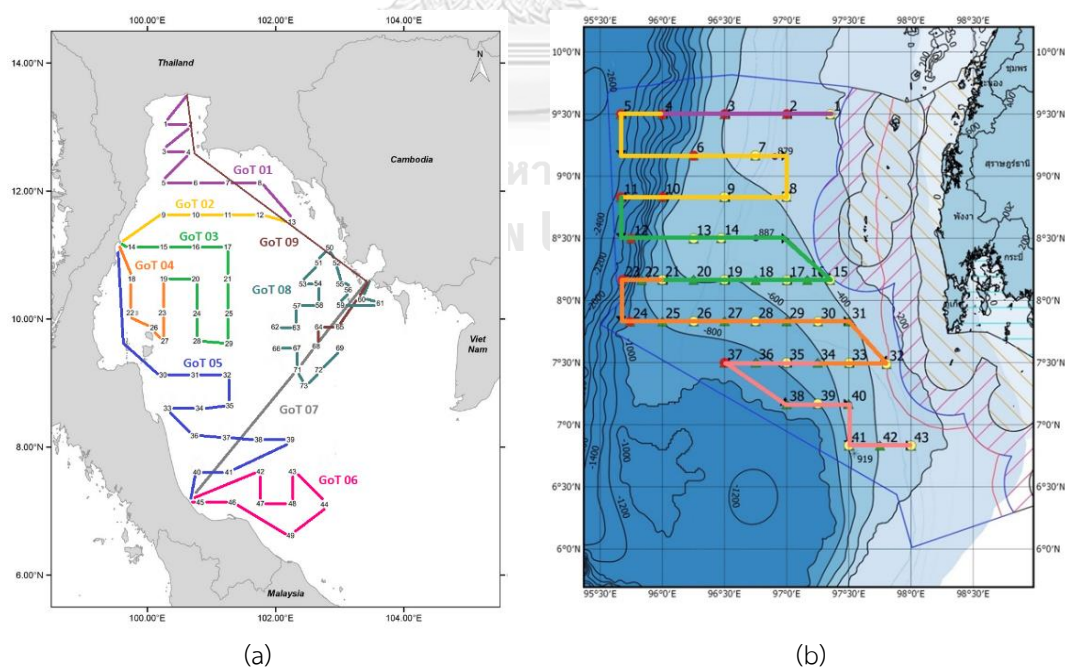
Figure 2.7 Marine aerosol sampling tracks onboard of (a) M.V. SEAFDEC-2 in the Gulf of Thailand, and (b) R.V. Dr.Fridtjof NANSEN in the Andaman Sea

(a)   (b)

(c)

Figure 2.8 Analytical equipment (a) SF-ICP-MS (Element 2) Thermo Fisher Scientific for metal analysis, (b) Multicollector ICP-MS (Neptune Plus) Thermo Fisher Scientific for Pb-isotope analysis, and (c) Ion Chromatography (IC, ICS-2500, DIONEX) for water soluble ion analysis

Analysis of water-soluble inorganic ions (WSIIs) was conducted in a Clean Laboratory at Department of Marine Science, Chulalongkorn University, and determined by ion chromatograph (Figure 2.8c) at the Center of Excellence on Hazardous Substance Management, Chulalongkorn University.

After sample collection the filters from terrestrial site were used for metal and Pb-isotope analysis, and the filters from ocean site were used for WSIIs analysis. Since the metals and Pb-isotopes can be extracted by the same procedure, therefore, the whole filters were extracted. While metals and WSIIs were extracted using different procedure, therefore, the filter has to be cut half, using a ceramic scissor, for each analysis (Figure 2.9)

2.4.2 Sample preparation for analysis of metals and Pb-isotopes

Sample preparation for metal and Pb-isotope analysis was conducted in Clean Room at EOS (Figure 2.10a). The PTFE filters were cut into a small size by the ceramic scissor and put into a Savillex® Teflon beaker. Between each sample, the scissor was cleaned by methanol and ultrapure water to prevent cross contamination. Adding of 5 mL of 50% (v/v) 3:1 HNO_3:HF mixture to the beaker containing sample filters. The tightly capped beakers were placed on the hotplate at 150°C for 12 hours (Figure 2.10b), following by sonication at 60°C for 1 hour. After extraction, the filters were removed from the solution using a Teflon tweezer. The solution was evaporated to nearly dryness on a hot plate at 120°C, then redissolved the extracted metals by adding 2 mL of 3% HNO_3. The final solution was separated into two aliquots, one half was for metal determination and another half was for Pb-isotope analysis.
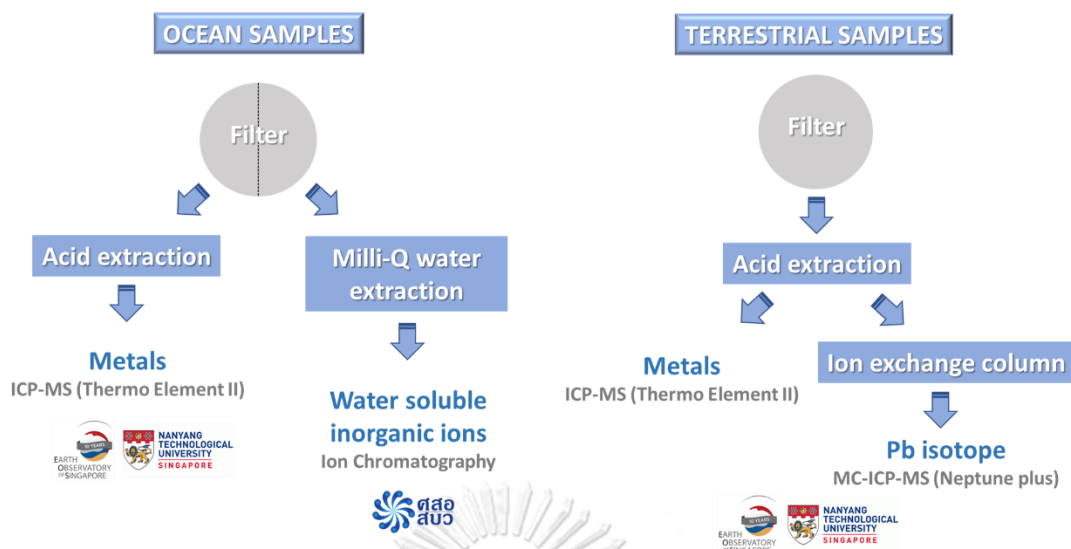
Figure 2.9 Management of filters after sample collection for chemical analysis

(a)   (b)
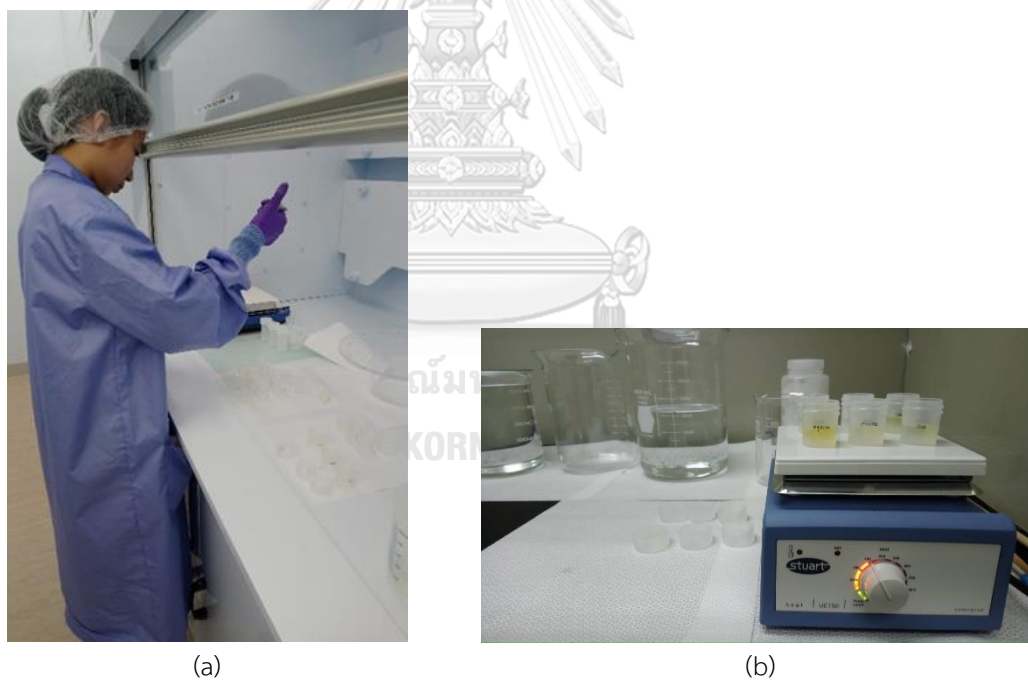
Figure 2.10 (a) Sample preparation for metal and Pb-isotope analysis in Clean Chemistry Laboratory-Class 1000 (Clean Room) of the Earth Observatory of Singapore (EOS), Nanyang Technological University, in Singapore, and (b) Savillex® Teflon beakers containing PTFE filters and acid were placed on the hotplate for metal extraction

2.4.3 Metal determination

One half of aliquot from 2.4.2 was used for trace metal analysis. One ppb of indium (In) was added into the solution as the internal standard. Instrumental drift was corrected by a combination of the internal indium standard and external bracketing multi-element standard from Inorganic Ventures (IV-ICPMS- 71A). Sixteen metals (e.g., Al, As, Ba, Ca, Cd, Cu, Cr, Fe, Mg, Mn, Na, Ni, Pb, Sr, V, Zn) were measured on a sector-field inductively coupled plasma mass spectrometer (SF-ICP-MS, an Element 2 from Thermo Fisher Scientific) (Figure 2.8a).

2.4.4 Pb isotope determination

Another half of aliquot from 2.4.2 was used for Pb-isotope analysis. The aliquots in Savillex® Teflon beakers were placed on the hotplate at 90°C until nearly dryness, then redissolved in 200 μL of 1.1 N HBr. The solution was loaded into a tiny ion exchange column filling with 200-400 mesh Eichrom AG-1X8 chloride form for Pb separation (Figure 2.11). Subsequently, rinse the beaker with 150 μL of 1.1 N HBr and pour the solution into the ion exchange column. Flush the column with 400 μL of 1.1 N HBr, following by 400 μL of 2 N HCl as a mobile phase to elute other metals. In this step, Pb still remained in the column. Ultimately, Pb was eluted from the ion exchange column by 500 μL of 6 N HCl and collected in the Savillex® Teflon beaker. The collected solutions were evaporated on the hotplate at 90°C until dryness and redissolved in 2% ultrapure HNO_3. The Pb isotopes were determined by a Multicollector ICP-MS (Neptune Plus from Thermo Fisher Scientific) (Figure 2.8b).
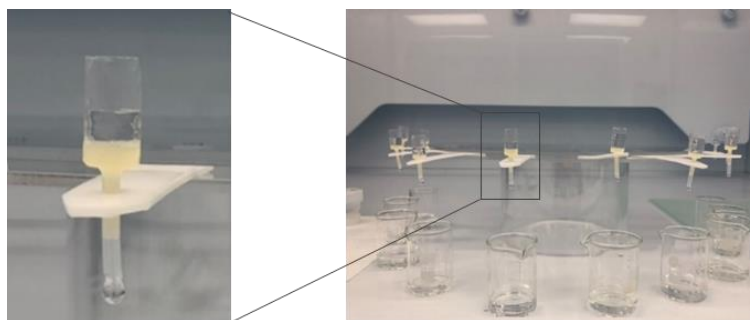
Figure 2.11 Ion exchange column for Pb separation for isotope analysis.

2.4.5 Sample preparation and determination of water-soluble inorganic ions

The PTFE filters were cut into a small size using a ceramic scissor and place in centrifuge tubes. Between each sample, the scissor was cleaned by Milli-Q water to prevent cross contamination. Five milliliters of Milli-Q water were added in centrifuge tube. The close capped centrifuge tubes were sonicated at room temperature for 1 hour to desorb and agitate the particles effectively. The PTFE filters were removed from solution using a Teflon tweezer. Then, the solution was filtered through 0.22 μm filter prior to analyze the WSIIs by Ion Chromatography (IC, ICS-2500, DIONEX) (Figure 2.8c). Anions were determined using anion-exchange column (4x250 mm, Dionex™ IonPac™ AS19, USA) and eluted with 10 mM KOH at a flow rate of 1.10 mL/min. Cations were determined using cation-exchange columns (4x250 mm, Dionex™ IonPac™ CS12A) in conductivity mode and eluted with 11 mM H_2SO_4 at the flow rate of 1.00 mL/min.

2.5 Quality assurance and quality control

Quality assurance and quality control (QAQC) of all data from chemical analysis was achieved by analysis of field blank and reagent blank. The field blank was the analysis of precleaned filter which brought to the sampling site and performed sampling as the same manner as normal sample collection unless no air pumping was conducted. This is to evaluate contamination which may exists on the impactor or during filter transfer process to and from the impactor. Regent blank was conducted in every analytical batch. Metal contamination in the blanks was determined and was subtracted from the metals concentration of the samples attained from the instrumental analysis.

Detection limit (LOD) of all chemical analyses (metals, Pb-isotopes and WSIIs) was calculated based on three times of the standard deviation (SD) of blank. For the SF-ICP-MS (Element 2) and the Multicollector ICP-MS (Neptune Plus) Thermo Fisher Scientific, different mass resolution modes were used to optimize the separation of measured isotopes from interfering polyatomic species (e.g., ^{75}As from $^{40}Ar^{35}Cl$) and improve detection limit of metals.

Indium (In) was used as an internal standard for metal analysis, while thallium (Tl) was used as an internal standard for Pb-isoptope analysis. The ^{203}Tl/^{205}Tl ratio of 0.418911 was used to correct for instrumental mass fractionation (Sen et al., 2016; White et al., 2000). The samples were measured at similar Pb/Tl ratios to the standards to avoid any analytical bias. The ^{202}Hg signal was used to correct the isobaric interference of ^{204}Pb by ^{204}Hg. The isotope ratios of the NBS-981 Pb standard were measured during the analytical sessions, indicating ^{206}Pb/^{204}Pb = 16.92599 ± 0.002, ^{207}Pb/^{204}Pb = 15.47794 ± 0.0027, ^{208}Pb/^{204}Pb = 36.6591 ± 0.0086, ^{206}Pb/^{207}Pb = 1.0935 ± 0.0001, and ^{208}Pb/^{207}Pb = 2.3684 ± 0.0002 (2 standard deviations, n = 22).

2.6 Data interpretation

2.6.1 Statistical analysis

Principal component analysis, a multivariate statistical technique, in SPSS$^{®}$ (version 22) software was used to emphasize variation and bring out strong patterns in a dataset. Source apportionment of metals during biomass burning was evaluated from the PCA results. Pearson's correlation coefficient was used to measure the strength of the correlation between the two variables. The statistical significance was accepted at $p < 0.05$.

2.6.2 Enrichment factor

The Enrichment Factor (EF) was used to indicate impacts of pollution according to the equation 2-1:

$$EF_{crust\ or\ sea} = (E/E_{ref})_{aerosol}/(E/E_{ref})_{crust\ or\ sea} \qquad (2\text{-}1)$$

where E is the concentration of interested element, E_{ref} is the concentration of reference metal in earth's crust or seawater. Calculation of EF_{crust} was based on the average upper continental crustal composition from Rudnick and Gao (2003) where aluminium (Al) was chosen as the reference element of crustal source. Owing to Al is the most abundant metal in the crust and its atmospheric cycle has been little altered by human impact. To evaluate the importance of the sea surface as a source for the marine aerosol, Na was used as the marine indicator element and the precursor source

composition was assumed to be that of bulk seawater (Chester and Bradshaw, 1991). EF can be classified into three categories as shown in Table 2.2.

Table 2.2 The degree of metal enrichment based on the EF_{crust} and EF_{sea} classification

EFcrust	EFsea	Degree of enrichment
EF < 10	EF < 10	Natural origin
10 ≤ EF < 100	EF > 100	Significant enrichment
EF > 100	EF > 100000	Extremely high enrichment

2.6.3 Air mass trajectory analysis

To investigate the potential sources of air mass, backward trajectory analysis was conducted by Hybrid Single Particle Lagrangian Integrated Trajectory (HYSPLIT) model that provided by NOAA Air Resources Laboratory (Stein et al., 2015). Wind directions were calculated at the altitudes between 100 and 1,000 m AGL (above ground level). These are atmospheric heights where the boundary layers are high enough to allow long range transport of aerosols.

As the aerosol samples over terrestrial cities were collected for 24 hours, the 72 hours backward trajectories, thus, were simulated to allow transport of aerosols from the sources to the sampling site. In addition, the 120 hours forward air-mass trajectories were simulated only at Chiangrai site to identify the dispersion of pollutants via air mass transport.

For marine aerosols over Thai waters, the aerosols only collected while the ship sailing, and the collecting time for aerosol sampling was up to 40 hours. Therefore, the 120 hours backward trajectories were simulated to ascertain the origins of the air masses.

CHAPTER 3

Sources of atmospheric lead (Pb) after quarter century of phasing out of leaded gasoline in Bangkok, Thailand

Jariya Kayee [a], Sujaree Bureekul [a,b], Penjai Sompongchaiyakul [a,b], Xianfeng Wang [c,d], Reshmi Das [d,e,*]

[a] Department of Marine Science, Faculty of Science, Chulalongkorn University, Bangkok, Thailand

[b] Center of Excellence on Hazardous Substance Management, Chulalongkorn University, Bangkok, Thailand

[c] Asian School of the Environment, Nanyang Technological University, Singapore

[d] Earth Observatory of Singapore, Nanyang Technological University, Singapore

[e] School of Environmental Studies, Jadavpur University, Kolkata, India

* Corresponding author. Jadavpur University, Kolkata, India.

E-mail address: reshmidas.sest@jadavpuruniversity.in (R. Das).

Highlights

- Aerosol Pb decreased in Thai aerosols 25 years after phasing out of leaded gasoline.

- Isotope ratios indicate a source shift to unleaded gasoline, diesel and coal combustion.

- Future studies intend to focus on quantifying Pb emissions from road traffic.

Abstract

After global phasing out of leaded gasoline, anthropogenic sources of atmospheric lead (Pb) are dominated by coal combustion emissions, high-temperature metallurgical processes, and vehicle exhausts. Thailand was one of the first countries in Southeast Asia to completely phase out leaded gasoline by the year 1994. This study investigates the sources of atmospheric Pb in Thai aerosols, a quarter-century after phasing out of leaded gasoline using a multiproxy approach, Pb isotopes in conjunction with trace metal composition of $PM_{2.5}$. Aerosol samples were collected for 1 year from January 2018 to April 2019 from Bangkok and Chonburi to understand the influence of seasonal variation on aerosol chemistry. Bangkok is the only megacity in Thailand and notorious for traffic congestion and Chonburi is a coastal town, 80 km southeast of Bangkok where the inter monsoon winds make landfall. Aerosol Pb concentrations significantly decreased in 25 years from 74 ± 5 ng/m^3 in 1994–1995 to 14 ± 13 ng/m^3 measured in Bangkok during Northeast (NE) monsoon winds. Concentrations of all the metals are higher in Chonburi compared to Bangkok in the NE monsoon wind, owing to the addition of local emissions from the megacity over the long-range transported metals before the winds reach the coastal town. The Pb isotope ratios have a wide range ($^{206}Pb/^{207}Pb$ range 1.1343–1.1685 and $^{208}Pb/^{207}Pb$ range 2.4138–2.4450) but the average ratios are not significantly different in Bangkok and Chonburi for all three seasons. However, present day $^{206}Pb/^{207}Pb$ ratios are more radiogenic than those measured 25 years ago in Bangkok. The Pb isotopes from both locations in all seasons have considerable overlap with unleaded gasoline and diesel used in Southeast Asia indicating automobile exhaust as an important source. Additionally, the NE monsoon winds are influenced by mixing of crustal dust (Al/Pb ratios correlates well with $^{206}Pb/^{207}Pb$, $r^2 = 0.63$) with coal combustion emission (strong inter-correlation of Pb, Zn, As and Cd, r^2 from 0.72 to 0.94) from China and Vietnam. Pb isotopes of the Southwest (SW) monsoon winds are also influenced by crustal dust and falls on the mixing line between coal combustion and ore processing emission from India in a Pb triple isotope plot. Chemical composition of aerosols in the inter-monsoon winds are similar to SW monsoon winds. After a quarter-century of leaded

gasoline banning in Thailand, the atmospheric Pb sources have changed from less radiogenic leaded gasoline exhaust and Chinese ore processing to more radiogenic unleaded gasoline and diesel exhaust and coal combustion.

1. Introduction

Lead (Pb) is a toxic, non-essential and ubiquitous pollutant in the ecosystem. It is a possible carcinogen (Class 2B), a potent neurotoxin (Lidsky and Schneider, 2003), and increases blood pressure which is one of the risk factors for cardiovascular disease (Alghasham et al., 2011). A recent report from UNICEF and Pure Earth finds that within 800 million children globally, 1 in 3 children has blood lead levels (BLL) at or above 5 micrograms per decilitre ($\mu g/dL$), a level that requires global and regional interventions as per World Health Organization (WHO) and the United States Centers for Disease Control and Prevention (CDC). Global anthropogenic fluxes of Pb to the atmosphere (4309 ± 72 Gg/yr) are an order of magnitude higher than natural fluxes (Sen and Peucker-Ehrenbrink, 2012). To minimize the exposure to this toxic metal it is important to determine the potential sources of atmospheric Pb. Before phasing out of leaded gasoline, the petro-fuel additive tetra-ethyl lead (TEL) was the primary source of the atmospheric lead (Nriagu, 1990). In the present-day atmosphere, the largest Pb emission source is coal combustion (Lee et al., 2014). Other significant sources include processing and smelting of base metal ores and automobile exhaust emission from diesel and unleaded gasoline combustion.

In 1991, phasing out of leaded gasoline started in Thailand, and by 1994, regular leaded gasoline was completely phased out (Sayeg, 1998). Since then, atmospheric Pb concentrations in Bangkok have significantly decreased (Hirota, 2006). The capital city of Bangkok is the largest city and the financial hub of Thailand and has close to 10 million automobiles and motorbikes. Even with low Pb concentrations in unleaded fuels (Gioia et al., 2017) millions of vehicles on road magnify Pb emission to the atmosphere (Thorpe and Harrison, 2008). The electricity demand in Thailand is growing since the 1980s and Thailand depends on natural gas and coal for power generation (ERIA, 2017). Thailand imports coal from Indonesia and Australia to meet the ever-

increasing demand for electricity (Energy Policy and Planning Office Ministry of Energy, www.eppo.ac.th). Hence coal combustion emission is also an important source of Pb in the atmosphere. The industrial zones in Thailand are home to numerous industries (Boonpeng et al., 2017; Saengsupavanich et al., 2009) including high-temperature metallurgy and ore processing which are potent sources of atmospheric Pb. The traditional nielloware art uses lead amalgam, which is poured into incised designs (Decharat et al., 2012) and such small scale industries are widespread in Thailand. As the residence time of Pb in the atmosphere is 5–10 days, transboundary pollution can also form an important source (Sturges and Barrie, 1987). China and India are the two largest emitters of coal combustion Pb in the region (Lee et al., 2014).

Aerosol samples collected from Bangkok in 1994–95 contained 74 ± 5 ng/m^3 Pb (Bollhöfer and Rosman, 2000; Bollhöfer and Rosman, 2001). Generally, $PM_{2.5}$ accumulates heavy metals more easily than PM_{10}. Previous studies observed that between 80 and 100% of Pb in PM_{10} was concentrated in the $PM_{2.5}$ fraction (Das et al., 2015; Kulshrestha et al., 2009; Wang et al., 2013). Hence a large fraction of Pb was possibly concentrated in the fine fraction of the aerosols collected in 1994–95. Isotope ratios indicated leaded gasoline and Chinese Pb ore to be the primary sources (Bollhöfer and Rosman, 2000; Bollhöfer and Rosman, 2001). Very high concentrations of airborne Pb (average 81.14 µg/m^3, range 9.0–677.2 µg/m^3) exceeding both the WHO recommended average annual limits (0.5 µg/m^3) and Thailand Air Quality Standards (monthly average of 1.5 µg/m^3) were reported in Nakhon Sri Thammarat Province from around nielloware factories that use Pb amalgams for the traditional artwork (Decharat et al., 2012). The factory workers had high BLL (mean 16.25 µg/dL; range 4.59–39.33 µg/dL) and correlated strongly with airborne Pb level. High BLL (mean 6.3 ± 2.2; range 2.5–16.2 µg/dL) was also reported in bus drivers of Bangkok (Kaewboonchoo et al., 2010) and workers of a battery manufacturing plant (range 17.4–22.3 µg/dL) (Lormphongs et al., 2003). The BLL in Bangkok children increased from approximately 5 µg/dL at birth to nearly 10 µg/dL in secondary school students (Ruangkanchanasetr and Suepiantham, 2002).

Often knowing the total concentration of Pb is not a sufficient parameter to understand the precise contamination sources. Pb isotopes that do not undergo physicochemical fractionation provide an important tool to track pollution sources (Komárek et al., 2008). However, pollution sources can have either distinctive or overlapping isotopic ratio ranges. When isotope fingerprinting proves inconclusive, often trace metal systematics of anthropogenic endmembers with distinctive trace metal signatures are combined with isotope ratios (Das et al., 2018; Kayee et al., 2020; Sen et al., 2016) for source identification. The objective of this study is to understand the status of atmospheric Pb pollution in central Thailand after two and half decades of complete phasing out of leaded gasoline. In this study, we use Pb concentrations of $PM_{2.5}$ in conjunction with Pb isotope ratios and trace metal concentrations to understand the sources of atmospheric Pb with changing season in Thai aerosol.

2. Materials and method

2.1 Sampling

$PM_{2.5}$ aerosol sampling was carried out between January 2018 to April 2019 in Bangkok (13.74°N, 100.53°E) and Chonburi (13.34°N, 100.93°E) in Thailand. $PM_{2.5}$ from each location were collected for 1 year to understand the influence of seasonal variation on the chemical composition of the aerosol. Bangkok Metropolis is located on the delta of the Chao Phraya River, approximately 40 km north of the Gulf of Thailand. The metropolis is notorious for traffic congestion and marred by air pollution from industrial emission, endless construction activities and traffic emissions. Chonburi is a coastal town, located on the east coast of the Gulf of Thailand, approximately 80 km southeast of Bangkok. Chonburi is a major tourist destination and an industrial estate. Oil refineries and a deep seaport is situated approximately 30 km south of Chonburi.

Aerosol samples were collected by personal modular impactor $PM_{2.5}$ (PMI, SKC Inc., USA) connected to a Deployable Particulate Sampler (DPS, Leland Legacy Pump, SKC Inc., USA) for 24 h with pumping efficiency of 10 L/min. The sampling dates are given in Table A-1 and Table A-2. The The $PM_{2.5}$ samples were collected on 47 mm

PTFE filters that were pre-washed with 1 N HCl at 140°C followed by rinsing with ultrapure water several times. The filters were dried in an oven at 60°C and sealed in petri dishes prior to sampling. In Bangkok, the pump was placed on 4th floor bridge connection of Khum-Watcharobol and Geology buildings, in Chulalongkorn University approximately ~20 m above ground level (AGL). In Chonburi, the pump was placed on 3rd floor of a research building, in Angsila Marine Animal Research Station at a height of ~20 m AGL. Thirty-seven aerosol samples from Bangkok and thirty-nine from Chonburi were packed in sterile petri dishes and stored in a desiccator after sampling. Three blank samples were collected by placing the Teflon filter in the filter cartridge and removed after ~5 min without turning on the pump. The blank filters were treated in the same way as the sample filters until further chemical analysis. The atmospheric circulation of Thailand is under the influence of the monsoon system, i.e. NE monsoon and SW monsoon. Hybrid Single Particle Lagrangian Integrated Trajectory Model (HYSPLIT) is used to compute 72 h backward air trajectory analysis to determine the origin of air masses at the two locations on the sampling days (Figure 3.1). The NE monsoon (mid-October to mid-February) transports aerosol from mainland China and upper South China Sea toward central Thailand. The SW monsoon (mid-May to mid-October) brings the air mass from the Indian Ocean. Inter-monsoon (mid-February to mid-May) is the transition period from NE monsoon to SW monsoon. The inter-monsoon wind originates over the South China Sea and blows towards Bangkok and Chonburi.
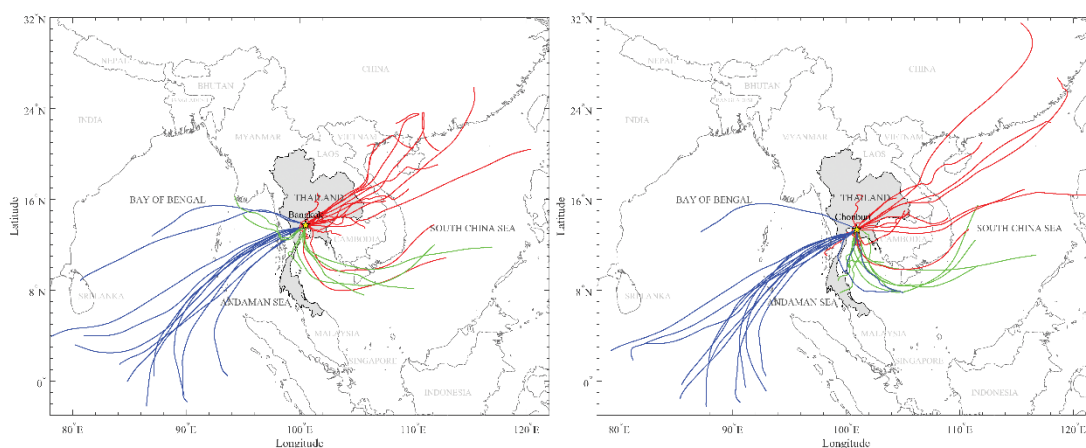
Figure 3.1 Backward wind trajectories for 72 h at 500 m above ground level (AGL) for the sampling days between January 2018 to April 2019 at Bangkok and Chonburi (red: NE monsoon, green: inter monsoon, and blue: SW monsoon). (For interpretation of the references to colour in this figure legend, the reader is referred to the Web version of this article.)

2.2 Metal analysis

Metal concentrations and Pb isotopic analysis were conducted in a class 1000 clean chemistry lab at the Earth Observatory of Singapore, Nanyang Technological University. All acids used for laboratory analysis were ultrapure grade from Seastar Chemicals and water used for dilution was ultrapure water with 18.2 MΩ cm resistivity (Super-Q, Merck Millipore). The PTFE filter samples (including blank filters) were cut into small sizes using a ceramic scissor and placed inside Savillex beakers. In between samples, the scissor was washed with methanol and ultrapure water to prevent any cross contamination. The filter papers were leached in 50% (v/v) of 3:1 HNO_3:HF mixture. The close capped Teflon beakers were sonicated at 60°C for 1 h and extracted at 150°C for 20 h. PTFE filters were removed from solution using a Teflon tweezer, washed with ultrapure water before discarding and the solution evaporated at 120°C till dryness. The metal extracts were re-dissolved in 2 mL of 7N HNO_3 several times to remove any traces of HF. Finally, the dried metal salts were dissolved in 2 mL of 2% HNO_3. Half of the solution was used for trace metal analysis and the other half was stored for Pb isotope analysis. For metal analysis, sixteen elements (e.g., Al, As, Ba, Ca,

Cd, Cu, Cr, Fe, Mg, Mn, Na, Ni, Pb, Sr, V, Zn) were determined using sectorfield ICP-MS (an Element 2 from Thermo Fisher Scientific). One ppb of Indium was added as an internal standard. Typical instrument sensitivity was about 1.8×10^6 cps/ppb for ^{115}In. Instrumental drift was resolved by a combination of internal Indium standard and external bracketing multi element standard from Inorganic Ventures (IV-ICPMS- 71A). Different mass resolution modes were used to optimize the separation of isotopes from interfering polyatomic species (e.g., ^{75}As from ^{40}Ar^{35}Cl) and improve detection limits. The final concentrations were blank corrected using the average blank filter concentrations that ranged from 1.3 to 3% of the average signal intensity of the samples. The extraction efficiency of all metals were >90% based on the analysis of SRM 2783 (urban particulate matter standard). The detection limit (LOD) of all metal analyte were calculated based on three times of the standard deviation (SD) of the blank. The value of LOD ranged from 0.0023 (Pb) to 2.2717 (Ca) ppb (n = 12). The details of the analytical techniques are given in (Kayee et al., 2020) and (Das et al., 2013).

2.3 Analysis of Pb isotope

The remaining half of the sample solutions (and blanks) were dried and dissolved in 1.1 N HBr before loading into the ion exchange column (Eichrom AG-1X8 chloride form, 200–400 mesh) for Pb separation. Then, 1.1 N HBr and 2 N HCl were used as mobile phase. Finally, the Pb sample was eluted with 6 N HCl and collected in Savillex beaker (Reuer et al., 2003). The collected solutions were evaporated at 90°C to dryness and re-dissolved with 2% ultrapure HNO_3. Pb isotope ratios were determined by Multi Collector ICP-MS (Neptune Plus from Thermo Fisher Scientific) adding thallium (Tl) as internal standard (White et al., 2000). The ^{203}Tl/^{205}Tl ratio of 0.418911 was used to correct for instrumental mass fractionation. The samples were measured at similar Pb/Tl ratios as the standards to prevent any analytical bias. ^{202}Hg signal was monitored to resolve the isobaric interference of ^{204}Hg on ^{204}Pb. The isotope ratios of NBS-981 Pb standard measured during the analytical sessions and the blank values are given in Table A-3 and Table A-4. The difference between the measured NBS-981 Pb isotope ratio during an analytical session and the true ratios as reported

by (Baker et al., 2004) were used to normalize the Pb isotope ratios of the measured samples (Das et al., 2018; Kayee et al., 2020).

3. Results and discussion

3.1 Particulate matter

$PM_{2.5}$ concentrations of Bangkok and Chonburi are taken from the Division of Air Quality Data, Air Quality and Noise Management Bureau, Pollution Control Department, Thailand. The statistical summary (mean, standard deviation and range) of $PM_{2.5}$ for the three seasons are given in Table 3.1. During all seasons, $PM_{2.5}$ in Bangkok was higher than Chonburi. $PM_{2.5}$ concentrations in Bangkok and Chonburi are highest during NE monsoon followed by inter monsoon and SW monsoon. Generally, anthropogenic emissions control $PM_{2.5}$ concentrations (Chen et al., 2020). The NE monsoon winds extensively travel over landmasses before reaching Bangkok and Chonburi. Hence $PM_{2.5}$ concentrations increases due to inputs from anthropogenic sources in addition to local pollution sources in Bangkok. Additionally, during NE monsoon season, low surface wind coupled with thermal inversion trap the aerosol over the ground surface. During the SW and inter monsoon, the winds originate over the ocean and are far less influenced by anthropogenic emission sources.

3.2 Metal concentrations

Sixteen metals were analyzed in this study. The statistical data of metal concentrations are shown in Table 3.1. Overall, the average metal concentrations in both locations followed similar trends, (Na, Ca, Fe, Al, Mg and Zn)> (As, Ba, Cr, Cu, Mn, Ni, Pb, Cd, Sr and V) in all the three seasons. Al, Fe, Ca, Mg and Mg are some of the most abundant elements in the Earth's crust (Rudnick and Gao, 2003). In addition to crustal dust, Na, Ca and Mg can also come from sea spray aerosols in the SW and inter monsoon winds. Zn is the most common anthropogenic metal and can be emitted from a variety of sources including road traffic, coal combustion and metal processing (Kravchenko and Lyerly, 2018; Žibret et al., 2013).

During the NE monsoon, concentrations of all the elements were higher in Chonburi compared to Bangkok, probably due to addition of local emissions from the metropolis over the long-range transported metals before the winds reached Chonburi. Na and Mg concentrations were higher in Chonburi during SW monsoon winds owing to the sea spray origin. Average Na concentration was highest (1846 ng/m^3) during the SW monsoon in the coastal town of Chonburi. Ca is comparable in both locations. Ca comes from sea spray, crustal dust and cement dust from construction sites. V, Ni, Cu concentrations are higher in Chonburi during the SW monsoon winds possibly due to presence of oil refineries south of the coastal town. The Pearson's correlation coefficient between the metals in two locations for the NE and SW monsoon winds are given in Table A-5, Table A-6, Table A-7 and Table A-8. In SW monsoon winds, V, Ni and Cu show moderately strong (r^2 from 0.61 to 0.74) inter-correlation indicating a common source.

The crustal Enrichment Factor (EF) defined by

EF = (metal/ref.metal)$_{aerosol}$/(metal/ref.metal)$_{crust}$ of Fe, Ca, Mg, when compared with Al as reference element showed values less than 10 for both locations in all seasons in spite of their high concentrations in the aerosol. Ideally, elements with crustal origin should have EF~1, however, EF of <10 is considered to have natural origin to account for the local variability of upper continental crust (UCC) composition which forms the immediate precursor of the aerosol metals. Average Zn concentrations in both the locations are high (range 26–171 ng/m^3) with very high EF (EF range 743–1871) indicative of anthropogenic sources. EF of Pb is > 100 in both locations with a similar trend of NE monsoon > inter monsoon > SW monsoon. Average concentrations of the remaining metals are less than 40 ng/m^3. However, Cd, As, Cu, Ni, Cr and V have high EF indicative of anthropogenic origin (Figure 3.2).

3.3 Pb concentrations and isotopic compositions

The Pb concentrations in Bangkok aerosols range from 1.1 to 46 ng/m^3 and those from Chonburi range from 0.29 to 46 ng/m^3. The lowest average Pb concentrations in Bangkok and Chonburi were recorded during the inter-monsoon followed by SW monsoon (Table 3.1). NE monsoon had the highest Pb concentrations in both locations owing to larger anthropogenic Pb input as compared to the SW and inter-monsoon winds, as the air mass mostly travelled over landmass.

The Pb isotopic composition has long been used as a "fingerprinting" tool to understand Pb sources as Pb isotopes do not fractionate in natural physical, chemical, and biological processes (Komárek et al., 2008). Pb isotope ratio of PM$_{2.5}$ over Bangkok and Chonburi are given in Table 3.2. The average ^{206}Pb/^{207}Pb ratios during NE monsoon (1.1519 ± 0.0056, 1SD, range 1.1462–1.1685) is higher than inter-monsoon (1.1467 ± 0.0062, 1SD, range 1.1343–1.1529) and SW monsoon (1.1474 ± 0.0047, 1SD, range 1.1382–1.1553) in Bangkok. In contrast, ^{206}Pb/^{207}Pb ratios at Chonburi during NE monsoon (1.1480 ± 0.0058, 1SD, range 1.1364–1.1603), is lower than inter-monsoon (1.1499 ± 0.0056, 1SD, 1.1377–1.1572), and SW monsoon (1.1526 ± 0.0038, 1SD, range 1.1448–1.1594) (Figure 3.3).

จุฬาลงกรณ์มหาวิทยาลัย
CHULALONGKORN UNIVERSITY
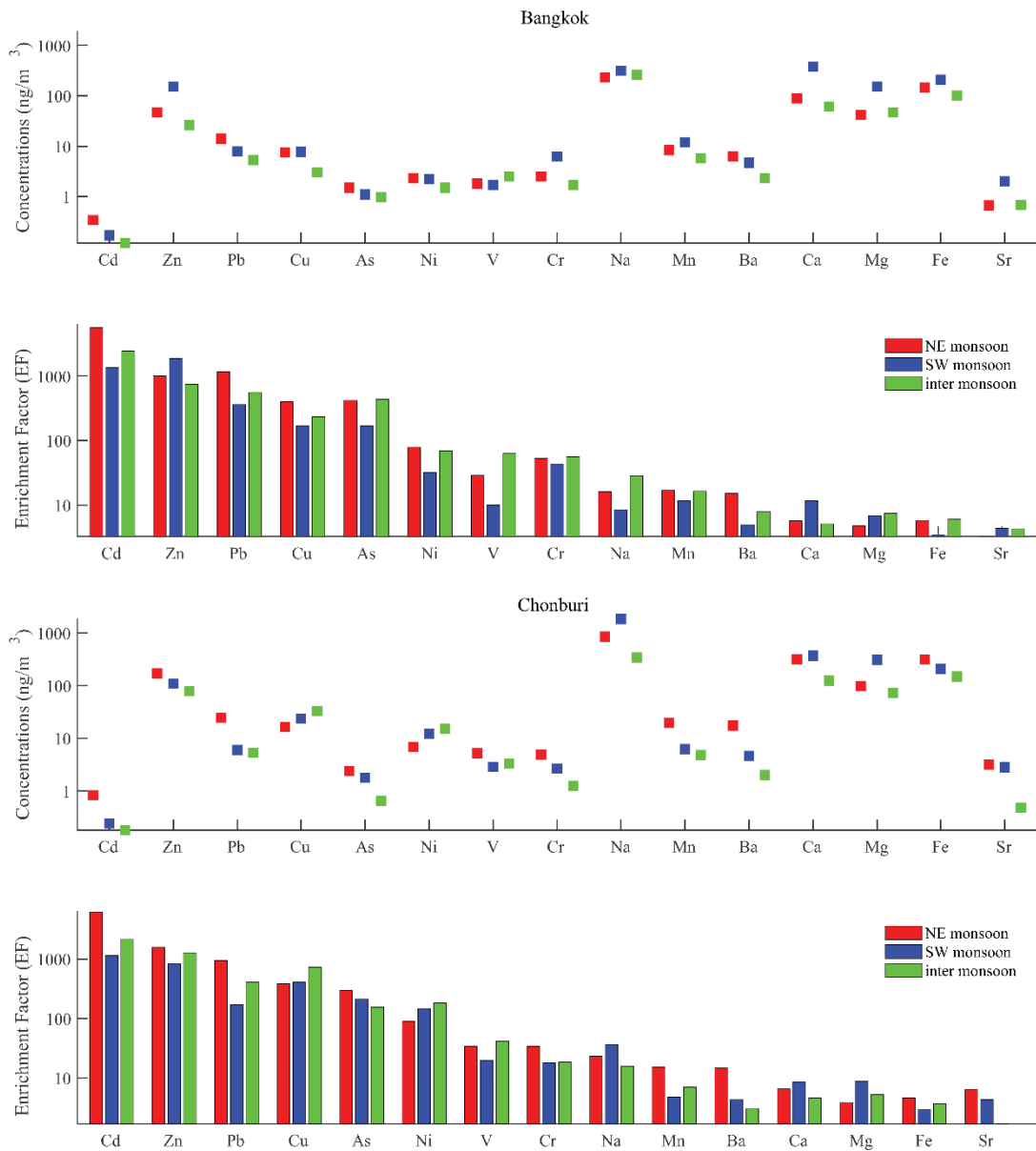
Figure 3.2 Average concentrations (squares) and Enrichment factors (EF) (bars) of metals from Bangkok and Chonburi for 3 seasons. EF is calculated using Al as reference element with respect to average upper continental crust (UCC) composition from Rudnick and Gao (2003) Metals with values of EFs < 10 have crustal sources, and those with values of EFs > 10 indicate anthropogenic influence

A time series plot of ^{206}Pb/^{207}Pb ratios and Pb concentration are shown in Figure 3.4. In Bangkok, average Pb concentration and isotope ratios were highest during the NE monsoon season but a weak negative correlation (r^2 = - 0.32) exists between the two. The SW and inter-monsoon aerosols do not show any significant correlation between Pb concentrations and isotope in Bangkok. In contrast, Chonburi aerosols show the lowest average value of ^{206}Pb/^{207}Pb during NE monsoon and a moderate positive correlation (r^2 = 0.50) with the Pb concentration. However, Pb concentration decreases with increasing ^{206}Pb/^{207}Pb ratios in Chonburi during SW (r^2 = - 0.50) and inter-monsoon (r^2 = - 0.75) winds.
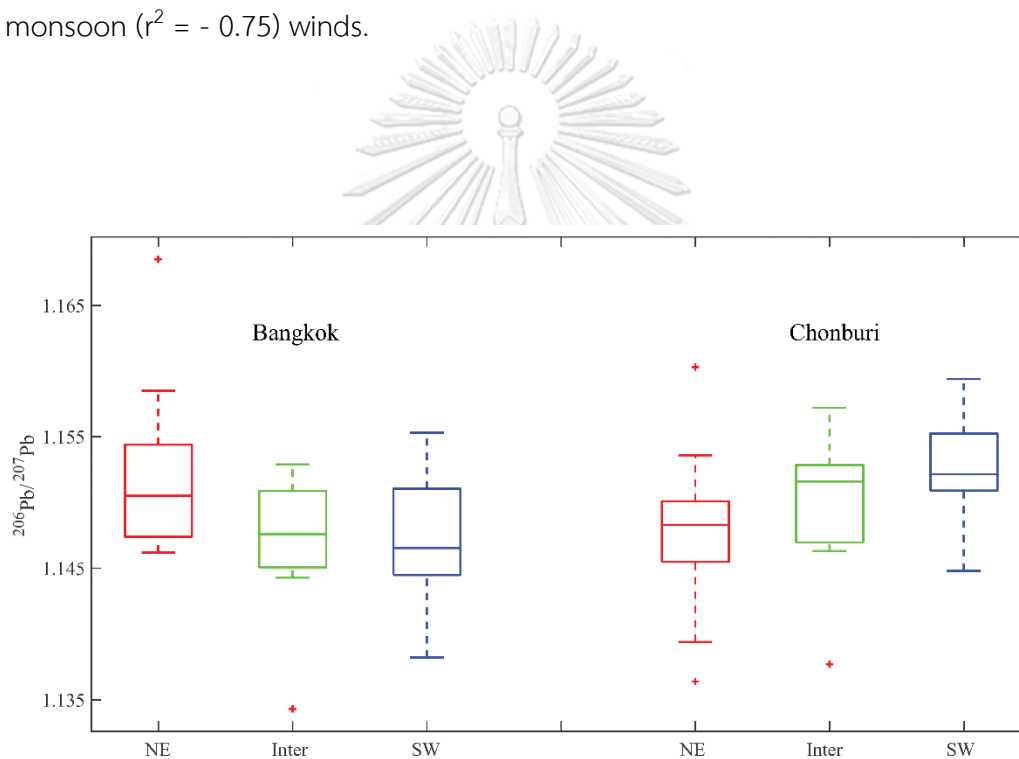
Figure 3.3 Box plot of ^{206}Pb/^{207}Pb ratios of PM$_{2.5}$ in Bangkok and Chonburi in 3 seasons

Table 3.1 The statistical summary of metal concentrations in ng/m^3 and PM$_{2.5}$ in µg/m^3

Location	Parameter	N	Al	As	Ba	Ca	Cd	Cr	Cu	Fe	Mg	Mn	Na	Ni	Pb	Sr	V	Zn	PM$_{2.5}$
Bangkok	**NE monsoon**	18																	
	Mean		52	1.5	6.3	88	0.34	2.5	7.5	145	42	8.4	234	2.3	14	0.67	1.8	47	124
	Min		19	0.2	1.6	48	0.05	0.73	2.2	61	24	3.6	104	0.64	1.1	0.25	0.32	4.8	80
	Max		103	4.7	17	173	0.82	7.1	18	274	83	19	682	12	46	1.5	5.5	153	177
	SD		19	1.4	3.7	31	0.22	1.8	4.4	68	15	4.7	143	2.7	13	0.38	1.4	40	33
	Inter-monsoon	7																	
	Mean		47	0.97	2.3	61	0.12	1.7	3.0	101	47	5.7	263	1.5	5.3	0.68	2.5	26	81
	Min		15	0.33	1.4	35	0.03	0.64	1.5	71	35	2.9	196	0.80	1.5	0.30	1.8	9.1	66
	Max		113	1.4	4.4	122	0.28	5.3	6.0	195	74	13	454	3.1	12	1.7	3.7	66	109
	SD		35	0.42	1.0	32	0.09	1.6	1.5	44	16	3.6	86	0.78	3.7	0.47	0.61	19	13
	SW monsoon	12																	
	Mean		138	1.1	4.7	375	0.17	6.2	7.7	209	153	12	311	2.2	7.9	2.0	1.7	152	65
	Min		50	0.28	2.2	55	0.04	1.0	2.9	122	43	4.3	85	0.84	3.2	N.D.	0.50	28	52
	Max		312	1.7	8.6	1684	0.39	41	32	407	468	31	538	9.1	11	6.5	6.3	517	78
	SD		77	0.47	1.9	602	0.11	11	7.9	86	121	8.3	153	2.4	3.1	1.8	1.6	169	10
Chonburi	**NE monsoon**	14																	
	Mean		146	2.4	17	315	0.83	4.9	17	314	99	20	848	6.8	24	3.1	5.2	171	96
	Min		73	0.57	4.1	100	0.21	1.0	7.7	121	53	7.3	332	2.0	7.3	0.69	0.74	21	56
	Max		366	5.0	129	1350	1.6	22	56	827	263	39	3793	39	46	18	15	770	162
	SD		79	1.5	32	328	0.45	5.3	12	180	52	10	943	9.6	12	4.5	4.3	212	36
	Inter-monsoon	9																	
	Mean		80	0.65	2.0	123	0.18	1.2	33	149	72	4.8	342	15	5.3	0.48	3.3	78	71
	Min		23	0.08	0.52	42	0.01	0.45	1.6	31	28	0.60	37	0.97	0.29	0.01	0.27	3.4	45
	Max		195	1.6	9.5	503	0.57	2.5	245	621	220	13	806	119	13	1.7	8.5	181	107
	SD		54	0.42	2.8	148	0.17	0.74	80	186	60	3.8	309	39	4.1	0.51	2.7	72	23
	SW monsoon	16																	
	Mean		150	1.8	4.6	370	0.24	2.7	24	207	307	6.2	1846	12	6.0	2.8	2.8	109	56
	Min		30	0.10	1.0	42	0.01	0.56	2.1	33	31	0.78	187	1.3	0.35	0.25	0.41	3.0	41
	Max		436	4.3	12	1116	0.93	7.7	100	540	1875	18	6436	26	19	8.4	8.2	347	69
	SD		126	1.5	3.5	327	0.30	2.1	26	165	449	5.8	2148	9.8	6.2	2.6	2.4	127	9.6

Table 3.2 Pb isotopic composition of $PM_{2.5}$

Location	Parameter	$^{206}Pb/^{204}Pb$	2se	$^{207}Pb/^{204}Pb$	2se	$^{208}Pb/^{204}Pb$	2se	$^{206}Pb/^{207}Pb$	2se	$^{208}Pb/^{207}Pb$	2se	Pb conc. (ng/m³)
Bangkok	**NE monsoon**											
	Mean	17.9641	0.0022	15.5917	0.0026	37.8544	0.0089	1.1519	0.0001	2.4298	0.0002	14
	Min	17.8573	0.0015	15.5758	0.0016	37.7331	0.0055	1.1462	0.0000	2.4244	0.0001	1.1
	Max	18.2626	0.0050	15.6254	0.0060	38.1744	0.0209	1.1685	0.0001	2.4450	0.0005	46
	SD	0.1016	0.0009	0.0127	0.0011	0.1143	0.0038	0.0056	0.0000	0.0054	0.0001	13
	Inter-monsoon											
	Mean	17.8763	0.0024	15.5862	0.0029	37.7773	0.0095	1.1467	0.0001	2.4258	0.0003	5.3
	Min	17.6562	0.0018	15.5617	0.0021	37.5332	0.0072	1.1343	0.0000	2.4138	0.0002	1.5
	Max	17.9914	0.0043	15.6025	0.0048	37.9378	0.0157	1.1529	0.0001	2.4337	0.0004	12
	SD	0.1105	0.0009	0.0136	0.0010	0.1295	0.0031	0.0062	0.0000	0.0064	0.0001	3.7
	SW monsoon											
	Mean	17.8775	0.0017	15.5769	0.0016	37.7330	0.0042	1.1474	0.0000	2.4224	0.0001	7.9
	Min	17.6990	0.0007	15.5496	0.0007	37.5337	0.0019	1.1382	0.0000	2.4138	0.0000	3.2
	Max	18.0565	0.0092	15.6458	0.0081	38.0096	0.0198	1.1553	0.0000	2.4308	0.0001	11
	SD	0.1003	0.0024	0.0252	0.0021	0.1228	0.0050	0.0047	0.0000	0.0047	0.0000	3.1
Chonburi	**NE monsoon**											
	Mean	17.8893	0.0025	15.5805	0.0028	37.7873	0.0095	1.1480	0.0001	2.4269	0.0003	24
	Min	17.6847	0.0007	15.5313	0.0008	37.5455	0.0022	1.1364	0.0000	2.4153	0.0001	7.3
	Max	18.1328	0.0043	15.6258	0.0049	38.1640	0.0168	1.1603	0.0001	2.4445	0.0005	46
	SD	0.1085	0.0009	0.0236	0.0011	0.1488	0.0042	0.0058	0.0000	0.0069	0.0001	12
	Inter-monsoon											
	Mean	17.8929	0.0027	15.5595	0.0025	37.7324	0.0064	1.1499	0.0000	2.4254	0.0001	5.3
	Min	17.7461	0.0014	15.5286	0.0012	37.6678	0.0033	1.1377	0.0000	2.4204	0.0000	0.29
	Max	18.0273	0.0038	15.5933	0.0035	37.8604	0.0086	1.1572	0.0000	2.4301	0.0002	13
	SD	0.0749	0.0009	0.0210	0.0007	0.0578	0.0017	0.0056	0.0000	0.0027	0.0000	4.1
	SW monsoon											
	Mean	17.9592	0.0010	15.5812	0.0010	37.8488	0.0026	1.1526	0.0000	2.4292	0.0001	6.0
	Min	17.8101	0.0003	15.5528	0.0003	37.6469	0.0008	1.1448	0.0000	2.4199	0.0000	0.35
	Max	18.0886	0.0031	15.6058	0.0026	37.9975	0.0066	1.1594	0.0000	2.4352	0.0001	19
	SD	0.0727	0.0006	0.0154	0.0005	0.1008	0.0013	0.0038	0.0000	0.0048	0.0000	6.2

Table 3.3 ^{206}Pb/^{207}Pb ratio of aerosol from this study compared with plausible anthropogenic and natural end members from the region

Location	Materials	^{206}/^{207} Pb		Reference
		Mean±1SD	Range	
Thailand (Bangkok)	Atmospheric aerosol	1.1494 ± 0.006	1.1343–1.1685	This study
Thailand (Chonburi)	Atmospheric aerosol	1.1503 ± 0.005	1.1364–1.1603	This study
Thailand (Bangkok)	Atmospheric aerosol	1.127 ± 0.001	1.091–1.155	Bollhöfer & Rosman (2000)
China (Shanghai)	Unleaded gasoline exhaust	1.1468 ± 0.004	1.1377–1.1601	Chen et al. (2005)
China (Shanghai)	Oil combustion	1.1507 ± 0.003	1.1468–1.1547	Chen et al. (2005)
Vietnam (Haiphong)	Oil combustion	1.1530 ± 0.005	1.1456–1.1577	Chifflet et al. (2018)
Taiwan (Taipei)	Oil combustion	1.1468 ± 0.003	1.1416–1.1507	Yao et al (2015)
China	Coal	1.1628 ± 0.010	1.1403–1.2077	Chen et al. (2005)
China	Coal	1.1926 ± 0.029	1.1546–1.2438	Chifflet et al. (2018)
India	Coal	1.2090 ± 0.006	1.2027–1.2180	Das et al. (2018)
Australia	Coal	1.2055	1.2053–1.2057	Díaz-Somoano et al. (2009)
Indonesia	Coal	1.1835 ± 0.004	1.1803–1.1881	Díaz-Somoano et al. (2009)
Vietnam	Coal	1.1768 ± 0.020	1.1494–1.1950	Chifflet et al. (2018)
Southeast Asia	River sediment	1.1934 ± 0.010	1.1818–1.2027	Millot et al. (2004)
South China Sea	Sediment	1.2077 ± 0.001	1.2062–1.2092	Zhu et al., 2003
India	Ores	1.0700 ± 0.037	1.0354–1.1138	Sangster et al. (2000)
Australia	Ores	1.1120 ± 0.078	1.0313–1.2257	Sangster et al. (2000)
China	Ores	1.1102 ± 0.060	1.0259–1.1905	Chifflet et al. (2018) and Sangster et al. (2000)

3.4 Isotopic composition of anthropogenic Pb

The three major anthropogenic sources of atmospheric Pb are coal combustion, ore processing and vehicle exhaust (Komárek et al., 2008). In some countries, it was reported that recirculation of historic Pb from leaded gasoline exhaust accounted for a major source (Flegal et al., 2010) (Morton-Bermea et al., 2011). However, as Thailand was one of the first countries in Southeast Asia to completely phase out leaded gasoline by 1994, it is unlikely that historic Pb is still recirculating in the atmosphere after ~25 years. Present-day traffic emissions from unleaded gasoline and diesel can be an important source of atmospheric Pb (Gioia et al., 2017). Since phasing out of leaded gasoline, Pb content has significantly reduced in petroleum fuel. However, the ever-increasing vehicular traffic on roads in developing countries of south and Southeast Asia can still contribute a significant quantity of Pb to the atmosphere. For example, vehicle exhausts from unleaded gasoline in Shanghai emitted 217 μg of Pb per gm of exhaust particles (Chen et al., 2005). The $^{206}Pb/^{207}Pb$ ratios in aerosol obtained from this study is compared with the anthropogenic end members from the region and natural background (Table 3.3). The $^{206}Pb/^{207}Pb$ ratios in the Thai aerosol ranged from 1.1343 to 1.1685 which overlaps with the $^{206}Pb/^{207}Pb$ ratios of the unleaded petroleum fuel from the region (Chen et al., 2005; Chifflet et al., 2018; Yao et al., 2015). Yao et al. (2015) measured gasoline and diesel used in Taipei and concluded that Pb isotopic ratios of vehicle exhaust have a considerable overlap with the reported aerosol data from Taiwan. Similar Pb isotope ratios were obtained from unleaded gasoline exhaust and oil combustion from Shanghai (Chen et al., 2005) and Vietnam (Chifflet et al., 2018) (Table 3.3). Though the oil combustion Pb isotope ratios have a considerable overlap with the ratios measured in Bangkok and Chonburi, some of the aerosol ratios are outside the range reported for gasoline exhaust in the region.

High radiogenic mixing endmembers such as coal and/or crustal dust can explain the radiogenic aerosol ratios ($^{206}Pb/^{207}Pb \geq 1.16$). In the region, the largest consumer of coal is China followed by India, Australia, Indonesia and Vietnam (Lee et al., 2014). Indian and Australian coal have similar Pb isotopic composition close to the crustal ratios of $^{206}Pb/^{207}Pb = 1.20$ (Das et al., 2018; Díaz-Somoano et al., 2009).

Indonesian and Vietnamese coal have lower average of ^{206}Pb/^{207}Pb ratios (Table 3.3). In contrast, Chinese coal has a large variation of ^{206}Pb/^{207}Pb ratios (Chifflet et al., 2018; Díaz-Somoano et al., 2009). The NE monsoon winds blowing from mainland China can transport Pb from Chinese and Vietnamese coal combustion emissions whereas Indian and Indonesian coal combustion emission can be significant sources for the SW monsoon wind. The natural background of Pb in atmospheric aerosol comes from crustal dust. The ^{206}Pb/^{207}Pb ratio of average UCC is 1.20 (Millot et al., 2004). However, there might be slight regional variation. Southeast Asian river sediments from large river deltas such as Salween, Brahmaputra, Mekong and the South China Sea sediments represent large-scale integrated weathering products of the present-day UCC from Southeast Asia. The ^{206}Pb/^{207}Pb ratio of the Asian rivers and South China Sea sediments vary between 1.1818 and 1.2092. Though the ^{206}Pb/^{207}Pb ratios of the natural background are higher than any of the observed ratios from Bangkok and Chonburi, it can form one of the radiogenic mixing end members for atmospheric Pb.

Base metal ore deposits are low in radiogenic Pb. In the region, Pb–Zn ores have a wide range of Pb isotopic composition (Table 3.3 and Figure 3.5). Chinese Pb ores are characterized by high ^{232}Th and hence higher ^{208}Pb/^{207}Pb compared to the other ores from the region (Chifflet et al., 2018; Sangster et al., 2000). Though the average ^{206}Pb/^{207}Pb of ores are much lower than the lowest ^{206}Pb/^{207}Pb ratio measured in this study, ores can form the low end member of mixing.
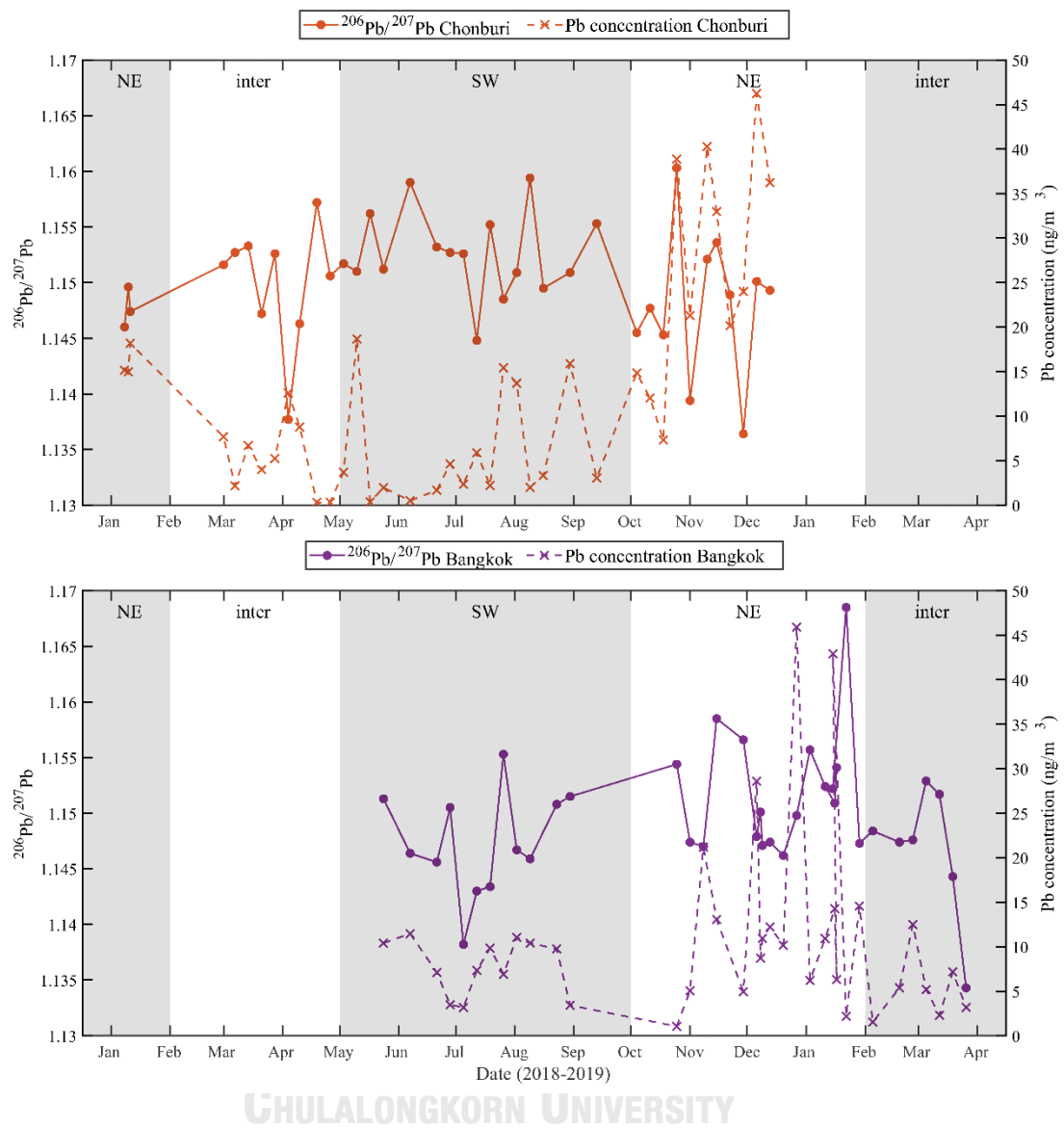
Figure 3.4 Time series plot of Pb concentration and ^{206}Pb/^{207}Pb ratios in Chonburi and Bangkok
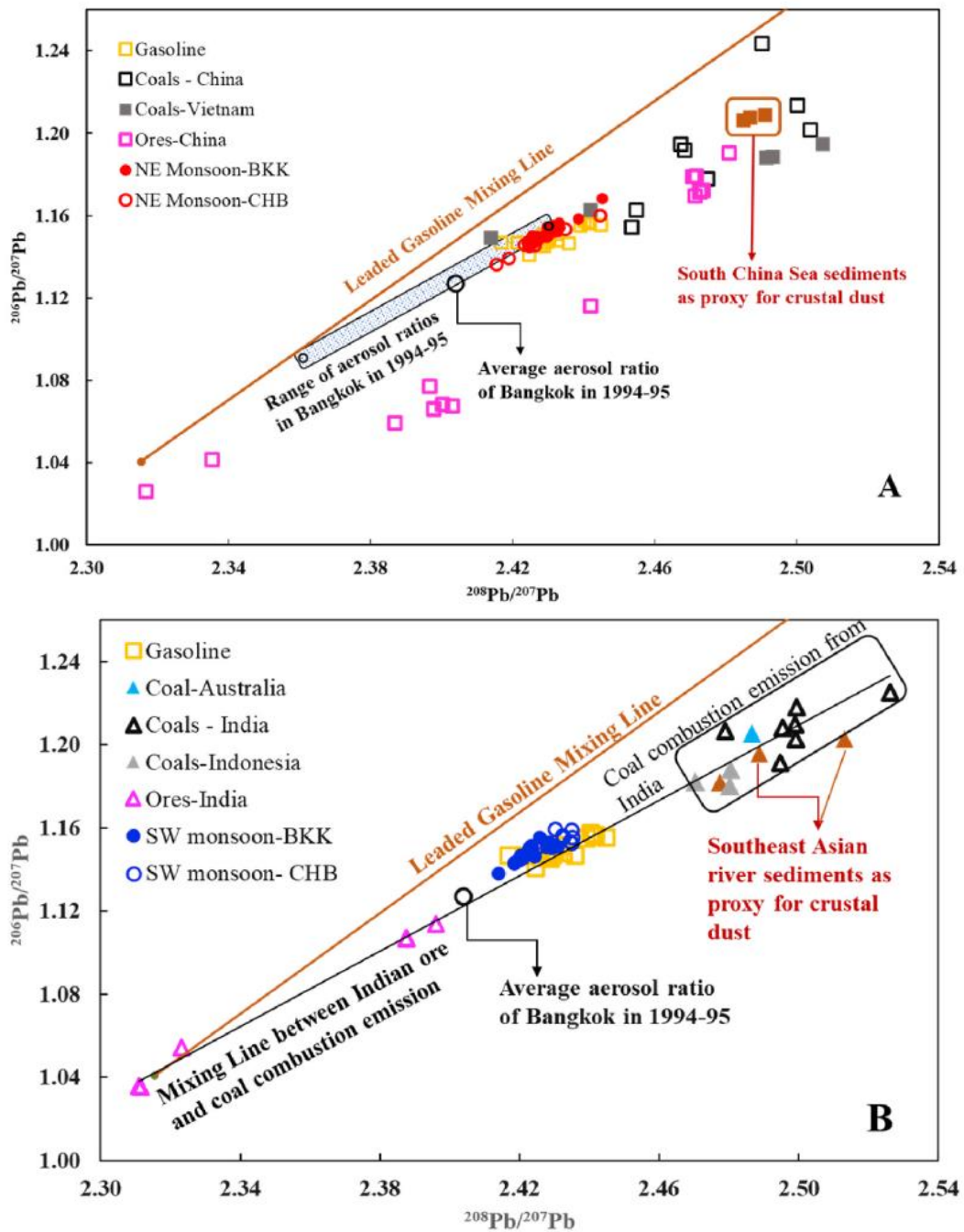
Figure 3.5 Pb triple isotope plot of aerosols during A) NE monsoon wind and B) SW monsoon wind along with the plausible anthropogenic and natural end members. The anthropogenic and natural end member composition are taken from references mentioned in Table 3.3

3.5 Sources of anthropogenic Pb in the Thai aerosols

The plausible anthropogenic end member isotope ratios indicate that present-day atmospheric Pb in Thailand can either be sourced from the vehicular exhaust and/or result from mixing between coal combustion emission and high-temperature metallurgical activities over the natural background. To further ascertain specific sources, we combine trace metal ratios with Pb isotopes, as different anthropogenic emission sources and natural background have distinctive trace metal signatures.

3.5.1   NE monsoon winds

The NE monsoon winds blow from over mainland China, northern Vietnam, Laos and northeast Thailand before reaching Bangkok and Chonburi (Figure 3.1). The possible anthropogenic contributors of Pb during NE monsoon could be coal combustion from Vietnam and China in addition to the natural background. From the triple isotope plot (Figure 3.5a), the linear trend of Pb–Zn ore from China does not overlap with the Pb isotope ratios and seems to be less likely to contribute towards aerosol Pb. Al/Pb ratios have been used by previous studies (Kayee et al., 2020; Millot et al., 2004) to trace crustal contributions. Al is the third most abundant element in the crust. Al/Pb ratios of Bangkok aerosols show good correlation with ^{206}Pb/^{207}Pb (r^2 = 0.63) indicating at least part of the Pb is from natural crustal dust (Table A-9). In Bangkok Pb, Zn, As and Cd strongly correlate with each other (r^2 from 0.72 to 0.94) and in Chonburi, Pb shows moderate to strong correlation with As (r^2 = 0.58) and Cd (r^2 = 0.72). Coal ash is a significant source of As, Cd, Zn and Pb emissions (Pacyna et al., 2009; Zhou et al., 2015). Pb isotopes of Vietnamese coal also overlap with the aerosol isotopes (Table A-5 and Table A-6). V/Pb ratios have often been used to distinguish between coal combustion emission (V/Pb > 1), traffic emission (V/Pb < 1) and industrial sources (V/Pb << 1) (Srinivasa Gowd et al., 2010). The Pb isotopes not only overlap the field for unleaded gasoline exhaust emission, but most of the aerosols also have Pb/V ratios of <1 in both the locations indicating traffic emission source for V and Pb. Average Pb/V ratio in Bangkok is 0.20 ± 0.26 and that in Chonburi is 0.26 ± 0.21. V and Pb (r^2 = 0.65) also correlates well in Bangkok. Hence the Pb sources of NE monsoon winds are

a mixture crustal dust with coal combustion emissions from Vietnam, China and unleaded gasoline/diesel exhaust.

3.5.2 SW monsoon winds

The SW monsoon winds blow from over the Indian Ocean and parts of Thailand before reaching Chonburi then to Bangkok (Figure 3.1). Hence, the possible significant regional anthropogenic Pb sources are emissions from India and Indonesia. Indian ores are much less radiogenic and coal from India and Indonesia are more radiogenic than the aerosols (Figure 3.5b). As India imports coal from Indonesia and Australia, Pb isotopes of Indian coal combustion emission is far from unique. During SW monsoon, aerosol Pb falls on the mixing line defined by the Indian ores, Indian, Australian and Indonesian coal and river sediments. The aerosols also overlap the field for gasoline exhaust like the NE monsoon winds. Pb correlates strongly with crustal elements such as Al (r^2 = 0.81) and Fe (r^2 = 0.90) at Chonburi. Al/Pb ratio also positively correlates with $^{206}Pb/^{207}Pb$ (r^2 = 0.61). However, after reaching Bangkok these correlations no longer exist possibly owing to mixing of local anthropogenic polluting sources. Hence crustal dust is a significant Pb source for the SW monsoon winds (Table A-7, Table A-8 and Table A-9).

Pb correlates well with As, Cd in both cities indicating coal combustion as contributors of atmospheric Pb (Cui et al., 2019; Deng et al., 2014; Pacyna et al., 2009). Pb also correlated strongly with Zn in both cities (but Zn does not correlate with As and Cd) indicating Pb–Zn ore processing as a significant source of Pb. In Chonburi, the SW monsoon winds have average V/Pb ratios of 0.94 ± 0.92 and in Bangkok 0.30 ± 0.48 indicating oil combustion as an important source of Pb. In Chonburi, V/Pb ratios exceed 1 for several days as is expected from coal combustion emissions. V/Pb ratios also positively correlate well with $^{206}Pb/^{207}Pb$ (r^2 = 0.67) in Chonburi indicating higher $^{206}Pb/^{207}Pb$ are possibly influenced by coal combustion emissions (Table A-9). In Chonburi Ni (r^2 = 0.61) and V (r^2 = 0.63), that are indicators of oil combustion, correlates well with Pb. The Ni, V can come either from road traffic of the oil refinery situated south of Chonburi. These correlations are not observed in Bangkok possibly due to mixing of local pollution sources of V and Ni. Overall Pb sources in the SW monsoon

winds are influenced by long-range transport of coal combustion emissions and ore processing and mixing with road traffic emissions in addition to the natural background. When the SW monsoon winds reach Bangkok, local pollution sources become significant contributors of aerosol Pb.

3.5.3   Inter monsoon winds

During the inter-monsoon season, majority of the air masses originate in the South China Sea and touches the southern tip of Vietnam before reaching Chonburi and Bangkok. There are several chemical similarities of the aerosols in the inter monsoon winds with the SW monsoon winds. $^{206}Pb/^{207}Pb$ ratios correlates well with Al/Pb ratios (r^2 = 0.53) in Chonburi indicating influence of natural background. Moderate to strong correlation of Pb with As, Cd, Zn indicates coal combustion and Pb–Zn ores as plausible sources of Pb. V/Pb ratios are <1 for the majority of the sampling days with several of the ratios exceeding 1.

3.6 Evolution of atmospheric Pb sources in Thailand in a quarter century

A year after phasing out of leaded gasoline from Thailand, Bollhöfer and Rosman (2000) measured Pb isotopic composition in Bangkok aerosol collected during the NE monsoon season (December 1994 to January 1995). The $^{206}Pb/^{207}Pb$ ratio ranged from 1.091 to 1.155, with an average of 1.127 ± 0.001 (Figure 3.5a). Average Pb concentration was 74 ± 5 ng/m^3. As the $^{208}Pb/^{207}Pb$ were slightly elevated compared to the leaded gasoline ratios it was interpreted to have been influenced by Chinese type Pb ores which are enriched in ^{208}Pb. Another possible source was suggested to be the influence of ^{232}Th rich material typically from soils, fly ash or coal burning. After 25 years, the average Pb concentrations in the NE monsoon winds have significantly decreased in Bangkok aerosol. The average and range of $^{206}Pb/^{207}Pb$ ratios in Bangkok and Chonburi increased for all three seasons possibly due to influence of coal combustion emission but still falls on the same trend line as measured by Bollhöfer and Rosman (Figure 3.5). Unleaded gasoline and diesel exhaust influence present day atmospheric Pb in Thailand as evident from a significant overlap in the isotope ratios.

4. Conclusions

Bangkok's population almost doubled in the last 25 years turning into a megacity with a current population of ~10.5 million. To keep pace with the growing population, road traffic in and around the city have increased at a rapid pace. As of 2018, there are approximately 9.7 million automobiles and motorbikes registered in Bangkok. Immediately after phasing out of leaded gasoline in 1994 from Thailand, the primary contributors of atmospheric Pb were leaded gasoline exhaust particles that were recirculating in the environment and high-temperature metallurgical processes that used Chinese Pb ores (Bollhöfer and Rosman, 2000). In the following 25 years, the atmospheric Pb sources evolved. Unleaded gasoline exhaust that still contains traces of Pb has become a significant source of atmospheric Pb is Bangkok and Chonburi. However, in absence of time series data of Pb concentration and/or isotope in Thailand, it is difficult to ascertain the precise timeline when this source shift occurred. Majority of the aerosol Pb isotopes measured in all the three seasons in both the locations overlaps with the unleaded gasoline and diesel exhaust reported from Taiwan, Vietnam and China. Trace element systematics and Pb isotopes of plausible end members indicates that the NE monsoon winds are influenced by long-range transport of coal combustion emissions from China and Vietnam and natural background of crustal soil dust. Pb concentrations in SW and Inter monsoon winds are less than the NE monsoon winds and contributed by natural background, gasoline exhaust and long-range transport of coal combustion and ore processing Pb from India and Indonesia. Future studies intend to focus on quantifying Pb emissions and isotope ratios from fuels (unleaded gasoline and diesel) used in Thailand to better understand the significance of traffic emission sources on atmospheric Pb in a country marred by the ever-increasing road traffic.

Acknowledgements

.

CHAPTER 4

Distribution and chemical composition of atmospheric aerosols over Thai waters during 2018 Southwest monsoon

Jariya Kayee[1], Sujaree Bureekul[1,2,*], Reshmi Das[3,4], Xianfeng Wang[4,5], Sukchai Arnupapboon[6], Penjai Sompongchaiyakul[1,2,*]

[1] Department of Marine Science, Faculty of Science, Chulalongkorn University, Bangkok, Thailand

[2] Center of Excellence on Hazardous Substance Management, Chulalongkorn University, Bangkok, Thailand

[3] School of Environmental Studies, Jadavpur University, Kolkata, India

[4] Earth Observatory of Singapore, Nanyang Technological University, Singapore

[5] Asian School of the Environment, Nanyang Technological University, Singapore

[6] Southeast Asian Fisheries Development Center/Training Department (SEAFDEC/TD), Thailand

*Corresponding author: bsujaree@gmail.com

*Corresponding author: spenjai@hotmail.com

Keyword: Andaman Sea, Gulf of Thailand, Trace metals, Water-soluble inorganic ions

Draft manuscript
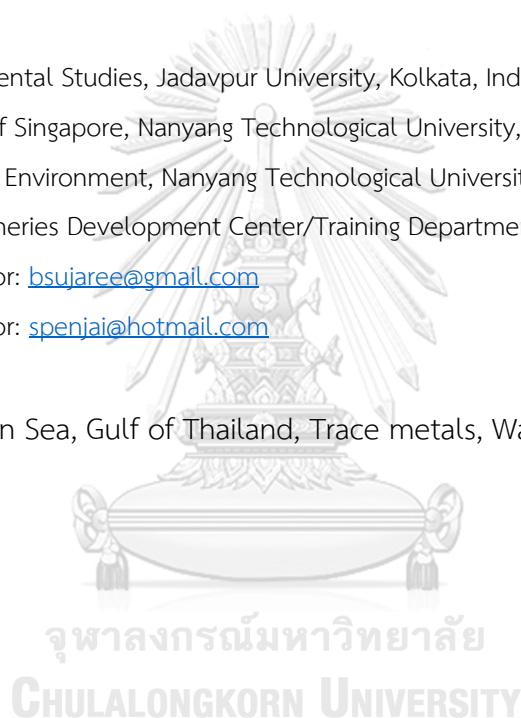
Abstract

The aerosols were collected over Thai waters during SW monsoon on board of M.V. SEAFDEC-2 (18th August to 18th October 2018) and R.V. Dr. Fridtjof Nansen (1st to 15th October 2018) in the Gulf of Thailand (GoT) and the Andaman Sea, respectively. $PM_{10-2.5}$ and $PM_{2.5}$ samples were collected in the GoT, while only $PM_{2.5}$ was collected in Andaman Sea. To investigate the distribution and chemical composition of atmospheric aerosol over Thai waters, the water-soluble inorganic ions and metal concentrations were determined. The results indicated the composition of both $PM_{10-2.5}$ and $PM_{2.5}$ were dominated by sea spray aerosols, especially $PM_{10-2.5}$. Near-shore aerosols, both $PM_{10-2.5}$ and $PM_{2.5}$, have shown signals of the continent sources. Anthropogenic activities also had an impact on these near-shore samples.

1. Introduction

Atmospheric particulate matter (PM) or aerosols refer to the mixture of solid particles and liquid droplets suspended in the air. Its present in the atmosphere has both direct (scattering and absorbing radiation) and indirect (influencing the droplet size distribution and albedo of marine boundary layer clouds) effects on climate variability. Based on particle size, PM is separated into two main groups; coarse particles ($PM_{10-2.5}$) having an aerodynamic diameter ranging from 2.5 to 10 μm and fine particles ($PM_{2.5}$) or smaller airborne particle having diameter less than 2.5 μm. These distinguished particle sizes differentiate due to its formation process and origins. Where coarse particles are mainly from natural processes such as crustal dust, volcanic debris, biogenic aerosol and sea spray (Prospero et al., 1983), fine mode mostly generated from anthropogenic activities such as industrial processes, vehicular emission, fossil fuels combustion, biomass burning, and high-temperature incineration processes. Originally, atmospheric particles emitted directly from sources into atmosphere are called "primary aerosols" while the secondary aerosols are those particles generated from gaseous molecules of natural or anthropogenic via particle conversion through heterogeneous chemical reactions (Jang and Kamens, 2001). The atmospheric lifetimes of aerosols are in the order of days to weeks and can travel a longer distance to other

areas (Duce et al., 1991) before removal via both wet and dry deposition processes (Arimoto et al., 1985; Majumdar et al., 2020).

Marine aerosols consider as one of the most important pathways for trace nutrients and metals inputs into the ocean(Mahowald et al., 2018). It defined for all various atmospheric particles found over the ocean varying in its chemical compositions including particles generated at sea surface as well as those chemically formed by atmospheric reaction after emitting from the sea. Also, the terrestrial aerosols that travel via long-distance transport (Saltzman, 2009). Under clean marine environment, sea salt ions such as Cl^-, Na^+, SO_4^{2-}, Mg^{2+}, Ca^{2+} and K^+ contribute significantly to the marine aerosol mass (Pósfai et al., 1995). However, aerosols originated from continental sources both natural and anthropogenic inputs may contribute to the changes in aerosol concentration mass, especially for NO^{3-}, SO_4^{2-}, Mg^{2+}, Ca^{2+} and trace metal composition (Duce et al., 2008; Xiao et al., 2018). Specifically, atmospheric deposition of leachable metals play an important role for supplying deficit micronutrients such as Fe, Zn, Mn, Ni, Cu and Co (Lohan and Tagliabue, 2018) to many oceans area and act as growth-limiting nutrient in the high nitrate low chlorophyll (HNLC) regions (Mahowald et al., 2008). Nevertheless, surplus of some trace metals such as Cu can be toxic at higher concentration and can restrains biological productivity to some plankton (Jordi et al., 2012). The inputs of micronutrient and trace metals originated from the terrestrial source via atmospheric deposition may even contribute to promote the higher productivity in Thai waters.

Nevertheless, none of the studies investigated chemical composition in atmospheric aerosol over Thai waters. Since, atmospheric inputs and circulation in Thailand is under the influence of the northeast and southwest monsoon. It can change chemical composition of marine aerosols over Thai waters seasonally. During northeast monsoon, aerosols transport from East-Asia continent toward this region, while in the southwest monsoon, marine aerosol from the Indian Ocean is brought by. Laterally, marine aerosol over the Thai waters is mixed with aerosol ejected from the local activities along the shoreline. Thus, this research focuses on the chemical composition of marine aerosol observed over the Thai waters during southwest

monsoon in 2018 over the Gulf of Thailand (GoT) by M.V. SEAFDEC2 and over Andaman Sea by R.V. Dr. Fridtjof Nansen research cruise to investigate the distribution and chemical composition of atmospheric aerosols. Atmospheric concentrations of sixteen metals (e.g., Al, As, Ba, Ca, Cd, Cu, Cr, Fe, Mg, Mn, Na, Ni, Pb, Sr, V and Zn) and water-soluble ions (e.g., Na^+, NH_4^+, K^+, Mg^{2+}, Ca^{2+}, Cl^-, NO_3^- and SO_4^{2-}) were analyzed in both coarse ($PM_{10-2.5}$) and fine ($PM_{2.5}$) particles. For Andaman Sea, the samples were determined only fine particles. Backward trajectories of the air masses were determined in conjunction with the enrichment factors (EF) to identify potential sources of atmospheric aerosols observed over the GOT during southwest monsoon.

2. Methods

2.1 Sample collection

Atmospheric aerosols were collected in the southwest monsoon by 2 cruises 1) over the GoT during 18th August to 18th October 2018 by M.V. SEAFDEC2 at a height of ~10 m above sea surface 2) over Andaman Sea during 1st to 15th October 2018 by R.V. Dr.Fridtjof Nansen, approx. 22 m above sea surface. The cruise track and sampling information are shown in Figure 4.1 and Table 4.1. Aerosol samples were collected on 47 mm PTFE filters with personal modular impactor (PMI, SKC Inc., USA) connected to air sampling pump (Gilian, AirCon-2) at flow rate 15 L/min. The sampler was operated during ship cruising to avoid the contamination from ship exhaust.

Before collecting the samples, the Teflon filters were cleaned with 1N HCl at 140°C for 2 hours, washed in Milli-Q water several times and dried in laminar flow hood for a few days. After collection, the filter samples were immediately sealed in the sterile Petri dishes, Ziploc bag and stored at -4°C until further chemical analysis. Field blanks were collected by placing the Teflon filter in the filter cartridge without running the pump and the filter was removed after ~3 min, approximately the time taken to change the sample filters to ascertain any contamination associated with handling and storage. The blank filters were stored in the same way as the sample filters.
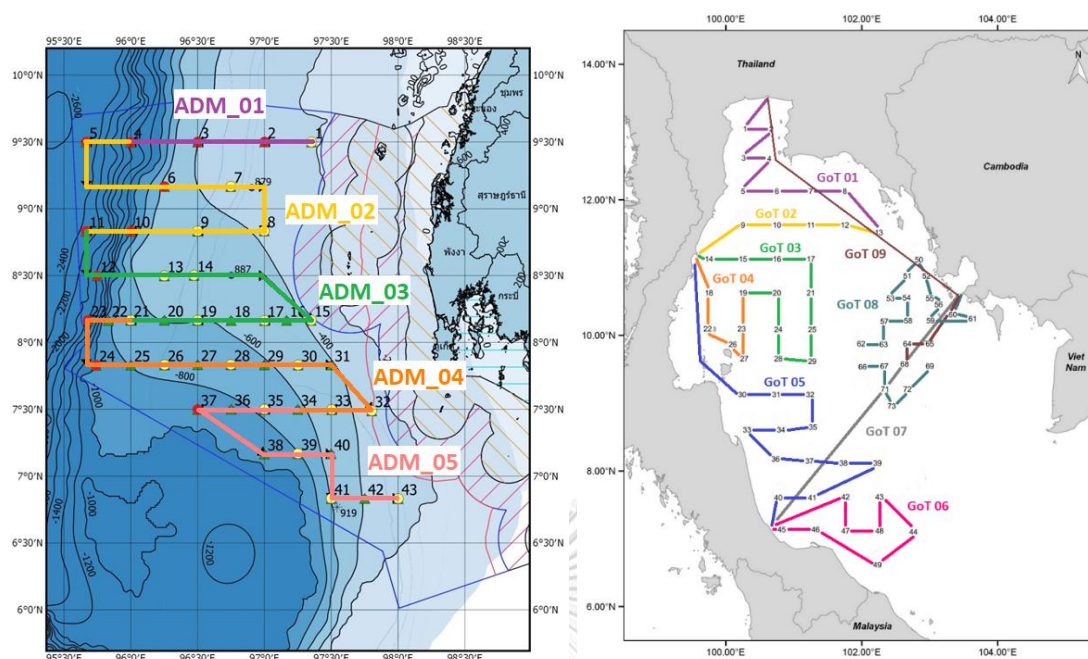
Figure 4.1 Survey map for aerosols collection over Thai water during SW monsoon (Left) on R.V. Dr. Fridtjof Nansen in Andaman Sea and (Right) on board of M.V. SEAFDEC-2 in the Gulf of Thailand. Color on cruise track mark different Aerosol samples

Table 4.1 Sampling information, including wind speed (WS), air temperature (AT), air pressure (AP) and relative humidity (RH)

Sample no.	End Date	End Location	WS (m/s)	AT (°C)	AP (hPa)	RH (%)	Sampling area
GoT_01	21/08/2018	11.77°N, 102.31°E	6.03	28.1	1010	90.9	Upper Gulf of Thailand
GoT_02	23/08/2018	11.42°N, 99.79°E	5.36	28.9	1012	89.0	Upper Gulf of Thailand
GoT_03	31/08/2018	10.98°N, 100.27°E	5.53	28.8	1014	86.6	Eastern Gulf of Thailand
GoT_04	03/09/2018	11.22°N, 99.56°E	5.21	29.1	1015	82.4	Eastern Gulf of Thailand
GoT_05	12/09/2018	7.75°N, 100.86°E	4.58	29.2	1015	85.0	Central Gulf of Thailand
GoT_06	20/09/2018	7.49°N, 100.79°E	4.94	28.3	1014	88.3	Southern Gulf of Thailan
GoT_07	27/09/2018	10.76°N, 103.57°E	-	-	-	-	Songkhla to Cambodia
GoT_08	10/10/2018	9.79°N, 103.19°E	2.61	28.6	1015	88.3	Waters of Cambodia
GoT_09	11/10/2018	13.57 N, 100.58 E	-	-	-	-	Cambodia to Chao Phra

2.2 Chemical analysis

2.2.1 Water-soluble ion analysis

Half of filter samples were cut into a small size using a ceramic scissor and place in the centrifuge tube. Between filters, the scissor was washed with Milli-Q water several times to avoid contamination. Five milliliters of Milli-Q water were added in centrifuge tube. The close capped centrifuge tubes were sonicated at room temperature for 1 h to desorb and agitate the particles effectively. PTFE filters were removed from solution using a Teflon tweezer. Then, the solution was filtered through 0.22 µm filter prior to analyze the water-soluble ions by Ion Chromatography (IC, ICS-2500, DIONEX). Three anions (e.g., Cl^-, NO^{3-}, SO_4^{2-}) were analyzed using column (4x250 mm, Dionex™ IonPac™ AS19, USA) and eluent with 10 mM KOH at flow rate of 1.10 mL/min. Five cations (e.g., Na^+, NH_4^+, K^+, Mg^{2+}, Ca^{2+}) were analyzed using cation-exchange columns (4x250 mm, Dionex™ IonPac™ CS12A) in conductivity mode and eluent with 11 mM H_2SO_4 at flow rate of 1.00 mL/min.

2.2.2 Metal analysis

The other half of filters were brought to the Earth Observatory of Singapore where all the chemical analyses were conducted in a class 1000 clean chemistry lab. Sample preparation and the details of the analytical techniques are following the methods described in (Das et al., 2015; Kayee et al., 2020). Sixteen metals (e.g., Al, As, Ba, Ca, Cd, Cu, Cr, Fe, Mg, Mn, Na, Ni, Pb, Sr, V and Zn) were measured on a sector-field inductively coupled plasma mass spectrometer (SF-ICP-MS, an Element 2 from Thermo Fisher Scientific). All acids used for metals analysis were ultrapure grade from Seastar Chemicals and water used for dilution was ultrapure water with 18.2 MΩ cm resistivity (Super-Q, Merck Millipore).

2.3 Source apportionment

2.3.1 Enrichment factors calculation

Enrichment factor (EF) is a widely used to explore the possible sources of atmospheric trace metals. The EF can indicate natural emissions and anthropogenic activities, according to the equation:

$$EF_{crust\ or\ sea} = (E/Ref)_{aerosol} / (E/Ref)_{crust\ or\ seawater} \qquad (4\text{-}1)$$

in which $(E/Ref)_{aerosol}$ is the ratio of the concentrations of an element E and reference metal in the aerosol, $(E/Ref)_{crust\ or\ seawater}$ is the ratio of their concentrations and reference metal in crust or seawater. Calculation of EF_{crust} is based on the average upper continental crustal (UCC) composition from Rudnick and Gao where Al was chosen as the reference element of crustal source (Rudnick and Gao, 2003). Owing to Al is the most abundant metal in the crust and its atmospheric cycle has been little altered by human impact. To evaluate the importance of the sea surface as a source for the marine aerosol, Na can be used as the marine indicator element and the precursor source composition is assumed to be that of bulk seawater (Chester et al., 1991). EF can be classified into three categories as shown in Table 4.2.

2.3.2   Statistical analysis

Statistical analysis (ANOVA) was performed using IBM SPSS statistic 22. Pearson's correlation coefficient is used to measure the strength of the correlation between the two variables. The statistical significance was accepted at $p < 0.05$.

2.3.3   Air mass backward trajectory

To investigate the potential sources of air mass, backward trajectory analysis was conducted by Hybrid Single Particle Lagrangian Integrated Trajectory (HYSPLIT) model that provided by NOAA Air Resources Laboratory (Stein et al., 2015). Backward air trajectories were simulated for 5 days (120 hours) from the end of sampling day to allow transport of aerosol from sources to the sampling area. Wind directions were calculated at different 3 altitudes, including 100, 500 and 1000 m AGL (above ground level) over the Gulf of Thailand. These are atmospheric heights where the boundary layers are high enough to allow long range transport of aerosol.

Table 4.2 The degree of metal enrichment based on the EF_{crust} and EF_{sea} classification

EF_{crust}	EF_{sea}	Degree of enrichment
EF < 10	EF < 10	Natural origin
10 ≤ EF < 100	EF > 100	Significant enrichment
EF > 100	EF > 100000	Extremely high enrichment

3. Results and discussion

3.1 Chemical composition

3.1.1   Water-soluble inorganic ions (WSIIs)

The water-soluble ion abundances over the Gulf of Thailand are generally consistent with dominant contributions of Na^+, NH_4^+, K^+, Mg^{2+}, and Ca^{2+} for the cations and Cl^-, NO_3^-, and SO_4^{2-} among the anions. Ion charge balance calculation has been generally used to understand the acid-base balance of ambient aerosols. The charge balance of cation and anions were estimated as following equations:

$$\text{Cation Equivalent } (\Sigma^+) = \frac{[Na^+]}{23} + \frac{[NH_4^+]}{18} + \frac{[K^+]}{39} + \frac{[Mg^{2+}]}{12} + \frac{[Ca^{2+}]}{20} \qquad (4\text{-}2)$$

$$\text{Anion Equivalent } (\Sigma^-) = \frac{[SO_4^{2-}]}{48} + \frac{[NO_3^-]}{62} + \frac{[Cl^-]}{35.5} \qquad (4\text{-}3)$$

Ion difference was estimated by using the following equation.

$$\text{Ion Difference (\%)} = \frac{(\Sigma^+ - \Sigma^-)}{(\Sigma^+ + \Sigma^-)} \times 100 \qquad (4\text{-}4)$$
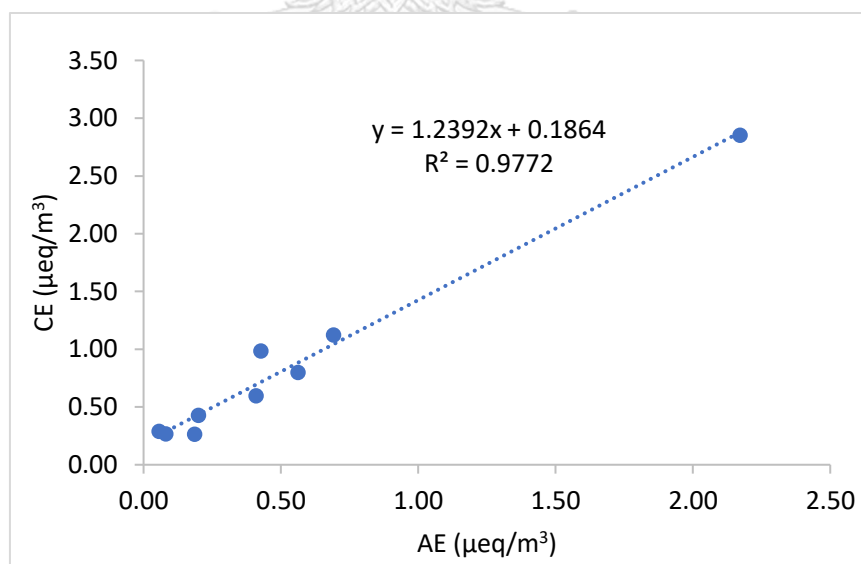
Figure 4.2 Ion charge balance

Significant correlations coefficient in charge balance were found at R^2 = 0.9772 (Table 4.3), indicating a good quality of datasets. The average ion difference was estimated to be 32%. The sum of total cation (Σ^+; µeq/m^3) should be equal to the sum of total anion (Σ^-; µeq/m^3). However, the average value of Σ^+/Σ^- ratio was found at 2.2 ± 1.2, indicating the presence of alkaline aerosols and the anion deficits were probably due to the unanalyzed inorganic (CO_3^{2-} and HCO_3^-) and organic ($HCOO^-$ and CH_3COO^-) anions. The statistical analysis of WSIIs is shown in Table 4.3. The orders in average ion mass concentrations of coarse particles were $Cl^- > Na^+ > K^+ > SO_4^{2-} > Ca^{2+} > Mg^{2+} > NO_3^- > NH_4^+$.

The ion concentrations in fine particles were distributed as $Cl^- > Na^+ > K^+ > Ca^{2+} > SO_4^{2-} > Mg^{2+} > NO_3^- > NH_4^+$, respectively. The concentrations of non-sea-salt (nss) components in water-soluble ions were estimated by using Na^+ as a sea-spray marker following,

$$[nss\text{-}SO_4^{2-}] = [SO_4^{2-}] - 0.25 \times [Na^+] \qquad (4\text{-}5)$$

$$[nss\text{-}K^+] = [K^+] - 0.036 \times [Na^+] \qquad (4\text{-}6)$$

$$[nss\text{-}Ca^{2+}] = [Ca^{2+}] - 0.038 \times [Na^+] \qquad (4\text{-}7)$$

Table 4.3 Statistical summary of WSIIs in µg/m^3 in atmospheric aerosol over GoT

Ions	PM$_{10\text{-}2.5}$					PM$_{2.5}$				
	Mean	SD	Median	Min	Max	Mean	SD	Median	Min	Max
Na^+	7.1	11	2.8	1.1	36	2.2	2.4	0.34	0.26	6.3
NH_4^+	0.11	0.13	0.07	0.00	0.38	0.03	0.05	0.01	0.00	0.13
K^+	3.9	4.2	2.2	0.28	10	1.3	2.5	0.33	0.04	7.9
Mg^{2+}	1.2	1.0	0.97	0.60	3.8	0.78	0.55	0.51	0.00	1.7
Ca^{2+}	1.4	0.84	1.1	0.78	3.4	1.2	0.62	0.89	0.64	2.4
Cl^-	11	18	4.2	1.0	58	4.0	4.9	0.32	0.23	13
NO_3^-	0.72	0.42	0.63	0.28	1.6	0.55	0.53	0.26	0.17	1.5
SO_4^{2-}	3.0	3.6	1.8	0.41	12	1.0	1.4	0.18	0.12	4.0

The result shows that all ion concentrations in coarse particles are higher than fine particles. It is probably due to marine aerosol constituent of coarse particle (Saltzman, 2009). Cl^- and Na^+ are the major ions, accounting for ~72.5% (range 55.6—82.6) of the total ions in coarse and ~64.1% (range 45.8—61.0) in fine particles. In addition, the Cl/Na ratio in coarse particles ranged from 0.66 to 2.0 (average 1.5 ± 0.38) and ranged between 0.87 and 2.0 (average 1.3 ± 0.49) for fine particles which is close to the Cl/Na ratio of marine aerosol in newly formed (1.8), observed in the marine atmosphere (1.3) (Duce and Hoffman, 1976; Kritz and Rancher, 1980; Wilkniss and Bressan, 1972) and not very different from seawater (1.16) (Chester and Jickells, 2012). Significant correlation between Cl^- and Na^+ in coarse (r = 0.999) and fine particles (r = 0.997) confirmed sea salt origin. Basically, coarse mode particles represent the natural aerosol such as dust and sea spray. The coarse particles show good correlation between Na^+, K^+, Mg^{2+}, Ca^{2+}, Cl^-, and SO_4^{2-} (range 0.555–0.999) indicating their same sources (Table 4.4).

Effects of the atmospheric anthropogenic inputs were observed by tracing the concentration of nss-PM$_{2.5}$. Nss-SO_4^{2-}, nss-K^+ and nss-Ca^{2+} were found mainly along the shore especially in the upper Gulf of Thailand. Overall, fraction of nss-SO_4^{2-} (a tracer for anthropogenic sources) was accounted for 52.5% of total SO_4^{2-} in fine samples and the upper Gulf of Thailand (GoT1-2) sample were recorded the high concentrations of nss-SO_4^{2-}. For the nss-SO_4^{2-} and nss-K^+ (a tracer for biomass burning) the moderate correlate (r = 0.548) was observed, indicating the significant influence of anthropogenic emissions (fossil fuel combustions and industrial emissions) and biomass burning. The highest concentration of nss-K^+ was also indicated in the upper Gulf of Thailand (GoT1). The nss-Ca^{2+} (a tracer for dust) found in relatively high concentrations nearby the shore in the sample in the upper and eastern Gulf of Thailand (GoT1-4) this suggested the possible influence of crustal dust.

Table 4.4 Correlation of WSIIs in coarse particle ($PM_{10-2.5}$) over GoT

	Na^+	NH_4^+	K^+	Mg^{2+}	Ca^{2+}	Cl^-	NO_3^-	SO_4^{2-}
Na^+	1							
NH_4^+	-0.317	1						
K^+	0.555	-0.358	1					
Mg^{2+}	0.981**	-0.351	0.608	1				
Ca^{2+}	0.911**	-0.428	0.672*	0.970**	1			
Cl^-	0.999**	-0.334	0.568	0.982**	0.915**	1		
NO_3^-	-0.160	0.510	0.181	-0.163	-0.197	-0.165	1	
SO_4^{2-}	0.953**	-0.027	0.446	0.923**	0.823**	0.947**	0.026	1

** Correlation is significant at the 0.01 level (two-tailed)

* Correlation is significant at the 0.05 level (two-tailed)

Table 4.5 The statistics of metals in ng/m^3 in atmospheric aerosol over GoT

Metals	$PM_{10-2.5}$					$PM_{2.5}$				
	Mean	SD	Median	Min	Max	Mean	SD	Median	Min	Max
Cd	0.13	0.16	0.07	0.02	0.52	0.04	0.04	0.03	0.01	0.12
As	1.3	1.7	0.71	0.18	5.6	0.35	0.46	0.13	0.04	1.2
Ba	3.2	2.8	2.1	0.29	7.0	2.9	4.5	0.45	0.27	12
V	3.3	2.6	2.4	0.14	7.0	2.6	4.3	0.82	0.17	12
Pb	5.2	8.5	2.3	0.27	27	1.4	1.8	0.62	0.16	4.7
Ni	5.6	4.2	3.9	1.6	15	5.8	6.2	3.4	0.58	18
Cu	6.6	3.1	6.6	2.6	12	5.0	3.4	4.3	1.1	12
Mn	8.8	7.0	8.9	1.5	21	12	18	0.85	0.45	51
Cr	10	13	8.0	2.0	43	17	38	3.9	1.3	119
Zn	17	18	14	2.8	63	21	20	11	5.2	62
Sr	39	72	9.8	1.6	227	8.2	13	0.66	0.27	34
Fe	333	311	160	52	819	348	488	57	15	1152
Al	293	332	94	44	895	346	587	40	25	1512
Ca	1451	2356	421	112	7437	485	594	187	60	1620
Mg	3315	4489	1213	211	13513	961	1310	93	44	3348
Na	22483	28686	10203	1741	89443	6844	8990	598	171	23411

3.1.2   Metal concentrations

Concentrations of sixteen metals are determined in coarse and fine particles. The statistical overview of coarse and fine concentrations are shown in Table 4.5. Overall, the concentrations in both particle sizes followed similar trends, (Na, Mg, Ca, Al and Fe) > (Zn, Sr, Cr, Mn, Ni, Cu, V, Pb, Ba, As and Cd). Al, Fe, Ca and Mg are some of the most abundant elements in the Earth's crust (Rudnick and Gao, 2003). In addition to crustal dust, Na, Ca, Mg and Sr can also come from sea spray aerosols (Fomba et al., 2013). The crustal dust and sea spray aerosol (Al, Fe, Sr, Ca, Mg and Na) are higher in coarse particles. Especially, the upper Gulf of Thailand (GoT1) significant high concentrations of sea spray aerosol such as Na, Mg, Ca and Sr. Moreover, the crustal dust has high concentrations in the eastern and central Gulf of Thailand (GoT3-5) such as Al, Fe and Mn. Fine particles also have high concentrations of crustal dust and sea spray (Al, Fe, Ca, Mg and Na) in the upper Gulf of Thailand. For the others, they may originate from several sources. Further Pearson's correlation coefficient, element ratio and enrichment factor were applied to explain the sources in the following section.

Metal dissolution from atmospheric aerosol deposition to the ocean has influence on marine biogeochemistry in term of increasing and reducing phytoplankton growth rates and modifying plankton community structure (Mahowald et al., 2018). Once aerosols are deposited on the ocean, the dissolution of the metals can be either rapid or gradual, with Zn and Cd dissolving more rapidly than other metals, and Ni, Al, Cu and Mn dissolving slower. Fe and Pb tend to react strongly in water, showing an increase and then decrease because sorption onto particles (Gledhill and Buck, 2012; Honeyman et al., 1988). The metal-binding is one of the major dissolutions in the ocean such as Fe and Cu. Copper is an essential biological trace metal whose speciation controlled by biogenic ligands. The ligand production of Cu may have two reasons: maintaining enough free Cu for nutrition while simultaneously preventing free Cu concentrations from reaching toxic levels (Mahowald et al., 2018).

3.2 Sources of marine aerosols over the Gulf of Thailand

3.2.1   Enrichment Factors

Marine aerosol can originate from either natural or anthropogenic sources. Thus, the enrichment factors are extensive tool for investigate sources of aerosol that natural emission or anthropogenic activities (Figure 4.4). In coarse particles, three of fifteen measured metals (Ba, Fe and Mn) have EF_{crust} less than 5 indicating crustal origin. V and Ca have EF_{crust} 16 and 45 indicating significant enrichment from anthropogenic sources. As, Cd, Cu, Cr, Ni, Pb, Sr, Zn, Mg and Na have $EF_{crust} > 100$ indicating an extremely high enrichment by anthropogenic sources (Figure 4.4a). Although Ca, Sr, Mg and Na have high EF_{crust}, these elements have EF_{sea} less than 6 indicating Ca, Sr and Mg from marine source (Figure 4.4b). Al and Fe are also high concentrations in coarse mode, especially in the eastern and central Gulf of Thailand (GoT3-5), possibly due to the long-range transport of crustal dust from south Thailand. Moreover, Sr is one of marine aerosols that indicates high concentrations in coarse particles.
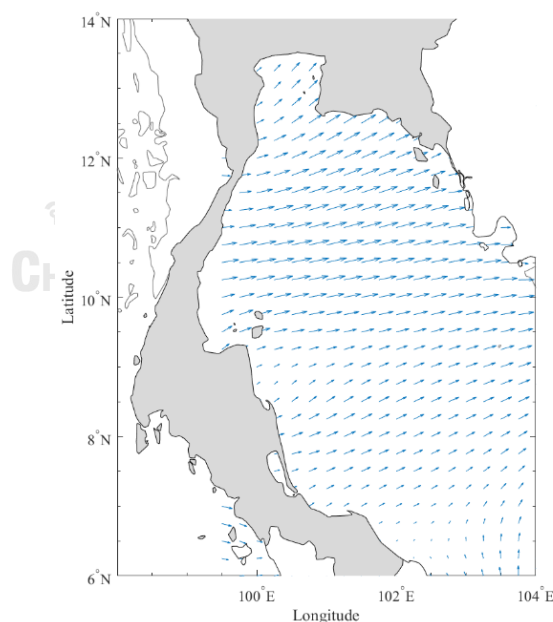
Figure 4.3 The wind velocities distribution (m/s) measured from 10 m above sea surface for August to October
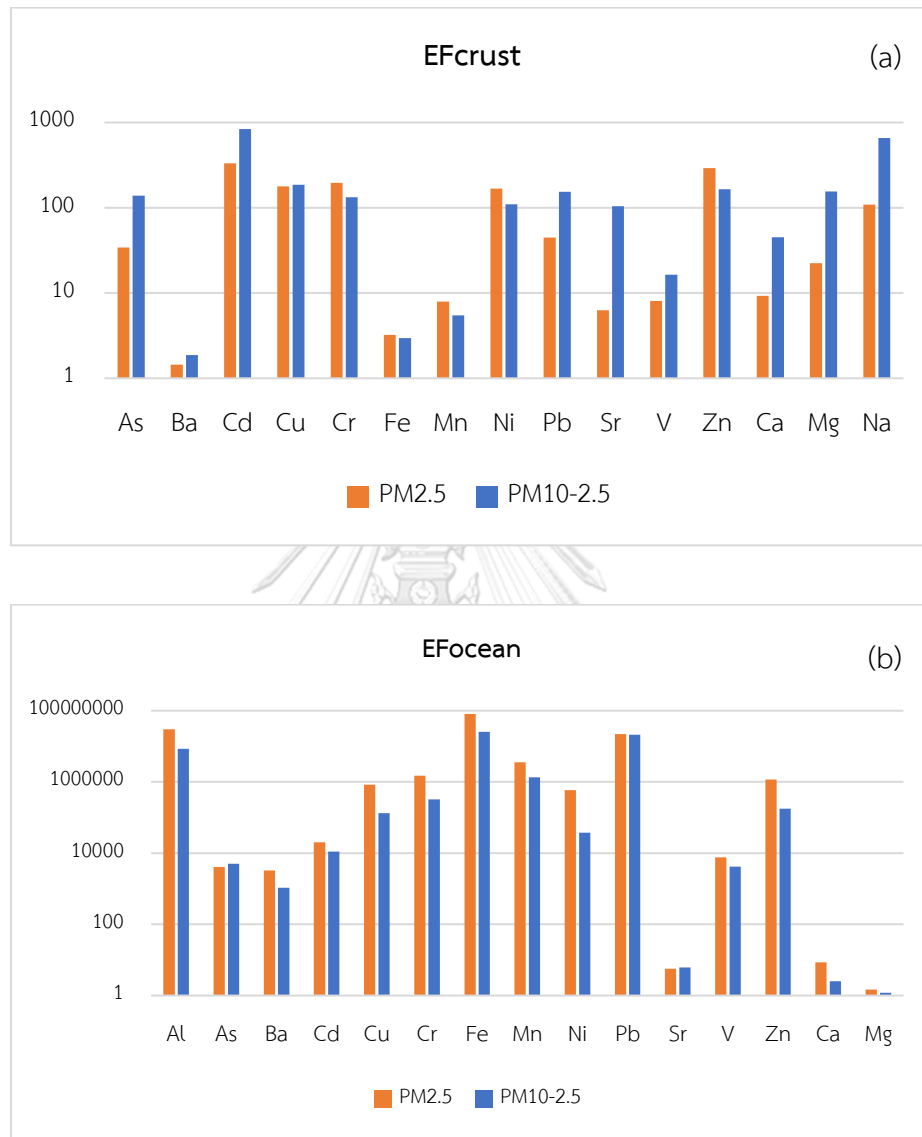
Figure 4.4 Enrichment factor of aerosol collected in GOT (a) for EF_{crust} and (b) for EF_{ocean}

Fine particles, Ba, Fe, Mn, Sr, V and Ca have EF_{crust} less than 10 probably because of crustal origin. As, Pb and Mg have EF_{crust} between 20 and 50 indicating moderate enrichment from anthropogenic sources. Cd, Cu, Cr, Ni and Zn have EF_{crust} > 100 indicating strong anthropogenic influence. The EF_{sea} of Ca, Sr, and Mg have the same trend with coarse mode particle. Nevertheless, Ca can come from a variety of sources including sea spray, crustal dust and cement dust from construction sites. Additionally, Ca has EF_{sea} more than 10 in southern Gulf of Thailand and Cambodia waters (GoT6-8) that probably from other sources.

As the results from EF, natural sources are counted for 99% of total metals and can divide into two major groups. The first group is marine aerosol (Sr, Ca, Mg and Na) that explains 95% (range 81-99). The second group (crustal sources) is associated with Al, Fe, Mn and Ba and can explains 4.6% of total metals which is consistent with the dust deposit to the ocean 5% (Mahowald et al., 2008). Only 0.63% (range 0.02-4.5) is observed in anthropogenic activities that shows loading of As, Cd, Cu, Cr, Ni, Pb, V and Zn. Although the EF can investigate both natural and anthropogenic sources, source apportionment of PM is difficult to complete solely based on EF and metal concentrations. To better understand the anthropogenic sources of trace metals in fine particles, element ratios and Pearson's correlation coefficient are used.

3.2.2 Air mass backward trajectory

All collected samples were analyzed for their air mass footprints. During southwest monsoon, the surface wind (10 m above sea surface) blow from southwest in the upper and southern Gulf of Thailand while the eastern Gulf of Thailand and Cambodia waters likely blow from west (Figure 4.3). Additionally, backward trajectory at the height of 100, 500 and 1000 m AGL are shown in Figure 4.5. Wind trajectories show that the climate over the Gulf of Thailand is strongly influenced by marine aerosol from the Indian Ocean during collecting sample. Only Cambodia waters (GoT8), air mass originate in China mainland and touch the southern tip of Vietnam before reaching Cambodia waters.
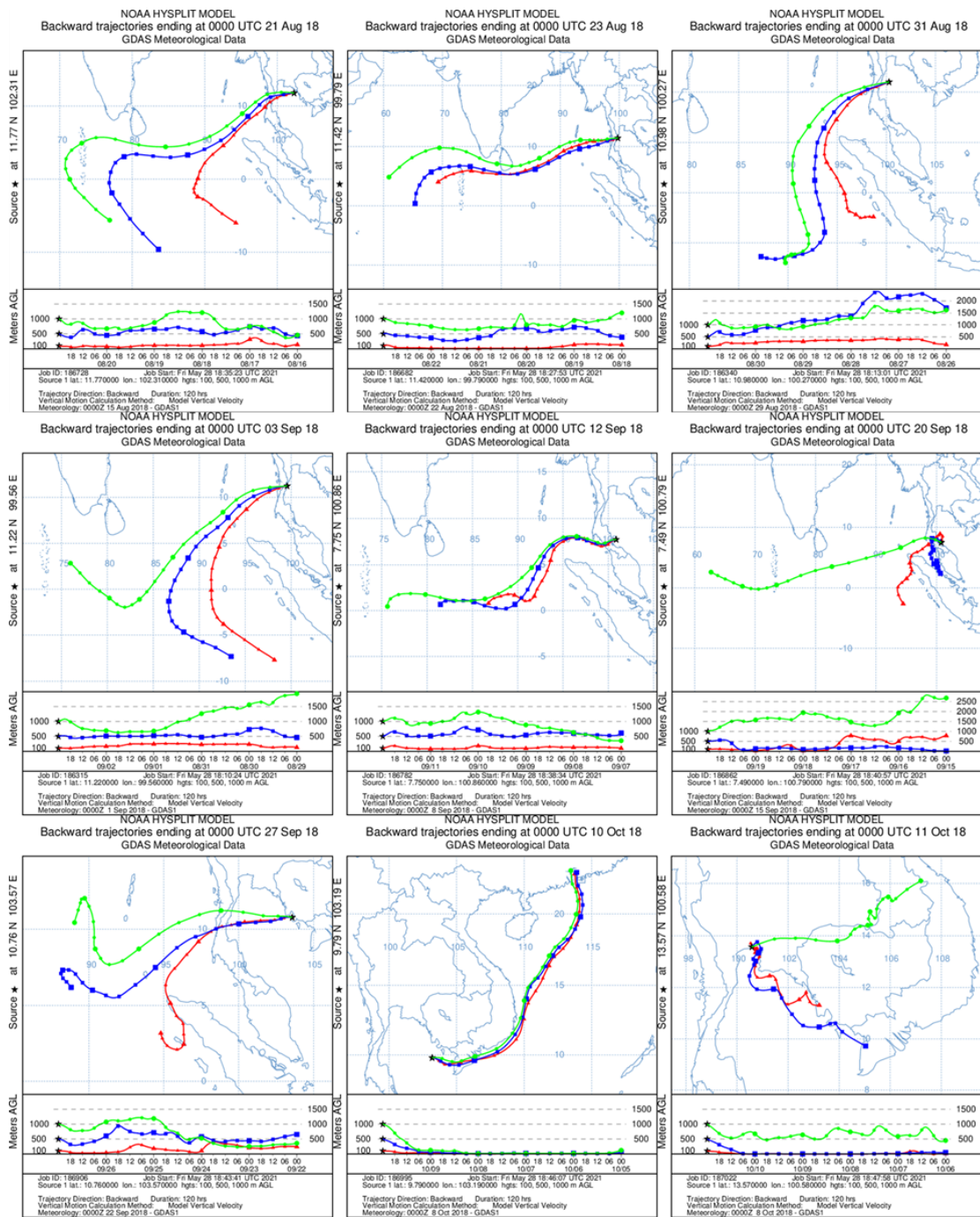
Figure 4.5 The 120 h backward trajectories for GoT1-9 at height of 100 (red line), 500 (blue line) and 1000 (green line) m for sampling collection in the GOT

3.3 Distribution of marine aerosol over the Gulf of Thailand

3.3.1   Upper Gulf of Thailand (GoT1-2)

The concentration of WSIIs such as Na^+, K^+, Mg^{2+}, Ca^{2+}, Cl^-, and SO_4^{2-} are highest in the upper Gulf of Thailand. Especially Na^+ and Cl^- in coarse particle are significant high concentration in GoT1, accounting for 41.4% and 42.9% of total ions, respectively. This is probably due to sea spray aerosol from the wind speed up to 9.26 m s^{-1} at the upper Gulf of Thailand (GoT1). Moreover, NH_4^+, NO_3^- and SO_4^{2-} in fine particles are highest in this area indicating influence of anthropogenic sources. Generally, anthropogenic emissions control fine particle (Chen et al., 2020). We consider the anthropogenic sources from metal tracer in fine particles.

The trace metal concentrations are highest in the upper Gulf of Thailand. As, Ba, Cd, Pb, Sr and V are highest in the upper Gulf of Thailand probably because of anthropogenic sources. Vanadium is considered to be a metal from oil combustion in residential, commercial, and industrial applications (Pacyna and Pacyna, 2001). The upper Gulf of Thailand (GoT1 and GoT2) indicate that high concentration of V as 12 and 7.6 ng m^{-3}, respectively. In addition, V/Ni ratios are 1.5 and 1.3 that close to petroleum fuel from traffic (1.49—2.4) (Lee et al., 2000; Thorpe and Harrison, 2008). Traffic is a major source of ground air pollution, especially in urban areas that can affect to the atmospheric around the upper Gulf of Thailand. Atmospheric aerosol study in surrounding area of the upper Gulf of Thailand at Bangkok and Chonburi (Kayee et al., 2021) has shown that trace metal concentrations in fine particles are influenced by anthropogenic sources including industrial emissions, coal combustion and traffic emission. Therefore, emissions from anthropogenic activities may have significant influence on trace metal in this region. Furthermore, Al and Fe are the 3rd and 4th most abundant elements in the Earth's crust and show highest concentrations and strong correlation (0.938) in the upper Gulf of Thailand (GoT1-2) suggest that the influence of crustal dust.

3.3.2   Eastern Gulf of Thailand (GoT3-4)

The concentration of WSIIs such as Na^+, K^+, Mg^{2+}, Ca^{2+}, Cl^-, and SO_4^{2-} are also high concentrations in the eastern Gulf of Thailand. Na^+ and Cl^- are the major ions and Cl/Na ratio is roughly 1.7 that consistent with the newly formed of marine aerosol (1.8) (Kritz and Rancher, 1980). The eastern Gulf of Thailand is also affected by marine aerosol from the Indian Ocean during the southwest monsoon (Figure 4.5).

The elements such as Cu, Cr, Mn, Ni, Pb, V, Zn, Fe, Al, Sr, Ca, Mg and Na are still high concentration in this region. The EF_{crust} indicates that crustal dust contributes Mn, Fe and Al. According to EF_{sea}, Sr, Ca, Mg and Na are derived from sea spray aerosol (Figure 4.4). However, the EF_{crust} of sample GoT4 is 54 which is significant enrichment of anthropogenic sources. Moreover, sample GoT4 has a high concentration of Cr and Mn of 119 and 51 ng/m^3, respectively, and a good correlation (0.814) that is possible due to the iron and steel industry around South Thailand (Pacyna and Pacyna, 2001). Pb and Zn are a common anthropogenic metal and can emit from a variety of sources including road traffic, coal combustion and industrial emissions.

3.3.3   Central Gulf of Thailand (GoT5)

The WSIIs such as Na^+, Mg^{2+}, Ca^{2+}, Cl^-, and SO_4^{2-} show high concentrations and strong correlation between each other (0.823—0.999, $p < 0.01$) in coarse particle. Moreover, Cl/Na ratio is 1.5 that consistent with marine aerosol (Duce and Hoffman, 1976; Kritz and Rancher, 1980; Wilkniss and Bressan, 1972). Backward trajectories of sample GoT5 indicates that the transport of air mass from the Indian Ocean. Thus, the air mass over the central Gulf of Thailand during southwest monsoon mostly contribute from marine aerosol. In general, NH_4^+, NO_3^- and SO_4^{2-} are major form of secondary inorganic aerosols. NH_4^+ and NO_3^- are highest in the central Gulf of Thailand. In addition, nitrogen deposition is estimated to be 80—100% from anthropogenic sources and it can absorb onto crustal dust particles and transport to the open ocean (Kim et al., 2014). Thus, it is producing higher concentrations of non-sea-salt aerosol over the ocean. The central Gulf of Thailand has moderate concentrations of trace

metal. However, the crust aerosol such as Mn (17.6 ng/m^3), Fe (795 ng/m^3) and Al (777 ng/m^3) indicate high concentrations in coarse particles.

3.3.4   Southern Gulf of Thailand (GoT6)

Sodium and chloride are the major ions of sea spray aerosols. The concentrations of Na$^+$ and Cl$^-$ are 1.56 and 1.03 µg/m^3, respectively. Other metals less than 1 µg/m^3 in coarse particles. The concentrations of WSIIs in fine particles less than 1 µg/m^3 except for K$^+$. The K$^+$ is generally used as a tracer for biomass and biofuel burning (Xiao et al., 2018). K$^+$ has high concentration (1.06 µg/m^3) in fine particles and nss-K$^+$ (1.05 µg/m^3) accounting for 99% of total K$^+$. The backward trajectories show that the air mass moved towards the southern Gulf of Thailand from Indian Ocean and Sumatra, Indonesia (Figure 4.5). The peatland fires in Sumatra, Indonesia are a major cause of transboundary haze pollution in Southeast Asia. The resulting haze problem is not only to Sumatra, Indonesia but also extends to neighboring countries such as Singapore, Malaysia and South of Thailand. The peatland burning peak for the period of July to September (Vadrevu et al., 2015). The GoT6 was collected on 16—20 September during southwest monsoon. It is possible that the peatland burning in Sumatra, Indonesia will reach to the southern Gulf of Thailand.

The element concentrations were lower than 10 ng/m^3 for most of the samples, except Zn, Fe, Al, Ca, Mg and Na. Ca, Mg and Na are represented the sea spray aerosols. Al and Fe are the abundant element in the Earth's crust while Zn can from a vary anthropogenic sources. In case of plants, Fe and Zn are micronutrients, however Al is considered as a toxin as inhibits root elongation. Moreover, Fe, Al, Ti and Zn in fine particles account for more than 85% of total metal concentration during peatland fire in Sumatra (Betha et al., 2013). Thus, the ratios of Zn, Fe and Al can used as a qualitative marker to determine the biomass burning source (Das et al., 2019). The Fe/Al ratio of fine particles over southern Gulf of Thailand (GoT6) is 0.43 while the Zn/Fe ratio is 0.71. Metals emitted from peat fire in Sumatra, Indonesia have an Fe/Al ratio (0.30—0.69) and a Zn/Al ratio (0.24—0.66). This indicates that the Fe/Al and Zn/Fe ratios are consistent with metals emitted from peat fire in Sumatra, Indonesia (See et al., 2007). However, sample GoT6 has low concentrations of WSIIs and trace metals

that probably because of rainfall. Rain or wet deposition is the major processes of atmospheric cleansing (Majumdar et al., 2020).

3.3.5   Cambodia waters

Sodium, chloride, and sulfate are higher than 2 µg/m^3 (2.10, 4.19 and 2.18 µg/m^3, respectively) in coarse particles. All WSIIs concentrations are less than 1 µg/m^3 in fine particles that probably less effect from sea spray aerosol. The backward trajectories show that the air mass originate from mainland China and pass though South China Sea and touch the tip of southern Vietnam before reach to Cambodia waters (Figure 4.5).

The element concentrations were lower than 10 ng/m^3 for most of the samples, except Cr, Ni, Zn, Fe, Al, Ca, Mg and Na. The crustal dust (Fe and Al) and sea spray (Ca, Mg and Na) are represented in this region. Cr, Ni and Zn are indicated high concentrations in urban/industrial area (Chifflet et al., 2018). Cr is shown high concentration and exceeded the Vietnamese ambient standard in Ho Chi Minh City that probably due to the effect of industrial activities and vehicle exhaust on city roads (Phan et al., 2020). This indicates that the aerosol over Cambodia water may influence by the air mass from Vietnam and marine aerosol from South China Sea.

3.3.6   Andaman Sea

As sampling height over Andaman Sea was higher than in the GoT, the WSIIs concentrations revealed in low concentrations. The metal concentrations and EFcrust and sea were showed in ng/m3 in Table 4.6. The results showed that the aerosols over Andaman Sea originate from marine sources (e.g., Mg, Ca and Sr). Beside marine sources, Al, Ba, Co, Fe, Mg, Mn, Na, Sr, V indicated that slightly influence from terrestrial. For Cu, Cr Ni, Pb and Zn probably affected by anthropogenic activities.

Table 4.6 Metal concentration, EF_{crust} and $EF_{seawater}$ over Andaman Sea

Metals	Min	Max	Mean	SD	EF_{crust}	$EF_{seawater}$
Al	22	48	36	11	–	3×10^8
Ba	0.20	1.1	0.47	0.41	2	3×10^4
Ca	34	433	200	170	17	168
Cu	0.46	2.0	1.2	0.62	94	4×10^6
Cr	0.66	2.3	1.5	0.85	36	3×10^6
Co	0.01	0.04	0.03	0.01	3	1×10^7
Fe	20	53	35	15	2	5×10^8
Mg	25	45	38	9.0	6	6
Mn	0.43	0.79	0.59	0.15	2	1×10^7
Na	31	105	62	32	6	–
Ni	0.47	2.3	1.2	0.79	54	1×10^6
Pb	0.07	0.39	0.24	0.13	29	1×10^8
Sr	0.11	0.44	0.29	0.14	2	25
V	0.06	0.14	0.11	0.03	2	2×10^4
Zn	2.0	13	8.8	5.4	280	1×10^7

4. Conclusion

This study presents an investigation of chemical composition (e.g., WSIIs and trace metals) in coarse and fine particles over the Thai waters during SW monsoon in 2018. The WSIIs were generally enriched with sea spray aerosol such as Na^+, K^+, Mg^{2+}, Ca^{2+}, Cl^-, and SO_4^{2-}. The EF_{sea} indicates that Sr, Ca, Mg and Na are from sea salt aerosol while EF_{crust} indicates that Ba, Fe, Mn and Al are from crustal dust. Besides, trace metals were used to verify the sources of the aerosols. The metals concentration is the highest in upper GoT followed by eastern GoT. The aerosols over the upper and eastern GoT are affected by the anthropogenic activities along the shoreline. The anthropogenic activities in southern Thailand may affected to the aerosols over eastern GoT. While the central GoT has high concentrations of sea spray aerosols and modurate concentration of trace metals. From elemental ratio and backward trajectory analysis, the peatland fires in Sumatra, Indonesia may influence to aerosols over the southern GoT. Cambodia waters has high concentrations of Cr which is exceed in Ho Chi Minh, Vietnamese and backward trajectory showed that the air mass may long distance transport to Cambodia waters. For Andaman Sea, the sampling height was higher than in the GoT, lower concentrations were found in the Andaman samples. The aerosols

over Andaman Sea originate from marine sources and little influence from terrestrial. However, the metal data indicated some samples had influenced by anthropogenic activities in a lesser extent.

CHAPTER 5

Metal concentrations and source Apportionment of PM$_{2.5}$ in Chiangrai and Bangkok, Thailand during a biomass burning season

Jariya Kayee[1], Penjai Sompongchaiyakul[1,2,*], Nivedita Sanwlani[3], Sujaree Bureekul[1,2], Xianfeng Wang[3,4], and Reshmi Das[4,5,*]

[1]Department of Marine Science, Faculty of Science, Chulalongkorn University, Bangkok, Thailand

[2]Center of Excellence on Hazardous Substance Management, Chulalongkorn University, Bangkok, Thailand

[3]Asian School of the Environment, Nanyang Technological University, Singapore

[4]Earth Observatory of Singapore, Nanyang Technological University, Singapore

[5]School of Environmental Studies, Jadavpur University, Kolkata, India

*Corresponding Author

penjai.s@chula.ac.th

reshmidas.sest@jadavpuruniversity.in

Keywords: biomass burning season, PM$_{2.5}$, aerosol optical depth, angstrom exponent, trace element, Pb isotope ratios
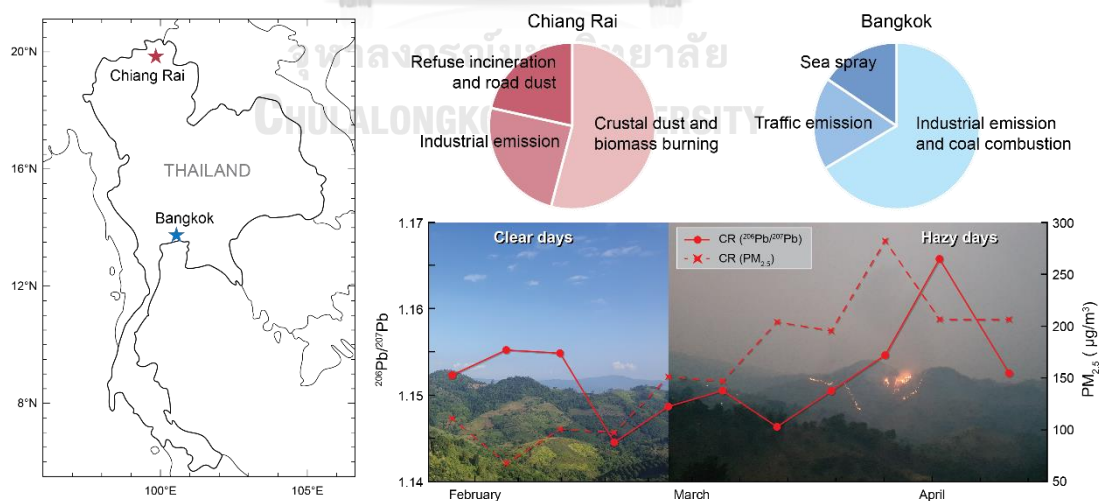
Abstract

One of the persistent environmental problems in the provinces of northern Thailand is severe air pollution during the dry season because of open vegetation burning by farmers for land clearance purpose. Aerosol optical depth and Ångström exponent data from MODIS-Terra satellite indicated that from mid-March to April, 2019, entire Thailand was covered with a high concentration of fine-sized aerosols. Trace metal concentrations of $PM_{2.5}$ collected from Chiang Rai in northern Thailand and Bangkok in southern Thailand between January and April 2019 were analyzed. Average concentrations of crustal metals such as Al, Ca, and Fe are higher in Chiang Rai compared to that in Bangkok. The Fe/Al ratio in Chiang Rai decreases from 1.65 during the onset of haze to 0.87 during the peak haze approaching a crustal ratio of 0.48. In contrast, Bangkok has higher Na, Mg, and Zn with an average Na/Mg ratio of 6.07 indicative of a sea spray (Na/Mg ~8) origin. Principal component analysis identifies three possible sources in Chiang Rai: (1) crustal dust and biomass burning, (2) industrial source, and (3) refuse incineration mixed with road dust; and for Bangkok (1) natural background, industrial emissions, and coal combustion, (2) traffic emission, and (3) sea spray. The ranges of Pb isotope ratios in the bulk fraction of $PM_{2.5}$ in Chiang Rai ($^{206}Pb/^{207}Pb$ = 1.1445—1.1657 and $^{208}Pb/^{207}Pb$ = 2.4244—2.4468) and Bangkok ($^{206}Pb/^{207}Pb$ = 1.1343—1.1685 and $^{208}Pb/^{207}Pb$ = 2.4138—2.4450) are not significantly different. However, in a time series plot, $^{206}Pb/^{207}Pb$ ratios in Chiang Rai follow $PM_{2.5}$ during the peak burning season and correlate well with the Al/Pb (r^2 = 0.61) ratios, indicating that at least part of the Pb is derived from crustal dust during peak fire. Using a binary mixing model, the most radiogenic Pb isotopes in Chiang Rai during the peak haze can be explained by ~5 to 30% mixing of crustal dust with ~35-40% biomass burning generated aerosols with the background. From the trace metal systematics and Pb isotope ratios, it is evident that (1) during the biomass burning season, trace metals from Chiang Rai are not transported down south to Bangkok and (2) in addition to metals released from biomass burning, the raging fire remobilizes crustal dust that forms an important source of Pb and other trace metals in the Chiang Rai aerosol.

1. Introduction

In Southeast Asia, countries such as Indonesia, Cambodia, Vietnam, Laos, Myanmar, and Thailand burn biomass for land clearing during the slash and burn agricultural waste creating severe air pollution (Vadrevu et al., 2019; Yin et al., 2019). Particulate matter (PM) generated from biomass burning has complex physicochemical properties. They are mixtures of polycyclic aromatic hydrocarbons (PAHs), carbonaceous (black and organic carbon) and nitrogenous compounds, organic and inorganic ions, and metals to name a few (Betha et al., 2013; See et al., 2006; See et al., 2007). Metals bound to the breathable fraction of the PM ($PM_{2.5}$) are of particular concern as the metals get deposited in the lower airways of the lungs and eventually mixes with the blood stream (Dockery and Pope, 1994; Dockery et al., 1993). In the Upper Silesia in Poland, high levels of Cd and Pb emissions caused an increase of spontaneous abortion in women during the first 3 months of pregnancy who were living close to the emission sources (Pacyna and Pacyna, 2011). Once emitted, the trace metals can get deposited on soils, fresh water, and marine ecosystems surrounding emission sources, as well as "en route" deposition during transport that can have far-reaching environmental impacts. Fe released from Indonesian wildfires stimulated a harmful algal bloom that caused extensive coral mortality off Sumatran coast (Abram et al., 2003). Fe-rich aerosols deposited over remote oceanic regions can augment photosynthesis, thus affecting marine biogeochemistry (Jickells et al., 2005). Because of a long residence time (0.5—2 years) of elemental Hg in the atmosphere, industrial emissions in Asia were found to be a major source of Hg in rainwater that falls along the California coast (Steding and Flegal, 2002). Besides the essential nutrients (e.g., iron and nitrogen compounds), PM-bound micronutrients (Zn, Cu, Mn, Mo, B, Ni, Se, etc.) can be very important both in marine and terrestrial ecosystems (Duce et al., 1991; Mahowald et al., 2018). Wildfires can lead to crustal dust entrainment by desiccating the soil and subsequently uplifting the dust by fire-related nearsurface strong wind (Schlosser et al., 2017; Wagner et al., 2018). Mineral dust can control the atmospheric radiation budget and affect climate changes (Choobari et al., 2014).

There have been several studies on source apportionment of metals in PM generated from biomass burning in Southeast Asia; (Ahmed et al., 2016; Betha et al., 2013; Das et al., 2019; See et al., 2007; See et al., 2006) however, none of the studies used isotope ratios as a "fingerprinting" tool. Lead (Pb) isotopes are an efficient tool for tracing the sources of Pb pollution (Bollhöfer and Rosman, 2001; Hamelin et al., 1989) as Pb isotopes do not fractionate during industrial and environmental processes and preserve the source signature even after degradation, processing, and transportation (Komárek et al., 2008). Several previous studies from South and Southeast Asia used Pb isotopic composition of atmospheric aerosol to understand the sources of Pb (Bollhöfer and Rosman, 2001; Carrasco et al., 2018; Das et al., 2018; Kumar et al., 2016; Sen et al., 2016). The identified Pb sources include industrial emission in Kanpur, India (Sen et al., 2016), Middle Eastern dust storm over Delhi, India (Kumar et al., 2016), coal combustion and industrial emission in Kolkata, India (Das et al., 2018), natural Pb, historic/remnant leaded petrol and present-day industrial and incinerated waste in Singapore (Carrasco et al., 2018), and industrial emission in Bangkok, Thailand (Bollhöfer and Rosman, 2001). However, none of the studies investigated Pb sources using isotopes during biomass burning.

The fire season in northern Thailand generally occurs during the months of February to April. Biomass (agricultural wastes of sugarcane, rice straw, and other crops) is burnt prior to the harvest season to quickly clear land and prepare the fields for the next crop cycle (Yin et al., 2019). Fire-related air pollution peaks in March and April in many provinces such as Lampang, Lamphun, Phrae, Nan, Mae Hong Son, Phayao, Uttaradit, Chiang Mai, and Chiang Rai in northern Thailand (Pongpiachan et al., 2013). Chiang Rai is the northernmost province of Thailand sharing borders with Laos and Myanmar. For 9—10 months in a year, Chiang Rai has a pristine atmosphere, which drastically changes during the burning season. Several studies on fire-related air pollution in northern Thailand primarily focused on quantifying PAHs, which are significantly higher during the haze season (Pongpiachan et al., 2017; Wiriya et al., 2013). Remote-sensing satellite data were used to monitor carbon monoxide (CO) and PM_{10} that showed a significant correlation with the forest fire hotspot counts, especially in

the rural areas (Sukitpaneenit and Kim Oanh, 2014). Furthermore, several studies reported regional scale mapping of fire-related near-ground PM$_{10}$ concentrations (Phayungwiwatthanakoon et al., 2014; Sayer et al., 2016).

   To the best of our knowledge, none of the previous studies investigated metal emissions during the burning season and tracked the long-range transportation of released metals from northern Thailand. Here, we study trace element compositions of the PM$_{2.5}$ generated during crop burning along with lead (Pb) isotope ratios to understand the sources (biomass vis a vis crustal dust) and the transportation pattern of the air pollution plume. MODIS-Terra aerosol optical (AOD) at 550 nm and Ångström Exponent (AE) for 550—860 nm were used to investigate spatiotemporal patterns in regional aerosol loading over Thailand for January—April 2019. Monthly variations in air mass forward trajectories over Chiang Rai were examined to understand the dispersion pattern of the atmospheric aerosols. Backward trajectories over Bangkok were computed to identify the potential dust emission sources and to determine whether burning-related air pollution reached far down south to Bangkok.

2. Methodology

2.1 Sampling

   Aerosol samples were collected from two different geographic locations in Thailand, Bangkok (13.83°N, 100.53°E) and Chiang Rai (19.85°N, 99.81°E) between January and April 2019 (Figure 5.1). Chiang Rai is the northernmost province of Thailand, approximately 800 km north of Bangkok. The atmospheric circulation of Thailand is characterized by the monsoon system. Cool dry continental winds prevail during the northeast monsoon (October-February) season that transports air pollution from distant areas as opposed to the southwest monsoon (May-September), which is generally maritime and clean. Air pollution in northern Thailand due to burning of agriculture wastes, forest fire, and waste incineration has been recognized as smog crisis during the dry season from January to April every year since 2007 (Wiwatanadate, 2014). In 2019, Thailand began to experience a haze from February that lasted until the end of April, peaking in March and April, which is the official crop burning season

in Chiang Rai (Pasukphun, 2018). We collected nonhaze samples till 20th February, after which the hazy days commenced. Generally during January to April, wind blows from north-northeast thus transporting the pollution plume down south. However, the wind rose diagram shows southeast and southwest as the dominant wind directions in Chiang Rai though northerly winds were present for some days during the sampling period (Figure 5.1). In Bangkok, the dominant wind direction was from south between January and April 2019.
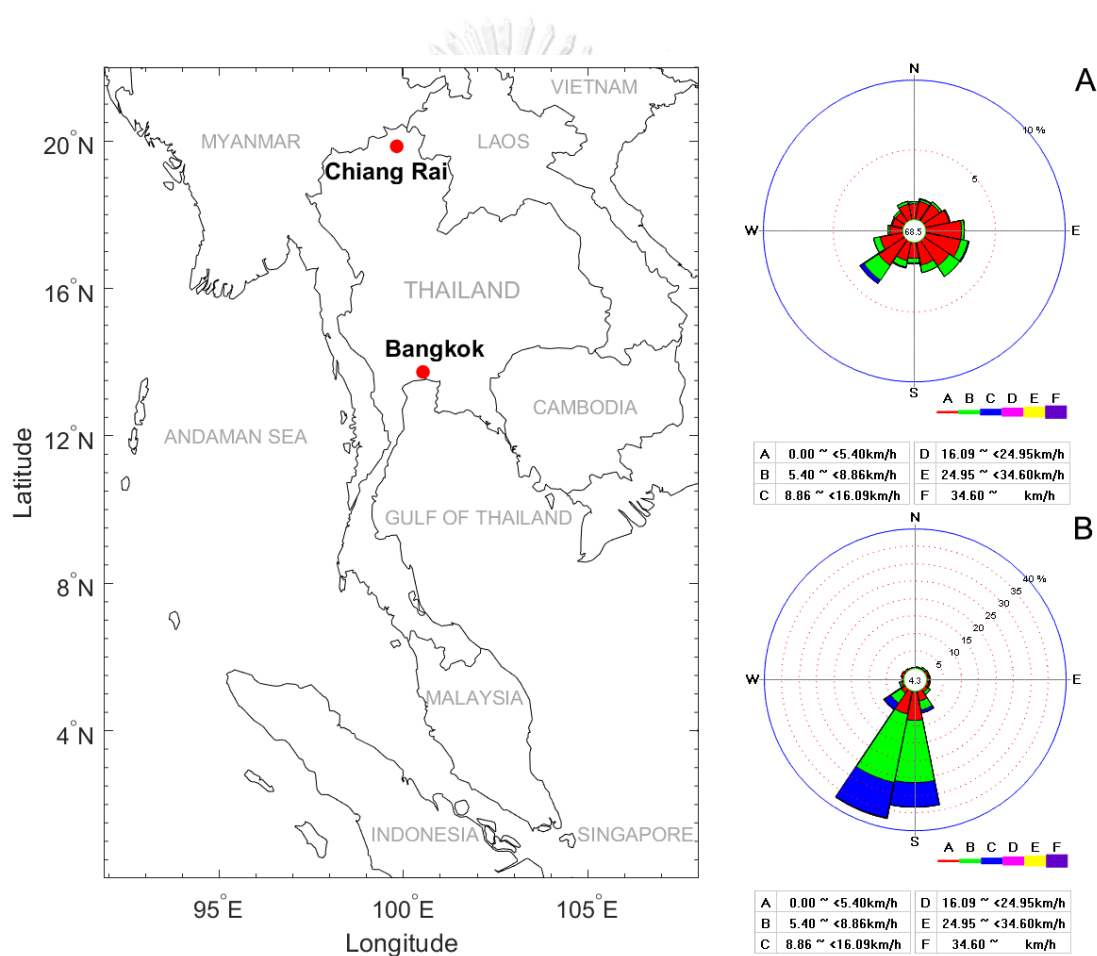
Figure 5.1 Aerosol sampling site and wind rose diagram to show the wind direction during January to April 2019 (A: wind rose at Chiang Rai and B: wind rose at Bangkok)

For the purpose, PM$_{2.5}$ samples were collected on 47 mm PTFE filters with personal modular impactor PM$_{2.5}$ (PMI, SKC Inc., USA) connected to a sampling pump (Gilian, AirCon-2) at a flow rate of 10 L/min. Samples were collected for 24 h from 6 AM, once every week. In Chiang Rai, the pump was placed on the roof top of a building at a height of ∼9 m above ground level (AGL). In Bangkok, the pump was placed on 4th floor bridge connection of Khum-Watcharobol and Geology buildings, Chulalongkorn University, approximately ∼22 m AGL. Before collecting the samples, the Teflon filters were cleaned with 1 N HCl at 140°C for 2 h, washed in ultrapure water several times, and dried in an oven. The filter samples were stored in a desiccator before sampling. Post collection, the filters were immediately sealed in the Petri dishes and stored inside the desiccator. Field blanks were collected by placing the Teflon filter in the filter cartridge without turning on the pump and the filter was removed after ∼5 min, approximately the time taken to change the sample filters. The blank filters were stored in the same way as the sample filters until further chemical analysis.

2.2 Satellite data and trajectory modeling

MODIS-Terra Collection 6.1, Level-2 product (MOD04_L2) based on the Dark Target and Deep Blue algorithms (Levy et al., 2013) was downloaded at a spatial resolution of 10 km from https://ladsweb.modaps.eosdis.nasa.gov/ for the period of January-April 2019 and a combined land and ocean AOD product centered at 550 nm was extracted. AOD centered at 550, 860, and 2100 nm over the ocean and AOD centered at 412, 470, and 650 nm over the land were used to derive combined AE over the spectral 550─860 nm range over land and ocean. The potential location of the emission source for Bangkok was inferred by back-tracing hourly air-mass trajectories at 750 m height above mean sea-level for 72 h (3 days) using the hybrid single-particle Lagrangian integrated trajectory (HYSPLIT) model (Stein et al., 2015). Similarly, hourly forward trajectories were computed for Chiang Rai to determine the dispersion of pollutants over a period of 120 h (5 days) using HYSPLIT at 750 m height above mean sea-level. Trajectory analysis was used to understand the atmospheric transport patterns and whether burning-related air pollution reached the capital city

of Bangkok. Cluster analysis was then carried out to assemble the trajectories into three or four major groups based on the wind speed and direction to estimate the median trajectories for each month.

2.3 Metal analysis

All chemical analyses were conducted in a class 1000 clean chemistry lab at the Earth Observatory of Singapore, Nanyang Technological University. Pekney and Davidson (2004) used 0.5% HF (∼0.30 M HF) to dissolve the silicate fraction in aerosols and calculated that less than 0.1% HF (∼0.06 M HF) is enough to completely dissolve 180 μg of SiO_2 present as crustal dust on aerosol filters (Pekney and Davidson, 2005). Other studies also used a dilute mixture of HF/HCl (4.5 M HF/1 M HCl) or HF/ HNO_3 for complete extraction of trace elements from atmospheric aerosol (Janssen et al., 1997). Assuming a large fraction of $PM_{2.5}$ can come from crustal dust in our samples, we decided to use ∼10 times more concentrated HF as compared to Pekney and Davidson (2004). Hence, 50% (v/v) of 3:1 HNO_3/HF (3.6 M HF/6M HNO_3) was used as the dissolution mixture. We tested our dissolution mixture on aerosol samples collected from Singapore. Half of the filter was leached in a concentrated 3:1 HNO_3/HF mixture and the other half in 50% (v/v) of 3:1 HNO_3/HF. No significant difference was observed in Pb isotope ratios between the two halves (Table B-1), indicating complete dissolution of natural Pb by the 3.6 M HF/6 M HNO_3 dissolution mixture. The PTFE filter samples (including SRM 2783 standard and blank filters) were leached with 5 mL of the dissolution mixture in Savillex beakers. The tightly capped Teflon beakers were sonicated at 60°C for 1 h and heated at 150°C for 12 h. PTFE filters were removed from the solution using a Teflon tweezer and washed with ultrapure water, and the solution was evaporated to dryness on a hot plate at 120°C. The dried extracts were redissolved in 7N HNO_3 and evaporated to dryness a couple of times to get rid of any traces of HF. Subsequently, the dried metal extracts were redissolved in 2 mL of 3% HNO_3 and separated into two parts. One aliquot was diluted for trace metal analysis and the other aliquot was stored for Pb isotope measurement. All acids used for analysis were of ultrapure grade from Seastar Chemicals and water used for dilution was ultrapure water with a 18.2 MΩ cm resistivity (Super-Q, Merck Millipore). The trace

metal concentrations were measured on a sector-field inductively coupled plasma mass spectrometer (SF-ICP-MS, an Element 2 from Thermo Fisher Scientific) at the Earth Observatory of Singapore (Das et al., 2013). One ppb of indium was added into the solutions as the internal standard. Instrumental drift was corrected by a combination of the internal indium standard and external calibration from the bracketing standard (IV-ICPMS-71A from Inorganic Ventures). Typical instrument sensitivity was about 1.8×10^6 cps/ppb for ^{115}In. All samples were measured for 15 elements including Al, As, Ba, Ca, Cu, Cr, Fe, Mg, Mn, Na, Ni, Pb, Sr, V, and Zn. Different mass resolution modes were used to optimize the separation of measured isotopes from interfering polyatomic species (e.g., ^{75}As from ^{40}Ar^{35}Cl) and improve detection limits. The final concentrations were blank corrected using the average blank filter concentrations. Averages of the procedural filter blanks ranged from 1.3 to 3% of the average signal intensity of the samples. SRM 2783 of urban PM samples was used to validate the method. Recoveries for all metals including Pb were found to be >90%. The detection limit (LOD) of all metal analytes was calculated based on three times of the standard deviation (SD) of blank. The value of LOD ranged from 0.0023 (Pb) to 2.2717 (Ca) ppb (n = 12).

2.4 Pb isotope analysis

The remaining aliquot of the sample solutions was passed through an ion exchange column (Eichrom AG-1X8 chloride form, 200—400 mesh) for separation of Pb. Sample solutions were dried and dissolved in 1.1 N HBr before loading into the columns. For column blanks, 1.1 N HBr was loaded instead of the sample. 1.1 N HBr and 2 N HCl were used as the mobile phase. Pb was eluted with 6N HCl and collected in a Savillex beaker (Reuer et al., 2003). The collected solutions were evaporated at 90°C to dryness and redissolved in 2% ultrapure HNO_3 and analyzed for Pb isotopes using a Multicollector ICP-MS (Neptune Plus from Thermo Fisher Scientific) at the Earth Observatory of Singapore (Das et al., 2018). Thallium (Tl) was added as an internal standard and a ^{203}Tl/^{205}Tl ratio of 0.418911 was used to correct for instrumental mass fractionation (Sen et al., 2016; White et al., 2000). The samples were measured at similar Pb/Tl ratios to the standards to avoid any analytical bias. The ^{202}Hg signal was

used to correct the isobaric interference of ^{204}Pb by ^{204}Hg. The isotope ratios of the NBS-981 Pb standard were measured during the analytical sessions, indicating ^{206}Pb/^{204}Pb = 16.92599 ± 0.002, ^{207}Pb/^{204}Pb = 15.47794 ± 0.0027, ^{208}Pb/^{204}Pb = 36.6591 ± 0.0086, ^{206}Pb/^{207}Pb = 1.0935 ± 0.0001, and ^{208}Pb/^{207}Pb = 2.3684 ± 0.0002 (2 standard deviations, n = 22). The ratio averaged between the measured NBS 981 Pb isotope composition during an analytical session and the true ratios as reported by Baker et al. (2004) were used to normalize the Pb isotope ratios of the measured samples (Baker et al., 2004; Das et al., 2018). The procedural blanks were measured and ranged from 0.05 to 0.77% of the sample concentration and were corrected for the reported concentration.

Table 5.1 Metal Concentrations in ng/m^3 and PM$_{2.5}$ in µg/m^3 (Source: Pollution Control Department) from Chiang Rai (CR 1–CR 11) and Bangkok (BKK 1–BKK 10)

	date	Al	As	Ba	Ca	Cu	Cr	Fe	Mg	Mn	Na	Ni	Pb	Sr	V	Zn	PM$_{2.5}$
CR1	29/01/2019	59	0.58	2.3	72	2.0	1.2	136	20	2.7	72	0.97	6.2	0.36	0.35	8.3	111
CR3	12/02/2019	91	0.35	2.3	93	2.7	19	193	26	16	73	7.3	2.9	0.42	0.52	7.3	101
CR4	19/02/2019	90	0.30	2.2	151	6.6	1.3	148	50	5.1	121	0.81	8.8	0.94	0.36	28	97
CR5	26/02/2019	147	0.65	3.6	122	2.1	1.1	155	43	8.5	67	0.56	9.1	1.2	0.64	21	151
CR6	05/03/2019	162	0.33	2.5	126	2.1	2.8	147	60	4.4	86	0.53	4.0	1.3	0.57	11	147
CR7	12/03/2019	230	0.76	3.4	191	2.8	1.0	213	85	13	75	1.3	17	3.4	0.76	31	203
CR8	19/03/2019	84	0.88	2.0	90	2.3	1.4	92	31	4.1	79	0.79	4.2	0.63	0.63	13	195
CR9	26/03/2019	62	0.40	1.3	60	1.3	0.55	63	26	2.5	65	0.39	2.4	0.39	0.53	6.9	281
CR10	02/04/2019	128	0.62	2.3	107	1.8	0.59	112	36	4.2	57	0.47	3.6	0.67	0.54	11	206
CR11	09/04/2019	159	0.55	2.6	117	1.8	0.93	158	58	5.4	50	0.55	5.3	1.1	0.46	11	206
mean		121	0.54	2.45	113	2.6	3.0	142	44	6.6	75	1.4	6.4	1.0	0.54	15	170
median		110	0.57	2.3	112	2.1	1.2	148	40	4.8	73	0.68	4.8	0.81	0.54	11	173
min		59	0.30	1.3	60	1.3	0.55	63	20	2.5	50	0.39	2.4	0.36	0.35	6.9	97
max		230	0.88	3.6	191	6.6	19	213	85	16	121	7.3	17	3.4	0.76	31	281
SD		54	0.19	0.66	38	1.5	5.7	44	20	4.5	19	2.1	4.4	0.90	0.13	8.7	59
	date	Al	As	Ba	Ca	Cu	Cr	Fe	Mg	Mn	Na	Ni	Pb	Sr	V	Zn	PM$_{2.5}$
BKK1	29/01/2019	103	3.8	17	173	14	2.5	274	58	15	353	2.1	43	1.5	2.4	61	157
BKK2	05/02/2019	30	0.53	2.3	98	2.3	1.6	83	56	6.0	389	1.4	2.2	0.53	2.6	11	99
BKK3	12/02/2019	51	1.0	6.7	90	7.0	1.9	168	42	12	302	2.2	15	0.76	4.0	79	87
BKK4	19/02/2019	15	0.33	1.4	35	1.5	0.90	79	35	2.9	234	0.80	1.5	0.30	2.1	9.1	66
BKK5	05/03/2019	38	1.0	2.0	86	2.9	0.89	76	39	3.7	226	1.0	5.4	0.69	1.8	26	80
BKK6	12/03/2019	113	1.4	4.4	122	6.0	1.6	195	74	13	255	1.7	12	1.7	2.5	66	75
BKK7	19/03/2019	39	0.80	1.8	49	2.2	0.64	79	67	4.6	454	1.3	5.2	0.72	2.6	26	109
BKK8	26/03/2019	19	0.56	1.9	41	2.5	5.3	99	38	7.2	247	1.4	2.3	0.52	2.2	14	83
BKK9	02/04/2019	75	1.4	2.5	54	3.4	1.2	107	39	4.5	196	3.1	7.2	0.49	3.7	25	79
BKK10	09/04/2019	26	1.3	1.9	42	2.6	1.1	71	37	3.7	232	1.1	3.2	0.34	2.4	19	75
mean		51	1.2	4.2	79	4.4	1.8	123	49	7.3	289	1.6	9.7	0.76	2.6	34	91
median		39	1.0	2.2	70	2.8	1.4	91	41	5.3	251	1.4	5.3	0.61	2.5	26	82
min		15	0.33	1.4	35	1.5	0.64	71	35	2.9	196	0.80	1.5	0.30	1.8	9.1	66
max		113	3.8	17	173	14	5.3	274	74	15	454	3.1	43	1.7	4.0	79	157
SD		35	1.0	4.8	44	3.8	1.4	68	14	4.4	84	0.69	13	0.47	0.69	25	26

3. Results and discussion

3.1 Particulate matter ($PM_{2.5}$)

The average $PM_{2.5}$ concentrations in Chiang Rai and Bangkok provided by Division of Air Quality Data, Air Quality and Noise Management Bureau, and Pollution Control Department of Thailand are 170 µg/m³ (range: 97—281 µg/m³) and 91 µg/m³ (range: 66—157 µg/m³), respectively (Table 5.1). Average $PM_{2.5}$ concentrations at Chiang Rai are higher than those at Bangkok during the sampling period (January to April 2019). The first four samples (CR 1 to CR 4) were collected during the non-haze period between January and mid-February. The onset of haze is evident from the increase in $PM_{2.5}$ concentrations in Chiang Rai from the end of February (26th February) to April (CR 5 to CR 11) from biomass burning (Khamkaew et al., 2016). The $PM_{2.5}$ concentrations during haze (average: 198 µg/m³) are significantly higher than those during nonhaze (average: 103 µg/m³) at Chiang Rai. In contrast, average Bangkok $PM_{2.5}$ in January-February was 102 µg/m³ (BKK 1 to BKK 4), which decreased to 83.5 µg/m³ (BKK 5 to BKK 10) after burning in Chiang Rai commenced. The higher concentrations of $PM_{2.5}$ in January-February in Bangkok are possibly because of thermal inversion in winter (Kim Oanh et al., 2013; Rungratanaubon et al., 2008). After the onset of haze in Chiang Rai, $PM_{2.5}$ concentrations in Bangkok do not show any increase, which indicates a minimal effect of biomass burning in the northern provinces on fine particle concentrations in Bangkok.

3.2 Aerosol optical depth and Ångström Exponent

Satellites routinely measure the spatial distribution of AOD, which represents the integrated extinction of electromagnetic radiation due to the amount of total column aerosol of all sizes. AE represents the spectral slope of AOD, indicating a systematic size distribution of the scattering particles (Balakrishnaiah et al., 2011; Quirantes et al., 2019). AOD acquired from satellite measurements has demonstrated to have a linear regression relationship with the near ground $PM_{2.5}$ (Guo et al., 2009; Zang et al., 2019). A good correlation has not only encouraged the use of AOD as a surrogate for $PM_{2.5}$ but has also been used for monitoring and nowcasting air quality

(Al-Saadi et al., 2005; He and Huang, 2018; Koelemeijer et al., 2006; Liu et al., 2005). Several different models have been proposed for studying the AOD-PM$_{2.5}$ relationship based on simple linear regression (Engel-Cox et al., 2004), multivariate regression including meteorological parameters (Li et al., 2017; Li et al., 2017; Liu et al., 2007; Pelletier et al., 2007), chemical transport models (Liu et al., 2004), and temporally structured models (Fang et al., 2016). MODIS-derived spatial distribution of AOD (550 nm) displays relatively clean marine areas (South China Sea) and a high concentration of fine particles prevalent over land areas (Figure 5.2). This can be attributed to various natural and anthropogenic sources influencing the Thailand environment. The spatial gradients of AE (550—860 nm) (Figure 5.3) indicate the abundance of fine particles (AE > 1) over the terrestrial region mainly from anthropogenic sources and biomass burning (Remer et al., 1998) and the dominance of coarse particles such as sea salt (AE < 1) over the marine environment (Eck et al., 1999).

A high AOD from the spatial distribution map (Figure 5.2) indicates a substantial amount of fine-sized (AE > 1) aerosol concentration around Bangkok during January and February, which is consistent with our high PM$_{2.5}$ in situ measurements. Chiang Rai depicts reduced aerosol load with relatively lower AOD and relatively coarser particles (~AE = 1) in coherence with lower PM$_{2.5}$ values in January and February. Mid-March onwards to April, entire Thailand including Chiang Rai is covered with a high concentration (high AOD) of fine-sized (AE > 1.5) aerosols (Figure 5.2) in coherence with high PM$_{2.5}$ measurements.
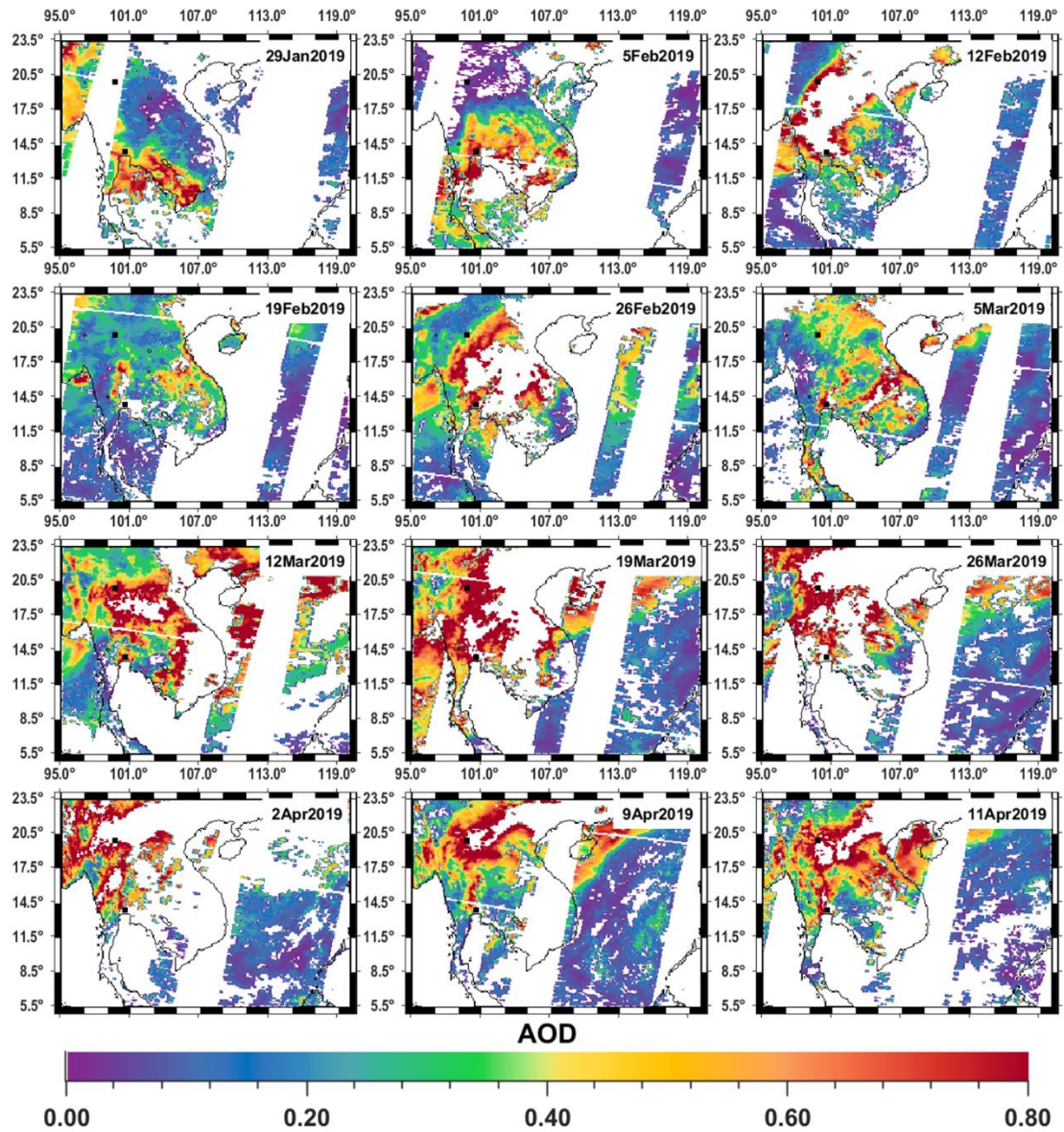
Figure 5.2 Spatial variation of AOD during the prehaze and haze periods for Chiang Rai and Bangkok. Each panel is 24 h average during the sampling period. The black dots represent the sampling locations (Chiang Rai and Bangkok)
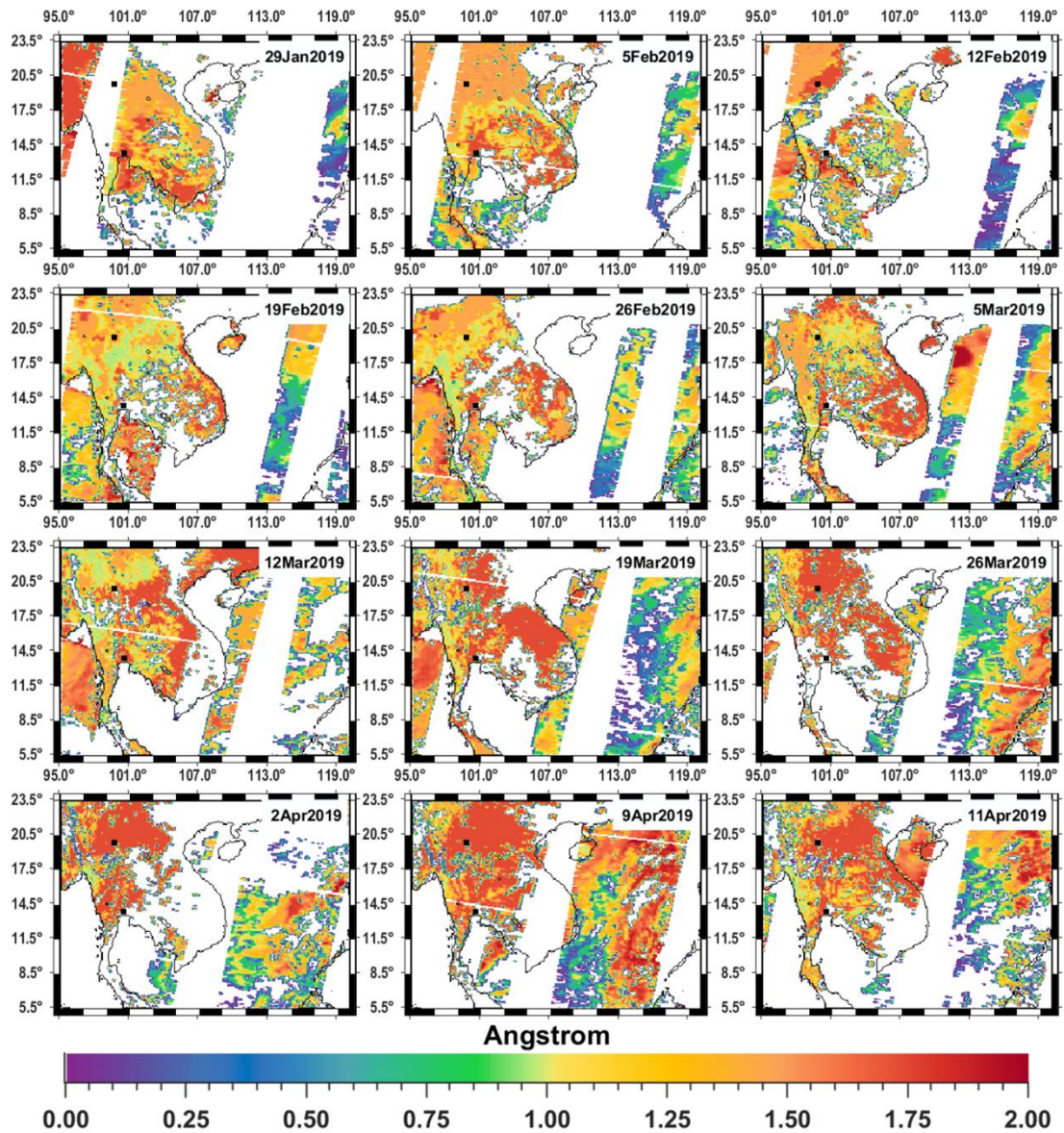
Figure 5.3 Spatial variation of AE during the pre-haze and haze periods for Chiang Rai and Bangkok. Each panel is 24 h average during the sampling period. The black dots represent the sampling locations (Chiang Rai and Bangkok)

3.3 HYSPLIT trajectory

Trajectory analysis is helpful for ascertaining the origins of air masses (back-trajectory) and identifying the transports of air mass from a location to determine the dispersion of pollutants (forward trajectory). Monthly variability of median air-mass trajectories (Figure 5.4) over Bangkok was carried out based on backward analysis to identify the potential source bringing the pollutants to Bangkok. In January, 72% of the cluster originated from the South China Sea and the rest came from Vietnam. All the clusters traveled long distances over land (Cambodia, Laos, Vietnam, and parts of Thailand) before reaching Bangkok. In February, the largest cluster (57%) originated in southern Vietnam and traveled over the Gulf of Thailand before reaching Bangkok. The remaining cluster came from the South China Sea, Cambodia, and Laos. Overall, the majority of the wind trajectories travel long distances over landmass in January and February before reaching Bangkok. In March, most of the air mass originates over sea such as Andaman Sea (55%), Gulf of Thailand (19%), and South China Sea (26%). In April, 33% of the cluster blows from Andaman Sea and the remaining from the Gulf of Thailand. Overall, wind clusters in March and April make minimal land travel before reaching Bangkok.

The forward trajectory (all the clusters) analysis showed that the atmospheric aerosols originating from northern Thailand are transported toward the north-east direction across from the pattern Chiang Rai Province predominantly toward mainland China and some part of northern Laos, and northern Vietnam throughout January-April. This observation is consistent with the general pattern of air mass movement observed in the northern Thailand province of Chiang Mai during the burning season (Punsompong and Chantara, 2015).
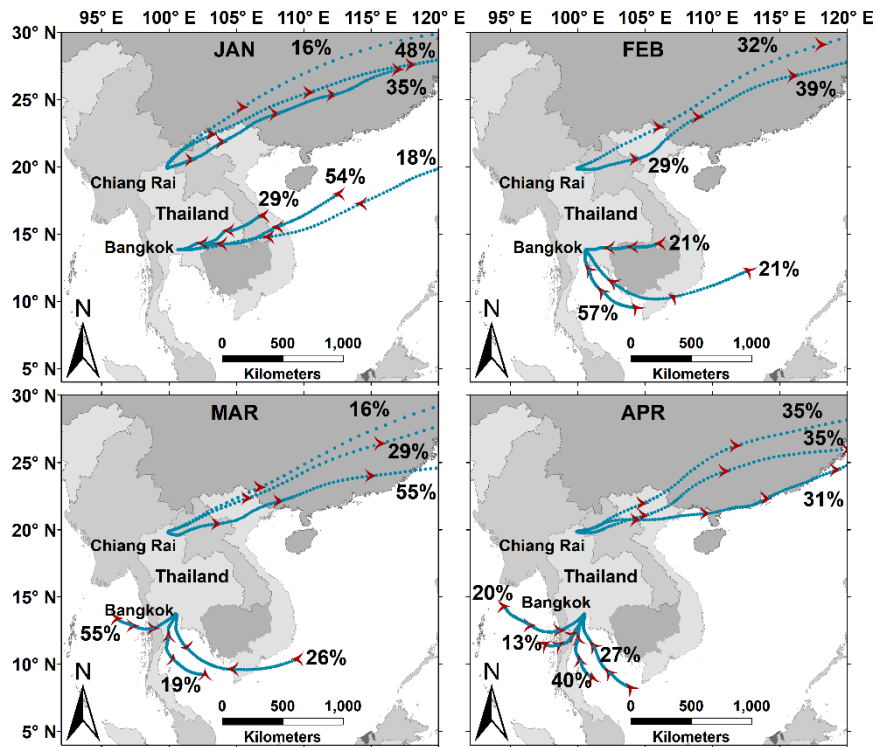
Figure 5.4 Median forward air-mass trajectories of the major clusters initiating at Chiang Rai forward-traced for 120 h and median backward air-mass trajectories of major clusters terminating at Bangkok backtraced for 72 h at 750 m above mean sea-level using the HYSPLIT model through January–April. Red arrows show the flow direction at a 24 h interval
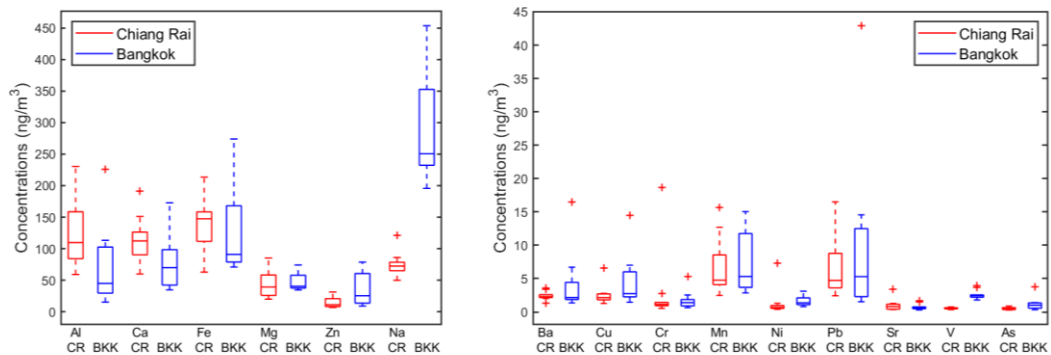
Figure 5.5 Box plot of metal concentrations in Bangkok and Chiang Rai

3.4 Metal concentrations

Concentrations of fifteen metals and metalloid (collectively referred to as metals in this study) are determined in the $PM_{2.5}$ fraction collected from Bangkok and Chiang Rai. The metal concentrations of $PM_{2.5}$ along with their mean, median, and concentration ranges are given in Table 5.1. Box plots of the metal concentrations are given in Figure 5.5. Average concentrations of typically crustal metals such as Al, Ca, Fe, and Sr are higher in Chiang Rai, and many of the industrial, traffic, high-temperature combustion, and sea spray-related metals such as Ba, Cu, Cr, Mg, Mn, Ni, V, Zn, Na, and As are higher in Bangkok. We use elemental ratios, Pearson's correlation coefficient, crustal enrichment factor (EF), and principal component analysis (PCA) to understand the sources of the metals in the two locations.

For mitigation efforts to be successful, source apportionment of metals in atmospheric chemistry is of utmost importance. Often the absolute concentrations are inadequate to pinpoint sources and elemental ratios are more useful. However, the range of emission factor of metals can vary within a factor of 2-10 and result in a large variation of the metal ratios (Nriagu and Pacyna, 1988). We use the ratios Zn/Al and Fe/Al as a qualitative marker to infer the relative importance of possible sources such as biomass burning and remobilized crustal dust (Schlosser et al., 2017; Wagner et al., 2018) by the raging fire. Al and Fe are the 3rd and 4th most abundant elements in the Earth's crust after oxygen and silicon, and the Fe/Al ratio 66 in the crust is typically ~0.48. Zn can come from a variety of sources including coal combustion, nonferrous metal production, and industrial emissions (Nriagu and Pacyna, 1988). In the case of plants, Fe and Zn are micronutrients that are preferentially taken up from soil while Al is considered as a toxin for plants as it inhibits root elongation (Das et al., 2019). Metals emitted from combustion experiments of vegetation from Indonesia (Das et al., 2019) have an Fe/Al ratio (0.20−2.73) and a Zn/Al ratio (0.06−1.70), which are higher than the values of haze-related $PM_{2.5}$ from Chiang Rai (Figure 5.6). The Fe/Al ratio of $PM_{2.5}$ in Chiang Rai ranges from 0.87 to 2.30 and shows a moderately strong negative correlation ($r^2 = -0.72$) with $PM_{2.5}$. This indicates that with increasing haze, the Fe/Al ratio decreases. Figure 5.6 shows that the non-haze $PM_{2.5}$ has Fe/Al > 2, which

decreases to 1.65 during the onset of haze and finally below 1 during the haze period approaching the crustal Fe/Al ratio of 0.48. In contrast, the Fe/Al ratio of Bangkok samples ranges between 1.42 and 5.14, indicating the anthropogenic input of Fe over the crustal background. The Zn/Al ratio of Chiang Rai PM during clear days ranges from 0.08 to 0.31, which decreases during the hazy days to 0.07 to 0.15. Sites with dominant crustal sources show a Zn/Al ratio of 0.05 ± 0.02 in Sagar Island in Bay of Bengal, India (Das et al., 2018) and 0.14 from rural sites near Delhi (Shridhar et al., 2009), which are in the range measured during hazy days in Chiang Rai. In contrast, the Zn/Al ratio of Bangkok PM is higher (0.34—1.54), indicating the anthropogenic input for Zn in Bangkok aerosols. Previous studies from Bangkok reported Zn/Al ratios of 0.13 and 0.20 from two residential sites (Chueinta et al., 2000) and attributed the Zn source to automobile exhaust. The Zn/Al values measured in Bangkok are common in urban settings with anthropogenic Zn sources and are similar to California, USA (1.15), Kashima, Japan (0.50), Ghent, Belgium (1.64), and Brisbane, Australia (0.9) (Chan et al., 1997; Chueinta et al., 2000).
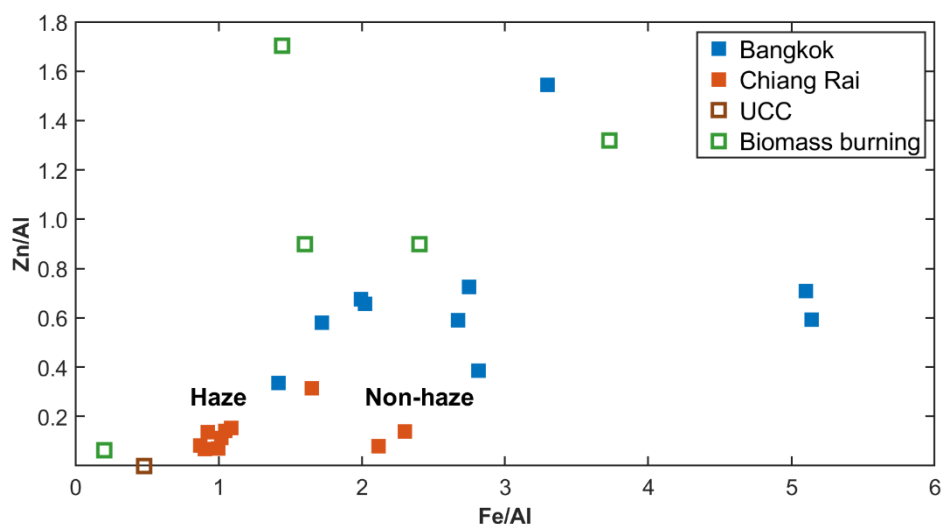
Figure 5.6 Relationship between Fe/Al and Zn/Al in Chiang Rai and Bangkok aerosols. Average UCC ratio and aerosol generated by biomass burning from Indonesia are plotted for reference

Bangkok is situated 30 km north of the Gulf of Thailand and is characterized by the presence of sea salt aerosol (Na = 289 ng/m^3). The Na/Mg ratio observed in Bangkok aerosol (range 3.43─7.17, average 6.07) is close to the typical Na/Mg ratio of sea spray aerosol (approximately 8). Na and Mg in Bangkok aerosol correlate well (r^2 = 0.64), indicating their similar source. Combustion in residential, commercial, and industrial applications can be a major source of Ni and V in PM. Bangkok is notorious for heavy road traffic, which might be the primary source of Ni and V (r^2 = 0.82). The average V/Ni ratio of Bangkok aerosol is 1.76, which is within the range (1.49─2.4) from road traffic (Chifflet et al., 2018). Pb and Zn can have a variety of anthropogenic sources including coal combustion, traffic emissions, and nonferrous metal smelting to name a few. Pb and Zn correlate well in both Chiang Rai (r^2 = 0.90) and Bangkok (r^2 = 0.68), indicating similar sources (Table B-2 and Table B-3). The concentrations of other trace metals such as Ba, Cu, Cr, Mn, and As in Bangkok are higher than those in Chiang Rai probably because Bangkok is located near the industrial estate of Samut Prakan, Chachoengsao, Rayong, and Samut Sakhon and is exposed to industrial emission sources (Yamsrual et al., 2019).

3.5 Enrichment factor

We use crustal EF to understand which of the elements in the aerosol have crustal dust as the primary source. The crustal EF can indicate natural emissions and anthropogenic activities. Calculations are generally based on the average upper continental crustal (UCC) composition given by Rudnick and Gao. The EF of an element in a PM sample is defined as

$$EF = (metal/ref.\ metal)_{aerosol}/(metal/ref.\ metal)_{crust}$$

Al and Fe are commonly used as reference elements although there are no strict requirements for which reference element to use. Bangkok has a high traffic congestion and has numerous industries nearby, both of which can be potential sources of Fe. Hence, Al was chosen as reference element. EF values <5 suggest elements have crustal sources and EF between 5 and 10 is likely to have a minor anthropogenic input over the natural background. Elements with EF between 10 and

100 are likely to be moderately enriched by anthropogenic sources. EF values greater than 100 are most probably related to industrial, high temperature combustion, and vehicular emissions (Sudheer and Rengarajan, 2012; Yin et al., 2012). In Chiang Rai, eight of fifteen measured metals (Ba, Ca, Na, Fe, Mg, Mn, Sr, and V) have EF less than 6 indicating crustal sources. In Bangkok, Ba, Ca, Fe, Mg, and Sr have EF between 4 and 10 indicating moderate enrichment from anthropogenic sources. In Chiang Rai, Ni, Cr, Cu, and As have EF between 10 and 100 and Pb and Zn have EF > 100. In Bangkok Na, Mn, V, Ni, and Cr have EF between 10 and 100 and Cu, As, Pb, and Zn have EF > 100 indicating a strong anthropogenic influence (Figure 5.7). In both the locations, Pb and Zn have the highest EF. A high EF of Zn (153—240) has been reported from Bangkok and the source was attributed to automobile exhaust and refuse incineration (Chueinta et al., 2000). EF of Pb > 100 has been observed in many previous studies and the sources were identified to be coal-based power stations and industrial and vehicular emissions (Pacyna et al., 2009; Yin et al., 2012). The common anthropogenic sources of the moderately enriched metals could be vehicular exhaust for Cu, coal combustion, and vehicular exhaust for Cr, coal combustion for As, and oil combustion for V and Ni. However, solely based on EF and elemental characteristics, source identification of PM cannot be achieved with a reasonable accuracy.
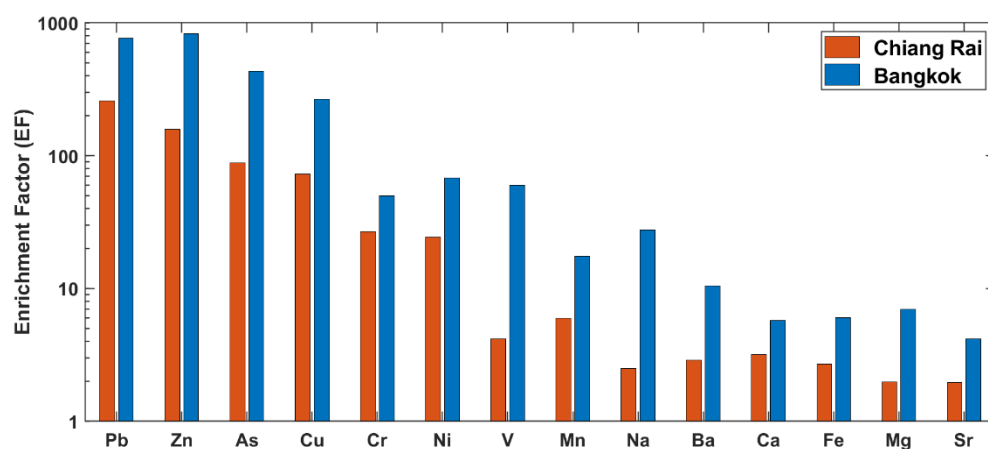
Figure 5.7 Enrichment factor of Chiang Rai and Bangkok aerosol

Table 5.2 Pb Concentration and Pb Isotope Composition of the PM$_{2.5}$ Aerosol Sample

sample	$^{206}Pb/^{204}Pb$	2se	$^{207}Pb/^{204}Pb$	2se	$^{208}Pb/^{204}Pb$	2se	$^{206}Pb/^{207}Pb$	2se	$^{208}Pb/^{207}Pb$	2se	Pb conc. (ng/m^3)	PM$_{2.5}$ (µg/m^3)
CR1	17.9666	0.0017	15.5871	0.0022	37.9279	0.0074	1.1523	0.00005	2.4353	0.00021	6.2	111
CR2	18.1441	0.0091	15.7091	0.0085	38.2184	0.0227	1.1552	0.00012	2.4350	0.00027	4.1	68
CR3	18.0356	0.0029	15.6134	0.0037	38.0025	0.0123	1.1548	0.00007	2.4361	0.00028	2.9	101
CR4	17.8541	0.0029	15.5945	0.0032	37.7718	0.0103	1.1445	0.00007	2.4244	0.00030	8.8	97
CR5	17.9380	0.0027	15.6123	0.0030	37.8613	0.0103	1.1487	0.00007	2.4270	0.00027	9.1	151
CR6	17.9587	0.0026	15.6046	0.0030	37.8546	0.0103	1.1505	0.00006	2.4280	0.00026	4.0	147
CR7	17.8834	0.0019	15.5975	0.0023	37.8015	0.0079	1.1463	0.00005	2.4256	0.00022	17	203
CR8	17.9602	0.0019	15.6068	0.0022	37.9082	0.0075	1.1505	0.00005	2.4310	0.00021	4.2	195
CR9	18.0325	0.0018	15.6138	0.0021	37.9754	0.0074	1.1546	0.00004	2.4341	0.00022	2.4	281
CR10	18.2426	0.0033	15.6453	0.0042	38.2504	0.0139	1.1657	0.00010	2.4468	0.00038	3.6	206
CR11	17.9960	0.0025	15.6105	0.0029	37.9512	0.0098	1.1525	0.00006	2.4331	0.00026	5.3	206
BKK1	17.9800	0.0033	15.6013	0.0044	37.9077	0.0149	1.1522	0.00010	2.4319	0.00041	43	157
BKK2	18.2626	0.0018	15.6254	0.0022	38.1744	0.0077	1.1685	0.00005	2.4450	0.00023	2.2	99
BKK3	17.8754	0.0018	15.5758	0.0022	37.7331	0.0075	1.1473	0.00005	2.4245	0.00021	15	87
BKK4	17.8993	0.0043	15.5842	0.0048	37.8153	0.0157	1.1484	0.00009	2.4285	0.00041	1.5	66
BKK5	17.8964	0.0023	15.5924	0.0028	37.7893	0.0097	1.1474	0.00006	2.4256	0.00028	5.4	80
BKK6	17.8990	0.0018	15.5925	0.0021	37.7910	0.0073	1.1476	0.00005	2.4258	0.00020	12	75
BKK7	17.9914	0.0018	15.6025	0.0021	37.9378	0.0072	1.1529	0.00004	2.4337	0.00020	5.2	109
BKK8	17.9641	0.0019	15.5940	0.0023	37.8689	0.0077	1.1517	0.00006	2.4305	0.00023	2.3	83
BKK9	17.8279	0.0019	15.5759	0.0024	37.7055	0.0081	1.1443	0.00005	2.4228	0.00023	7.2	79
BKK10	17.6562	0.0029	15.5617	0.0034	37.5332	0.0111	1.1343	0.00007	2.4138	0.00028	3.2	75
	$^{206}Pb/^{204}Pb$	2SD	$^{207}Pb/^{204}Pb$	2SD	$^{208}Pb/^{204}Pb$	2SD	$^{206}Pb/^{207}Pb$	2SD	$^{208}Pb/^{207}Pb$	2SD		
NBS 981 (true value)	16.93736						1.0933	0.0004	2.3704	0.0012		
NIST 981 (n = 22)	16.9259	0.0022	15.4779	0.0027	36.6591	0.0086	1.0935	0.0001	2.3684	0.0002		
procedural blank (n = 3)	18.9395	0.3205	17.1765	0.2892	40.4743	0.6835	1.1051	0.0030	2.3632	0.0023		

^{a}NBS 981 true value is taken from Baker et al., 2004.[43]
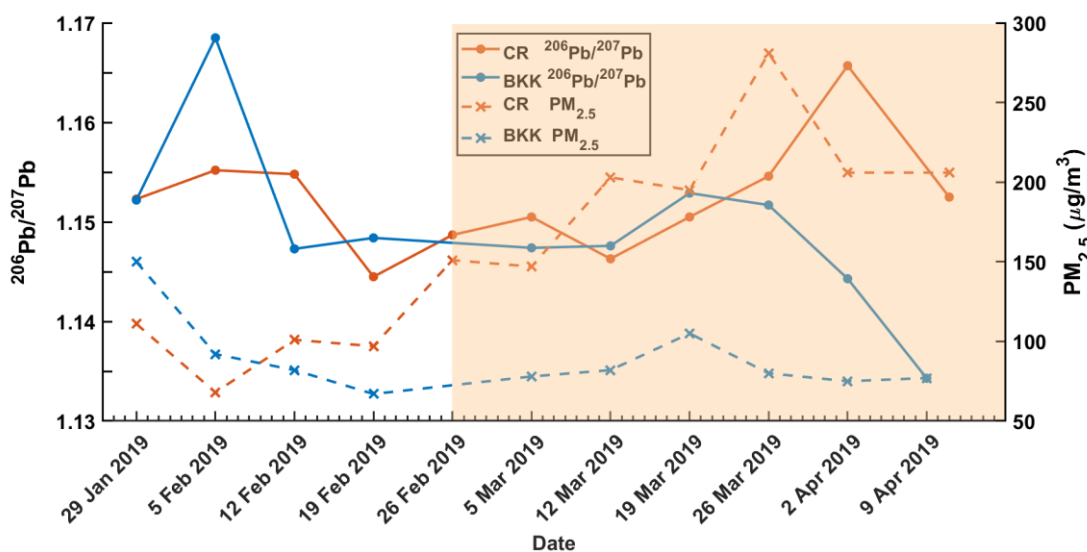
Figure 5.8 Time series plot of the $^{206}Pb/^{207}Pb$ ratio and $PM_{2.5}$ during January to April 2019 in Bangkok and Chiang Rai. The shaded area shows the burning season.

3.6 Statistical Analysis

We use PCA of the Statistical Package for the Social Sciences (SPSS) version 22 to analyze sources of metals during the burning season in the two different locations. PCA is a statistical technique based on variations in the sequencing data and brings out strong patterns in a dataset. It is often used in environmental studies. Only the factors with eigenvalues higher than 1 were selected. The Varimax rotated Kaiser-normalized component matrix results indicate three possible factors representing three different contributing sources in both the locations. The loadings of variables on factors, communalities, eigenvalues, percentage variance, and percentage cumulative variance are given in Table B-4.
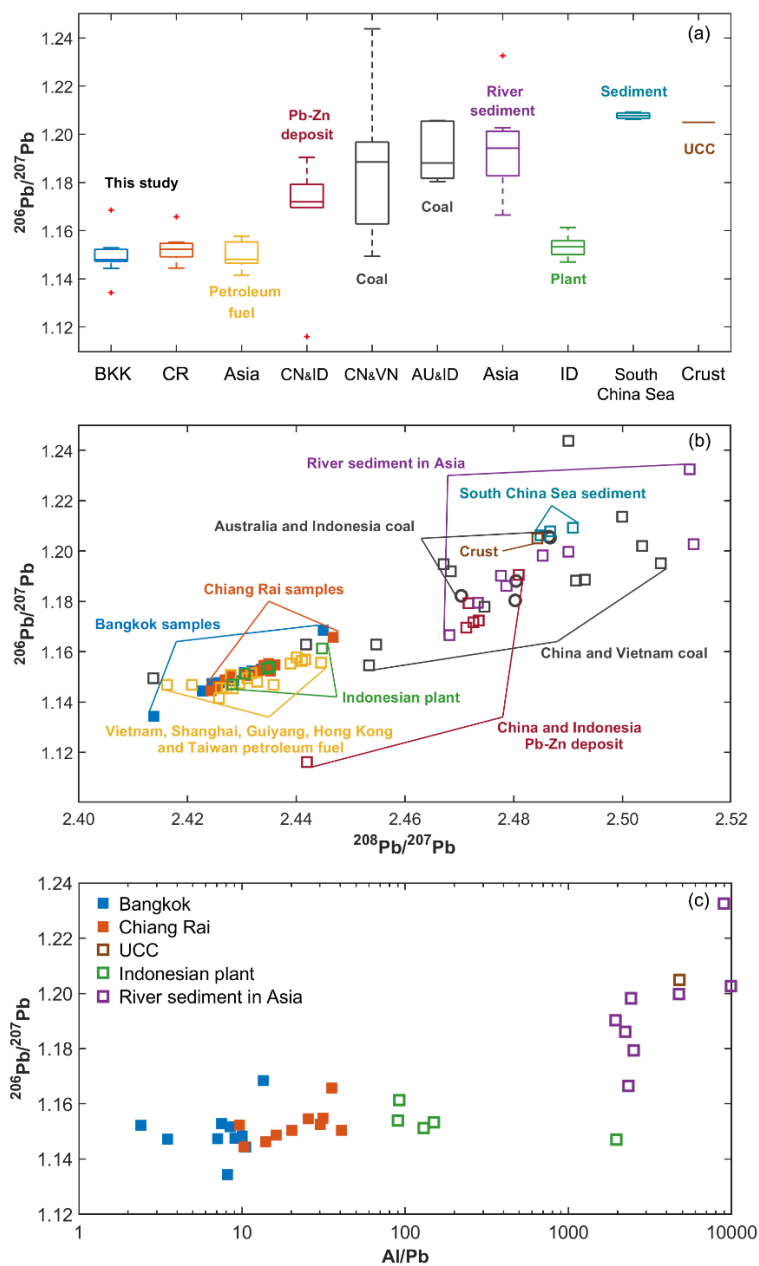
Figure 5.9 (a) Box plot of the ^{206}Pb/^{207}Pb ratio in this study (Bangkok and Chiang Rai), in comparison with petroleum fuels from southeast Asia, Pb–Zn ore deposits from China (CN) and Indonesia (ID), coal from China (CN), Vietnam (VN), Australia (AU), and Indonesia (ID), river sediment in Asia, Indonesian plant (Das et al., 2019-Goldschmidt abstract), South China Sea sediment, and average UCC. (b) Pb triple isotope Plot of Chiang Rai and Bangkok aerosols, in comparison with different possible anthropogenic end members. (c) Plot of ^{206}Pb/^{207}Pb ratio vs Al/Pb of Chiang Rai and Bangkok aerosols from this study, in comparison with average UCC and river sediments in Asia as representative of crust soil in the region and Indonesian plant as representative of biomass burning aerosol from northern Thailand

In Chiang Rai, 86.14% of the variation can be explained by three factors. The first factor explains 46.59% variance of the data and shows high loading for Al, Ba, Ca, Fe, Mg, Pb, Sr, V, and Zn (0.608-0.959). Most of these metals (except Pb and Zn) have EF < 6 indicating the crustal origin. Hence, the first factor possibly denotes metals with crustal dust (Kim et al., 2012) and biomass burning (Pb and Zn) as the primary source (Ryu et al., 2004). The second factor explains 20.96% of the variance and shows a high loading for Cr, Ni, and Mn (0.852-0.974). These metals indicate emission from the industrial source (Qi et al., 2016). The third factor shows a high loading of Cu (0.937) and Na (0.914) explaining 18.59% of the variance. Strong correlation between Cu and Na (0.889) (see the Table B-2) suggests that the two metals have similar emission sources such as refuse incineration mixed with road dust (Council, 2000; Ooki et al., 2002).

In Bangkok, 54.97% of the variance is observed in factor 1 that shows a high loading of Al, Ba, Ca, Cu, Fe, Mn, Pb, Sr, Zn, and As (0.704-0.973). These metals represent a mixture of natural and anthropogenic sources. Cu, Pb, and Zn have EF > 100 and can originate from industrial emissions and coal combustion (Aunela-Tapola et al., 1998). Factor 2 explains 14.78% variance and has a high loading of Ni (0.855) and V (0.947). Strong correlation of Ni and V coupled with a V/Ni ratio in the range of road traffic emission (see the Table B-3) suggests that the two metals are sourced from fossil fuel combustion (Chifflet et al., 2018). Factor 3 shows a high loading of Mg (0.864) and Na (0.700) and has 12.98% variance of the data. Mg and Na show good correlation with the Na/Mg ratio close to that of marine aerosol (Magesh et al., 2020; Pani et al., 2017; Wu et al., 2019). During the biomass burning season in the northern provinces, entire Thailand is covered by fine PM. However, the disparity in trace metal systematics between Chiang Rai and Bangkok indicates that the metals are possibly not transported down south to Bangkok.

3.7 Pb isotopic composition

Atmospheric Pb can be emitted by anthropogenic processes such as vehicle exhausts, coal combustion, and high-temperature industrial processes. Pb isotopes provide a powerful tool to investigate Pb pollution and identify the origin of the metal. The amount of Pb isotopes presented in a system is determined by the relative proportion of initial U-Th-Pb, which varies with the origin or geological conditions. The Pb isotope ratios, Pb, and $PM_{2.5}$ concentrations are given in Table 5.2. The Pb isotope ratios of the NBS 981 standard and procedural blank are also given in Table 5.2.

Pb concentrations in the $PM_{2.5}$ in Chiang Rai and Bangkok range from 2.43 to 16.50 (6.29 ± 4.25, 1SD) and 1.53 to 42.91 (9.69 ± 12.47, 1SD) ng/m^3, respectively. However, if only the burning season is considered, average Pb in Bangkok (5.95 ± 3.64, 1SD) is lower than that in Chiang Rai (6.44 ± 4.91, 1SD). Pb concentrations in both Bangkok and Chiang Rai do not correlate with $PM_{2.5}$. However, in Bangkok, only BKK 1 shows very high Pb (42.91 ng/m^3) and $PM_{2.5}$ (157 $\mu g/m^3$) concentrations. The $^{206}Pb/^{207}Pb$ ratios in Chiang Rai range from 1.1445 to 1.1657 (1.1523 ± 0.0056, 1SD) and the $^{208}Pb/^{207}Pb$ ratios range from 2.4244 to 2.4468 (2.4324 ± 0.0063, 1SD), and the $^{206}Pb/^{207}Pb$ ratios in Bangkok show a larger variation, 1.1343—1.1685 (1.1495 ± 0.0085, 1SD) and the $^{208}Pb/^{207}Pb$ ratios range between 2.4138 and 2.4450 (2.4282 ± 0.0081, 1SD).

A time series plot of the $^{206}Pb/^{207}Pb$ ratio and $PM_{2.5}$ in Chiang Rai and Bangkok shows that the $^{206}Pb/^{207}Pb$ ratio in Chiang Rai follows the $PM_{2.5}$ during the burning season and the ratio increases with $PM_{2.5}$ (Figure 5.8), indicating that at least a part of the Pb is burning related. Normally, Bangkok records high $PM_{2.5}$ concentrations during December and January due to thermal inversion. For the remaining ten months, average Bangkok $PM_{2.5}$ remains lower than 100 $\mu g/m^3$ (Wimolwattanapun et al., 2011). During the haze, the $PM_{2.5}$ concentration and the $^{206}Pb/^{207}Pb$ ratio in Bangkok do not show much variation. The Pb isotopic composition of atmospheric aerosol results from mixing of many different sources. We present an overview of the Pb isotopic compositions (mainly $^{206}Pb/^{207}Pb$) of different possible anthropogenic sources from the region as published in the literature to understand the source(s).

Figure 5.9a presents the range of $^{206}Pb/^{207}Pb$ ratios of Chiang Rai and Bangkok aerosols along with the plausible end members of anthropogenic Pb. Atmospheric Pb emission from vehicular exhaust has significantly reduced in Thailand after 1991 when leaded gasoline was phased out (Sayeg, 1998). However, even considering the very low Pb concentrations in fuels, the heavy road traffic, particularly in Bangkok, must magnify Pb emissions to the atmosphere (Thorpe and Harrison, 2008). $^{206}Pb/^{207}Pb$ ratios of the unleaded petroleum fuel from the region (Vietnam, Shanghai, Guiyang, Hong Kong, and Taiwan) range from 1.1415 to 1.1577 (Chen et al., 2005; Chifflet et al., 2018; Duzgoren-Aydin et al., 2004; Yao et al., 2016; Zhao et al., 2015). Most of the aerosols collected from Bangkok (except BKK 2 and BKK 10) and Chiang Rai (except CR 10) plots in this range. Hence, the gasoline exhaust can be a potential source of Pb, at least in Bangkok aerosols.

The second plausible Pb source can be high-temperature industries such as roasting and smelting of ores in nonferrous metal smelters. Pb-Zn ores from different geochemical provinces in the region (north and northeast China, Yangtze Province, and Indo-china geochemical Province) have a wide range of $^{206}Pb/^{207}Pb$ (1.091-1.194) (Bing-Quan et al., 2002). However, in a Pb triple isotope plot ($^{206}Pb/^{207}Pb$ vs $^{208}Pb/^{207}Pb$) (Figure 5.9b), the Pb-Zn ores do not plot on a linear mixing trend with the aerosol samples implying they are less likely to be a major contributor to the aerosol Pb.

Post phasing out of leaded gasoline, Pb emissions from coal combustion have increased by an order of magnitude (Lee et al., 2014). Thailand imports coals from Indonesia and Australia (Energy Policy and Planning Office Ministry of Energy, www.eppo.ac.th). The $^{206}Pb/^{207}Pb$ ratios of Indonesian coal range from 1.1804 to 1.1881 (Díaz-Somoano et al., 2009), whereas those of Australian coal range between 1.2053 and 1.2057 (Díaz-Somoano et al., 2009). Though all the $^{206}Pb/^{207}Pb$ ratios in the Bangkok and Chiang Rai aerosols are lower than those in Australian and Indonesian coal, the coal combustion emissions can be a mixing end member. The residence time of Pb aerosols in the atmosphere is around ∼5-10 days (Sturges and Barrie, 1987). Hence, transboundary pollution remains an important source of atmospheric aerosols. Long-range transport of coal combustion Pb is also a possibility from Southeast Asian

countries. Pb isotopes of coal from Vietnam (Bollhöfer and Rosman, 2000; Chifflet et al., 2018) ($^{206}Pb/^{207}Pb$ ranges between 1.1494 and 1.1950) and China (Chen et al., 2005; Díaz-Somoano et al., 2009; Mukai et al., 1993; Zhao et al., 2015) ($^{206}Pb/^{207}Pb$ ranges between 1.1546 and 1.2438) are plotted for reference in Figure 5.9a,b.

Apart from the above-mentioned anthropogenic sources, Pb can come from biomass burning in Chiang Rai. Remobilized mineral dust from the desiccated soil during wildfire could be a significant source of atmospheric Pb (Ito and Shi, 2016; Wagner et al., 2018). $^{206}Pb/^{207}Pb$ of average UCC is 1.1924 (Millot et al., 2004), river sediments in Asia are 1.1672—1.2325 (Millot et al., 2004) and biomass from the region is 1.1410-1.1613 (Das et al., 2019- Goldschmidt abstract, https://goldschmidtabstracts.info/abstracts/abstractView?id=2019001124).

In summary, the Pb isotope ratios of the PM alone are unable to differentiate between the possible end member sources because their isotopic compositions have overlapping ranges (Figure 5.9a) and several of the plausible end members plot on linear mixing trend (Figure 5.9b). In order to understand the source(s) of atmospheric Pb, we combined Pb isotope ratios and trace metal systematics because natural and anthropogenic end members should have distinct trace metal signatures. From trace metal systematics, it is evident that during haze, dominance of crustal metals such as Al increases in Chiang Rai. Hence, we select Al to ratio with Pb. In Figure 5.9c, the Al/Pb ratio of the Chiang Rai samples ranges from 9.61 to 40.63 and correlates well with $^{206}Pb/^{207}Pb$ (r^2 = 0.61). The Bangkok aerosols have a much lower Al/Pb ratio (2.39—13.52) and do not show any significant correlation with the Pb isotopes (r^2 = 0.33). However, it is to be noted that sample BKK 2 has the highest $^{206}Pb/^{207}Pb$ ratio among all the Bangkok aerosols and also the highest Al/Pb ratio (13.52). This indicates that crustal dust can play an important role during the fire and contribute significantly toward atmospheric Pb. For comparison, the Al/Pb ratios of biomass from Indonesia and average UCC (Rudnick and Gao, 2003) and river sediments in Asia (Millot et al., 2004) are plotted in Figure 5.9c.

From the trace metals and Pb isotopes, it is evident that during haze, there is some degree of mixing of PM from biomass burning and crustal dust with the background. The average Pb isotope ratios ($^{206}Pb/^{207}Pb$ = 1.1517 ± 0.0050, 1SD and $^{208}Pb/^{207}Pb$ = 2.4327 ± 0.0056, 1SD) during clear day is considered to be the background. Biomass and mineral soil composition from northern Thailand were not measured in this study, and hence, we had to rely on the existing literature for these plausible end member Pb isotopic compositions. We use the average of the Indonesian plants (Das et al., 2019-Goldschmidt abstract) for biomass composition. For regional crustal sediment composition, average of the large river sediments from South and Southeast Asia (Millot et al., 2004) (India, Bangladesh, Myanmar, and Vietnam) is used. Sediment samples from large river deltas are large-scale integrated samples of the weathering products of the present-day UCC. To obtain an isotope-mixing model, iterative percentages of each component's abundance were used. The most radiogenic Pb isotopes (CR 9 and CR 10) during peak haze can be explained by ~5 and 30% mixing of crustal dust with ~35 and 40% biomass burning generated aerosols with the background.

A decade-long study on wildfires in western United States demonstrated that crustal dust is significantly enhanced in wildfire plume identified based on enrichments of typical crustal metals such as Si, Ca, Al, Fe, and Ti in fine aerosol (Schlosser et al., 2017). High resolution large-eddy simulation, conducted with the all scale atmospheric model demonstrated that the energy released by the fires controls the near-surface wind patterns and mobilize dust particles (Wagner et al., 2018). However, to what extent mineral dust will be mobilized depends primarily on fire properties such as fire size, intensity, and shape, in addition to the ambient wind velocities.

4. Conclusion

Air pollutants released from forest fires and stubble burning in northern Thailand are of major concern to human health, ecosystem, and climate. Images of size-resolved aerosols from MODIS-Terra satellite show that entire Thailand is covered with high concentrations of fine-sized aerosol during the peak fire from mid-March to April. However, forward air mass trajectories from northern Thailand provinces show winds mostly flow toward north and northeast toward mainland China, whereas Bangkok in southern Thailand receives air mass from the South China Sea and Bay of Bengal. Metal composition of $PM_{2.5}$ from Chiang Rai during haze shows high concentrations of crustal metals and may have three primary sources: 1, crustal dust and biomass burning, 2, industrial source, and 3, refuse incineration mixed with road dust. Bangkok $PM_{2.5}$ metals are influenced by 1, natural background mixed with industrial emissions and coal combustion, 2, traffic emission, and 3, sea spray. The Pb isotope ratio ($^{206}Pb/^{207}Pb$) in Chiang Rai aerosol increases with increasing haze (and $PM_{2.5}$) and correlates well with the crustal metal to Pb ratio (Al/Pb), indicating that at least part of the Pb is derived from crustal dust during increasing fire. However, no such pattern is observed in Bangkok. From the $PM_{2.5}$ concentrations, wind trajectories, AOD and AE observations, and trace metal and Pb isotope analysis, it is concluded that during peak fires, crustal dust can form a significant source of Pb and other metals in the aerosol. Though entire Thailand is covered with fine aerosols during the peak fire in northern provinces, it is not evident that long-range atmospheric metal transport occurs from fire hotspots to southern Thailand. Local sources and sea spray remain the primary sources of metals in $PM_{2.5}$ in Bangkok.

Acknowledgments

จุฬาลงกรณ์มหาวิทยาลัย

CHULALONGKORN UNIVERSITY

CHAPTER 6 SUMMARY AND CONCLUSIONS

Bangkok, Chonburi and Chiangrai are located in different geographical region of Thailand. Bangkok and Chonburi are the coastal cities with distinct characteristics. Bangkok is a capital city which current population is approx. 10.5 million. Traffic congestion in Bangkok is one of the top ranks in the world. Consequently, the well-known of air pollution which resulting from traffic emission and endless construction activities, as well as industrial emissions. Chonburi is situated along the east of the upper Gulf of Thailand (GoT). It is a major tourist destination and an industrial estate. Chonburi is included in the National Economic and Social Development Plan of Thailand since the discovery of natural gas in the GoT. Many industries including industrial estates, oil refineries and deep-sea port were developed under the Eastern Seaboard Development Program since 1982. Recently, Chonburi is included in the Eastern Economic Corridor (EEC), a strategic plan under Thailand 4.0 announced in 2016. Meanwhile, Chiangrai is the utmost northern province of Thailand sharing the border with Laos and Myanmar. Land use and Land cover in Chiangrai and neighboring areas are mainly natural forest and agricultural land, with scattering small towns and municipals. Most time of the year (9—10 months), Chiangrai has a pristine atmosphere, which drastically changes during agricultural field open burning either pre-harvest or post-harvest. Biomass open burning, both forest fires from land clearing and agricultural residue burnings, is an on-going manmade activity which create air pollutants into the atmosphere. In northern part of Southeast Asia (Thailand, Myanmar, Laos and Cambodia), it generally occurs in January to April, while in Indonesia is during July to September. These are a major cause of transboundary haze pollution in Southeast Asia.

The atmospheric circulation of aerosols in Thailand is controlled by monsoons, e.g., NE monsoon, SW monsoon and inter-monsoon (Figure 6.1). The backward trajectories indicate that the NE monsoon winds travel extensively over landmasses before reaching Thailand. In SW monsoon, the wind originates over the Indian ocean blow toward Thailand. While inter-monsoon period the wind blow from the South

China Sea and pass-through Vietnam before reaching Thailand. In detail during NE monsoon Bangkok has low surface wind coupled with thermal inversion, the aerosols can trap over the ground surface. While Chonburi is situated along the coast, the atmosphere is dominated by marine aerosol all over the year. In Chiangrai, the atmosphere during January to April is influences by biomass open burning.
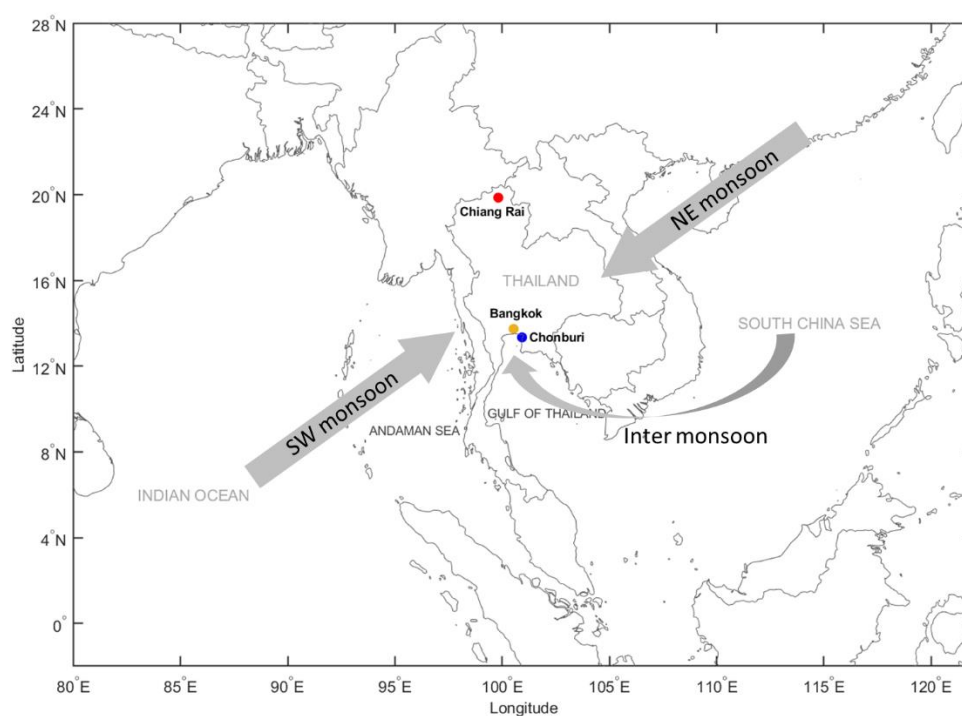
Figure 6.1 The atmospheric circulation of aerosol in Thailand

6.1 Seasonal variation and air-sea-land influences on chemical composition of aerosols over coastal cities

The PM$_{2.5}$ aerosols samples in Bangkok and Chonburi were collected in three monsoon periods during 2018-2019, with weekly or bi-weekly sampling intervals.

The PM$_{2.5}$ concentrations in Bangkok was higher than Chonburi for all seasons. Moreover, PM$_{2.5}$ concentrations in Bangkok and Chonburi are highest during NE monsoon followed by inter monsoon and SW monsoon. The NE monsoon winds blow over landmasses before reaching Bangkok and Chonburi, whereas during the SW and

inter monsoons, the wind originates over the ocean and are far less influenced by anthropogenic emission sources.

During NE monsoon, sea spray aerosols concentrations in the atmospheric over Bangkok and Chonburi are high, especially Chonburi. Sodium (Na), a tracer for marine aerosols, was in the range of 104–682 and 332–3793 ng/m with the average 234 and 300 ng/m in Bangkok and Chonburi, respectively. The results of Pb isotope ratios revealed that the possible anthropogenic contributors in both Bangkok and Chonburi could be influenced by long-range transport of coal combustion emissions from China and Vietnam and natural background of crustal soil dust. It is well known that traffic emission is one of the major problems in both locations.

The concentrations of Na and Mg were the highest during SW monsoon in comparison to other periods owing to the sea spray origin. The high concentration of V, Ni and Cu, which are indicator of oil combustion, in Chonburi during the SW monsoon winds indicated possible influences from oil refineries located south of the coastal town. In general, sources of Pb metals in Chonburi's aerosols during SW monsoon were influenced by long-range transport of coal combustion emissions and ore processing and mixing with road traffic emissions in addition to the natural background. When the SW monsoon winds reach Bangkok, local pollution sources become significant contributors of aerosols.

Chemical composition in aerosols in the inter monsoon winds had several chemical similarities with those of the SW monsoon winds. Overall sources in inter-monsoon winds were influenced by natural background and coal combustion.

6.2 Chemical composition of the aerosols over Thai waters

The sampling was conducted during SW monsoon 2018 in both GoT and Andaman Sea. Aerosols sample was collected by M.V. SEAFDEC-2 (18th August to 18th October) in GoT and R.V. Dr.Fridtjof Nansen (1st to 15th October) in Andaman Sea. The GoT samples were collected at approx. 10 m above sea surface, while the Andaman samples were operated approx. 22 m above sea surface. Two size classes of aerosols

were collected in the GoT, $PM_{10-2.5}$ and $PM_{2.5}$, while Andaman Sea only $PM_{2.5}$ was collected.

The chemical composition of the aerosols over the GoT was studied in $PM_{10-2.5}$ and $PM_{2.5}$. The WSIIs results in $PM_{10-2.5}$ indicated the domination of sea spray components, e.g., Na^+, K^+, Mg^{2+}, Ca^{2+}, Cl^-, and SO_4^{2-}. The Cl^- and Na^+ ions are the major ions, accounting for ~72.5% and ~64.1% of the total ions in coarse and fine particles, respectively. In addition, the Cl/Na molar ratio of 1.5 and 1.3 for coarse and fine particles, respectively, which are close to the Cl/Na ratio of marine aerosols. While coarse particles ($PM_{10-2.5}$) contain mostly sea salt aerosols, fine particles ($PM_{2.5}$) are the mixture of low concentration sea salt aerosols and anthropogenic aerosols (nss-$PM_{2.5}$). Nss-SO_4^{2-}, nss-K^+ and nss-Ca^{2+} were mainly found in near-shore aerosols especially in the upper GoT, indicating the anthropogenic sources. The fraction of nss-SO_4^{2-}, a tracer for anthropogenic sources, in overall marine aerosols of the GoT accounted for 52.5% of total SO_4^{2-} in $PM_{2.5}$.

Metal is another tracer of anthropogenic sources. Metals (such as Sr, Ca, Mg and Na) in $PM_{2.5}$ showed high concentration of ions from sea spray. Crustal dust containing Mn, Fe, and Al can be found in the near-shore aerosols. The EF of As, Pb, Cd, Cu, Cr, Ni and Zn indicated the influence of anthropogenic activities. V which is considered to be a metal from oil combustion, is found in significant amount in aerosols collected over the upper GoT and Cambodian waters. V/Ni ratios show that the aerosols in both areas were influences by petroleum fuel from traffic. For the upper GoT, it was most likely impacted by traffic emissions from coastal cities around, while Cambodian waters was likely southern Vietnam being one of the sources affecting. The aerosols over the southern GoT indicated somewhat significant influences by peatland burning from Sumatra, Indonesia. However, it needs to be confirmed by Pb isotope ratios.

The chemical composition in the aerosols over the Andaman Sea was analyzed only in $PM_{2.5}$. As the sampling height was higher than those in the GoT, lower concentrations were found in the Andaman samples particularly sea salt ions. However, the aerosols were clearly dominated by sea spray. From metal Enrichment

Factor and 72 hours back-trajectory analysis reveals that aerosols over Andaman Sea originate from marine sources and little influence from terrestrial. However, the metal data indicated some samples had influenced by anthropogenic activities in a lesser extent.

6.3 Influence of biomass burning in northern Thailand on aerosols over Bangkok metropolis

The weekly $PM_{2.5}$ aerosols were sampled during 2019 burning season (January to April) in both Bangkok and Chiangrai. During the peak fire from mid-March to April, northern Thailand is covered with high concentrations of fine particles. Elemental ratios coupled with Pb isotope ratios indicate influences of (1) crustal dust and biomass burning, (2) industrial source, and (3) refuse incineration mixed with road dust, in Chiangrai's aerosols. Meanwhile, Bangkok during haze period is influenced by (1) natural background mixed with industrial emission and coal combustion, (2) traffic emission, and (3) sea spray, indicated that the effect of biomass burning did not reach Bangkok. This is confirmed by forward air mass trajectories from northern Thailand provinces. Thus, it was not evident that long-range atmospheric metal transport occurred from fire hotspots reaching Bangkok. Local sources and sea spray remained the primary sources of metals in Bangkok's aerosols.

6.4 Recommendation for further study

Metals in aerosols often exist in trace amounts (low ng/m^3 level), so contamination of dust in the laboratory might dramatically change in metal concentration and incorrect isotope ratios, leading to overestimate metal concentration and misinterpretation in source apportionment. Therefore, clean technique has to be applied, and clean laboratory is required in sample preparation steps of metal analysis. The clean environment at least in the laminar flow cabinet or clean bench is a basic need in the preparation step of environmental samples for metal analysis.

Furthermore, rainwater is one of the important that remove aerosols and the associated contaminants from the atmosphere through wet deposition. Therefore, it is worth to take rainwater into account for the future research.

REFERENCES

Abram, N.J., Gagan, M.K., McCulloch, M.T., Chappell, J. and Hantoro, W.S. Coral reef death during the 1997 Indian Ocean Dipole linked to Indonesian wildfires. Science 301(5635) (2003): 952-955.

Ahmed, M., Guo, X. and Zhao, X.-M. Determination and analysis of trace metals and surfactant in air particulate matter during biomass burning haze episode in Malaysia. Atmospheric Environment 141 (2016): 219-229.

Al-Saadi, J., Szykman, J., Pierce, R.B., Kittaka, C., Neil, D., Chu, C.A., Remer, L., Gumley, L., Prins, E., Weinstock, L., MacDonald, C., Wayland, R., Dimmick, F. and Fishman, J. Improving National Air Quality Forecasts with Satellite Aerosol Observations. Bulletin of the American Meteorological Society 86(9) (2005): 1249-1262.

Alghasham, A.A., Meki, A.-R.M.A. and Ismail, H.A.S. Association of Blood Lead level with Elevated Blood Pressure in Hypertensive Patients. International journal of health sciences 5(1) (2011): 17-27.

Arimoto, R., Duce, R.A., Ray, B.J. and Unni, C.K. Atmospheric trace elements at Enewetak Atoll: 2. Transport to the ocean by wet and dry deposition. Journal of Geophysical Research: Atmospheres 90(D1) (1985): 2391-2408.

Aunela-Tapola, L.A., Frandsen, F.J. and Häsänen, E.K. Trace metal emissions from the Estonian oil shale fired power plant. Fuel Processing Technology 57(1) (1998): 1-24.

Baker, J., Peate, D., Waight, T. and Meyzen, C. Pb isotopic analysis of standards and samples using a ^{207}Pb–^{204}Pb double spike and thallium to correct for mass bias with a double-focusing MC-ICP-MS. Chemical Geology 211(3) (2004): 275-303.

Balakrishnaiah, G., Raghavendra, K.K., Suresh, K.R.B., Rama, G.K., Reddy, R.R., Reddy, L.S.S., Nazeer A.Y., Narasimhulu, K. and Suresh, B.S. Analysis of optical properties of atmospheric aerosols inferred from spectral AODs and Ångström wavelength exponent. Atmospheric Environment 45(6) (2011): 1275-1285.

Betha, R., Pradani, M., Lestari, P., Joshi, U.M., Reid, J.S. and Balasubramanian, R. Chemical speciation of trace metals emitted from Indonesian peat fires for health risk assessment. Atmospheric Research 122 (2013): 571-578.

Bing-Quan, Z., Yu-Wei, C. and Xiang-Yang, C. Application of Pb isotopic mapping to environment evaluation in China. Chemical Speciation & Bioavailability 14(1-4) (2002): 49-56.

Bollhöfer, A. and Rosman, K.J.R. Isotopic source signatures for atmospheric lead: the Southern Hemisphere. Geochimica et Cosmochimica Acta 64(19) (2000): 3251-3262.

Bollhöfer, A. and Rosman, K.J.R. Isotopic source signatures for atmospheric lead: the Northern Hemisphere. Geochimica et Cosmochimica Acta 65(11) (2001): 1727-1740.

Bond, T.C., Bhardwaj, E., Dong, R., Jogani, R., Jung, S., Roden, C., Streets, D.G. and Trautmann, N.M. Historical emissions of black and organic carbon aerosol from energy-related combustion, 1850–2000. Global Biogeochemical Cycles 21(2) (2007).

Boonpeng, C., Polyiam, W., Sriviboon, C., Sangiamdee, D., Watthana, S., Nimis, P.L., and Boonpragob, K. Airborne trace elements near a petrochemical industrial complex in Thailand assessed by the lichen Parmotrema tinctorum (Despr. ex Nyl.) Hale. Environmental Science and Pollution Research 24(13) (2017): 12393-12404.

Brimblecombe, P. 10.14 - The Global Sulfur Cycle. in Holland, H.D. and Turekian, K.K. (eds.), Treatise on Geochemistry (Second Edition). 559-591. Oxford: Elsevier, 2014.

Buck, C.S., Aguilar-Islas, A., Marsay, C., Kadko, D. and Landing, W.M. Trace element concentrations, elemental ratios, and enrichment factors observed in aerosol samples collected during the US GEOTRACES eastern Pacific Ocean transect (GP16). Chemical Geology 511 (2019): 212-224.

Carrasco, G., Chen, M., Boyle, E.A., Tanzil, J., Zhou, K. and Goodkin, N.F. An update of the Pb isotope inventory in post leaded-petrol Singapore environments. Environmental Pollution 233 (2018): 925-932.

Chan, Y.C., Simpson, R.W., McTainsh, G.H., Vowles, P.D., Cohen, D.D. and Bailey, G.M. Characterisation of chemical species in $PM_{2.5}$ and PM_{10} aerosols in Brisbane, Australia. Atmospheric Environment 31(22) (1997): 3773-3785.

Charlson, R.J., Lovelock, J.E., Andreae, M.O. and Warren, S.G. Oceanic phytoplankton, atmospheric sulphur, cloud albedo and climate. Nature 326(6114) (1987): 655-661.

Chen, J., Tan, M., Li, Y., Zhang, Y., Lu, W., Tong, Y., Zhang, G. and Li, Y. A lead isotope record of shanghai atmospheric lead emissions in total suspended particles during the period of phasing out of leaded gasoline. Atmospheric Environment 39(7) (2005): 1245-1253.

Chen, Z., Chen, D., Zhao, C., Kwan, M-P., Cai, J., Zhuang, Y., Zhao, B., Wang, X., Chen, B., Yang, J., Li, R., He, B., Gao, B., Wang, K. and Xu, B. Influence of meteorological conditions on $PM_{2.5}$ concentrations across China: A review of methodology and mechanism. Environment International 139 (2020): 105558.

Chester, R., Berry, A.S. and Murphy, K.J.T. The distributions of particulate atmospheric trace metals and mineral aerosols over the Indian Ocean. Marine Chemistry 34(3) (1991): 261-290.

Chester, R. and Bradshaw, G.F. Source control on the distribution of particulate trace metals in the North Sea atmosphere. Marine Pollution Bulletin 22(1) (1991): 30-36.

Chester, R. and Jickells, T. The Transport of Material to the Oceans: The Atmospheric Pathway. in Marine Geochemistry. 52-82, 2012.

Chifflet, S., Amouroux, D., Bérail, S., Barre, J., Van, T.C., Baltrons, O., Brune, J., Dufour, A., Guinot, B. and Mari, X. Origins and discrimination between local and regional atmospheric pollution in Haiphong (Vietnam), based on metal(loid) concentrations and lead isotopic ratios in PM_{10}. Environmental Science and Pollution Research 25(26) (2018): 26653-26668.

Choobari, O.A., Zawar-Reza, P. and Sturman, A. The global distribution of mineral dust and its impacts on the climate system: A review. Atmospheric Research 138 (2014): 152-165.

Chuang, M.-T., Lee, C.-T., Chou, C.C.-K., Engling, G., Chang, S.-Y., Chang, S.-C., Sheu, G.-R., Lin, N.-H., Sopajaree, K., Chang, Y.-J. and Hong, G.-J. Aerosol transport from Chiang Mai, Thailand to Mt. Lulin, Taiwan – Implication of aerosol aging during long-range transport. Atmospheric Environment 137 (2016): 101-112.

Chueinta, W., Hopke, P.K. and Paatero, P. Investigation of sources of atmospheric aerosol at urban and suburban residential areas in Thailand by positive matrix factorization. Atmospheric Environment 34(20) (2000): 3319-3329.

Chuesaard, T., Chetiyanukornkul, T., Kameda, T., Hayakawa, K. and Toriba, A. Influence of Biomass Burning on the Levels of Atmospheric Polycyclic Aromatic Hydrocarbons and Their Nitro Derivatives in Chiang Mai, Thailand. Aerosol and Air Quality Research 14(4) (2014): 1247-1257.

National Research Council. Waste Incineration and Public Health. Washington, DC: The National Academies Press, 2000.

Cui, W., Meng, Q., Feng, Q., Zhou, L., Cui, Y. and Li, W. Occurrence and release of cadmium, chromium, and lead from stone coal combustion. International Journal of Coal Science & Technology 6(4) (2019): 586-594.

Dani, K.G.S. and Loreto, F. Trade-Off Between Dimethyl Sulfide and Isoprene Emissions from Marine Phytoplankton. Trends in Plant Science 22(5) (2017): 361-372.

Das, R., Bin Mohamed Mohtar, A.T., Rakshit, D., Shome, D. and Wang, X. Sources of atmospheric lead (Pb) in and around an Indian megacity. Atmospheric Environment 193 (2018): 57-65.

Das, R., Bizimis, M. and Wilson, A.M. Tracing mercury seawater vs. atmospheric inputs in a pristine SE USA salt marsh system: Mercury isotope evidence. Chemical Geology 336 (2013): 50-61.

Das, R., Khezri, B., Srivastava, B., Datta, S., Sikdar, P.K., Webstar, R.D. and Wang, X. Trace element composition of $PM_{2.5}$ and PM_{10} from Kolkata – a heavily polluted Indian metropolis. Atmospheric Pollution Research 6(5) (2015): 742-750.

Das, R., Wang, X., Itoh, M., Shiodera, S. and Kuwata, M. Estimation of Metal Emissions From Tropical Peatland Burning in Indonesia by Controlled Laboratory Experiments. Journal of Geophysical Research: Atmospheres 124(12) (2019): 6583-6599.

Decharat, S., Kongtip, P., Thampoophasiam, P. and Thetkathuek, A. An examination of blood lead levels in thai nielloware workers. Safety and health at work 3(3) (2012): 216-223.

Deng, S., Shi, Y., Liu, Y., Zhang, C., Wang, X., Cao, Q., Li, S. and Zhang, F. Emission characteristics of Cd, Pb and Mn from coal combustion: Field study at coal-fired power plants in China. Fuel Processing Technology 126 (2014): 469-475.

Díaz-Somoano, M., Kylander, M.E., López-Antón, M.A., Suárez-Ruiz, I., Martínez-Tarazona, M.R., Ferrat, M., Kober, B. and Weiss, D.J. Stable Lead Isotope Compositions In Selected Coals From Around The World And Implications For Present Day Aerosol Source Tracing. Environmental Science & Technology 43(4) (2009): 1078-1085.

Dockery, D.W. and Pope, C.A. Acute respiratory effects of particulate air pollution. Annual Review of Public Health 15(1) (1994): 107-132.

Dockery, D.W., Pope, C.A., Xu, X., Spengler, J.D., Ware, J.H., Fay, M.E., Ferris, B.G. and Speizer, F.E. An Association between Air Pollution and Mortality in Six U.S. Cities. New England Journal of Medicine 329(24) (1993): 1753-1759.

Duce, R.A. and Hoffman, E.J. Chemical Fractionation at the Air/Sea Interface. Annual Review of Earth and Planetary Sciences 4(1) (1976): 187-228.

Duce, R.A., LaRoche, J., Altieri, K., Arrigo, K.R., Baker, A.R., Capone, D.G., Cornell, S., Dentener, F., Galloway, J., Ganeshram, R.S., Geider, R.J., Jickells, T., Kuypers, M.M., Langlois, R., Liss, P.S., Liu, S.M., Middelburg, J.J., Moore, C.M., Nickovic, S., Oschlies, A., Pedersen, T., Prospero, J., Schlitzer, R., Seitzinger, S., Sorensen, L.L., Uematsu, M., Ulloa, O., Voss, M., Ward, B. and Zamora, L. Impacts of Atmospheric Anthropogenic Nitrogen on the Open Ocean. Science 320(5878) (2008): 893.

Duce, R.A., Liss, P.S., Merrill, J.T., Atlas, E.L., Buat-Menard, P., Hicks, B.B., Miller, J.M., Prospero, J.M., Arimoto, R., Church, T.M., Ellis, W., Galloway, J.N., Hansen, L., Jickells, T.D., Knap, A.H., Reinhardt, K.H., Schneider, B., Soudine, A., Tokos, J.J., Tsunogai, S., Wollast, R. and Zhou, M. The atmospheric input of trace species to the world ocean. Global Biogeochemical Cycles 5(3) (1991): 193-259.

Duzgoren-Aydin, N.S., Li, X.D. and Wong, S.C. Lead contamination and isotope signatures in the urban environment of Hong Kong. Environment International 30(2) (2004): 209-217.

Eck, T., Holben, B., Reid, J., Dubovik, O., Smirnov, A., Neil, N.T., Slutsker, I. and Kinne, S. Wavelength dependence of the optical depth of biomass burning, urban, and desert dust aerosols. Journal of Geophysical Research: Atmospheres 104(D24) (1999): 31333-31349.

Engel-Cox, J.A., Holloman, C.H., Coutant, B.W. and Hoff, R.M. Qualitative and quantitative evaluation of MODIS satellite sensor data for regional and urban scale air quality. Atmospheric Environment 38(16) (2004): 2495-2509.

ERIA. Coal-fired power plants in Thailand. in *Creating Better Social Acceptance for Electric Power Infrastructure*, Murakami, T., Editor. 2017. 3-18.

Fang, X., Zou, B., Liu, X., Sternberg, T. and Zhai, L. Satellite-based ground $PM_{2.5}$ estimation using timely structure adaptive modeling. Remote Sensing of Environment 186 (2016): 152-163.

Flegal, A.R., Gallon, C., Hibdon, S., Kuspa, Z.E. and Laporte, L.F. Declining—but Persistent—Atmospheric Contamination in Central California from the Resuspension of Historic Leaded Gasoline Emissions As Recorded in the Lace Lichen (Ramalina menziesii Taylor) from 1892 to 2006. Environmental Science & Technology 44(14) (2010): 5613-5618.

Fomba, K.W., Müller, K., van Pinxteren, D. and Herrmann, H. Aerosol size-resolved trace metal composition in remote northern tropical Atlantic marine environment: case study Cape Verde islands. Atmospheric Chemical and Physics 13(9) (2013): 4801-4814.

Gioia, S.M.C.L., Babinski, M., Weiss, D.J., Spiro, B., Kerr, A.A.F.S., Veríssimo, T.G., Ruiz, I. and Prates, J.C.M. An isotopic study of atmospheric lead in a megacity after phasing out of leaded gasoline. Atmospheric Environment 149 (2017): 70-83.

Gulson, B.L., Tiller, K.G., Mizon, K.J. and Merry, R.H. Use of lead isotopes in soils to identify the source of lead contamination near Adelaide, South Australia. Environmental Science & Technology 15(6) (1981): 691-696.

Guo, J.-P., Zhang, X.-Y., Che, H.-Z., Gong, S.-L., An, X., Cao, C.-X., Guang, J., Zhang, H., Wang, Y.-Q., Zhang, X.-C., Xue, M. and Li, X.-W. Correlation between PM concentrations and aerosol optical depth in eastern China. Atmospheric Environment 43(37) (2009): 5876-5886.

Hamelin, B., Grousset, F.E., Biscaye, P.E., Zindler, A. and Prospero, J.M. Lead isotopes in trade wind aerosols at Barbados: The influence of European emissions over the North Atlantic. Journal of Geophysical Research: Oceans 94(C11) (1989): 16243-16250.

He, Q. and Huang, B. Satellite-based mapping of daily high-resolution ground $PM_{2.5}$ in China via space-time regression modeling. Remote Sensing of Environment 206 (2018): 72-83.

Hirota, K. Review of Lead Phase Out for Air Quality Improvement in the Third World Cities Lessons from Thailand and Indonesia. Studies in Regional Science 36(2) (2006): 527-541.

Hsu, Y.-C., Lai, M.-H., Wang, W.-C., Chiang, H.-L. and Shieh, Z.-X. Characteristics of Water-Soluble Ionic Species in Fine ($PM_{2.5}$) and Coarse Particulate Matter ($PM_{10-2.5}$) in Kaohsiung, Southern Taiwan. Journal of the Air & Waste Management Association 58(12) (2008): 1579-1589.

Hu, J., Wu, L., Zheng, B., Zhang, Q., He, K., Chang, Q., Li, X., Yang, F., Ying, Q. and Zhang, H. Source contributions and regional transport of primary particulate matter in China. Environmental Pollution 207 (2015): 31-42.

Ismal, I.M., Basahi, J., Hassan, I., Summan, A. and Hammam, E. Source of Heavy Metals in Aerosol Particles in Atmosphere of Jeddah City, Saudi Arabia. in, 2018.

Ito, A. and Shi, Z. Delivery of anthropogenic bioavailable iron from mineral dust and combustion aerosols to the ocean. Atmospheric Chemistry and Physics 16(1) (2016): 85-99.

Jang, M. and Kamens, R.M. Atmospheric Secondary Aerosol Formation by Heterogeneous Reactions of Aldehydes in the Presence of a Sulfuric Acid Aerosol Catalyst. Environmental Science & Technology 35(24) (2001): 4758-4766.

Janjai, S., Núñez, M., Masiri, I., Wattan, R., Buntoung, S., Jantarach, T. and Promsen, W. Aerosol Optical Properties at Four Sites in Thailand. Atmospheric and Climate Sciences 02 (2012).

Janssen, N.A.H., Van Mansom, D.F.M., Van Der Jagt, K., Harssema, H. and Hoek, G. Mass concentration and elemental composition of airborne particulate matter at street and background locations. Atmospheric Environment 31(8) (1997): 1185-1193.

Jeong, C.H., Wang, J.M. and Evans, G.J. Source Apportionment of Urban Particulate Matter using Hourly Resolved Trace Metals, Organics, and Inorganic Aerosol Components. Atmospheric Chemistry and Physics Discussions 2016 (2016): 1-32.

Jickells, T.D., An, Z.S., Andersen, K.K., Baker, A.R., Bergametti, G., Brooks, N., Cao, J.J., Boyd, P.W., Duce, R.A., Hunter, K.A., Kawahata, H., Kubilay, N., Laroche, J., Liss, P.S., Mahowald, N., Prospero, J.M., Ridgwell, A.J., Tegen, I. and Torres, R. Global Iron Connections Between Desert Dust, Ocean Biogeochemistry, and Climate. Science 308(5718) (2005): 67-71.

Jordi, A., Basterretxea, G., Tovar-Sánchez, A., Alastuey, A. and Querol, X. Copper aerosols inhibit phytoplankton growth in the Mediterranean Sea. Proceedings of the National Academy of Sciences 109(52) (2012): 21246.

Kaewboonchoo, O., Morioka, I., Saleekul, S., Miyai, N., Chaikittiporn, C. and Kawai, T. Blood lead level and cardiovascular risk factors among bus drivers in Bangkok, Thailand. Industrial Health 48(1) (2010): 61-5.

Kanabkaew, T. Prediction of Hourly Particulate Matter Concentrations in Chiangmai, Thailand Using MODIS Aerosol Optical Depth and Ground-Based Meteorological Data. EnvironmentAsia 6 (2013): 65-70.

Kang, M., Guo, H., Wang, P., Fu, P., Ying, Q., Liu, H., Zhao, Y. and Zhang, H. Characterization and source apportionment of marine aerosols over the East China Sea. Science of The Total Environment 651 (2019): 2679-2688.

Kayee, J., Sompongchaiyakul, P., Sanwlani, N., Bureekul, S., Wang, X. and Das, R. Metal Concentrations and Source Apportionment of $PM_{2.5}$ in Chiang Rai and Bangkok, Thailand during a Biomass Burning Season. ACS Earth and Space Chemistry 4(7) (2020): 1213-1226.

Keene, W.C., Pszenny, A.A.P., Galloway, J.N. and Hawley, M.E. Sea-salt corrections and interpretation of constituent ratios in marine precipitation. Journal of Geophysical Research: Atmospheres 91(D6) (1986): 6647-6658.

Keller, M.D. Dimethyl Sulfide Production and Marine Phytoplankton: The Importance of Species Composition and Cell Size. Biological Oceanography 6(5-6) (1989): 375-382.

Khamkaew, C., Chantara, S., Janta, R., Pani, S.K., Prapamontol, T., Kawichai, S., Wiriya, W. and Lin, N.-H. Investigation of Biomass Burning Chemical Components over Northern Southeast Asia during 7-SEAS/BASELInE 2014 Campaign. Aerosol and Air Quality Research 16(11) (2016): 2655-2670.

Kim Oanh, N.T., Kongpran, J., Hang, N.T., Parkpian, P., Hung, N.T.Q., Lee, S.B. and Bae, G.N. Characterization of gaseous pollutants and $PM_{2.5}$ at fixed roadsides and along vehicle traveling routes in Bangkok Metropolitan Region. Atmospheric Environment 77 (2013): 674-685.

Kim, W.-H., Song, J.-M., Ko, H.-J., Kim, J.S., Lee, J. and Kang, C.-H. Comparison of Chemical Compositions of Size-segregated Atmospheric Aerosols between Asian Dust and Non-Asian Dust Periods at Background Area of Korea. Bulletin of the Korean Chemical Society 33 (2012): 3651-3656.

Koelemeijer, R.B.A., Homan, C.D. and Matthijsen, J. Comparison of spatial and temporal variations of aerosol optical thickness and particulate matter over Europe. Atmospheric Environment 40(27) (2006): 5304-5315.

Komárek, M., Ettler, V., Chrastný, V. and Mihaljevič, M. Lead isotopes in environmental sciences: A review. Environment International 34(4) (2008): 562-577.

Kravchenko, J. and Lyerly, H.K. The Impact of Coal-Powered Electrical Plants and Coal Ash Impoundments on the Health of Residential Communities. North Carolina Medical Journal 79(5) (2018): 289-300.

Kritz, M.A. and Rancher, J. Circulation of Na, Cl, and Br in the tropical marine atmosphere. Journal of Geophysical Research: Oceans 85(C3) (1980): 1633-1639.

Kulshrestha, A., Satsangi, P.G., Masih, J. and Taneja, A. Metal concentration of $PM_{2.5}$ and PM_{10} particles and seasonal variations in urban and rural environment of Agra, India. Science of The Total Environment 407(24) (2009): 6196-6204.

Kumar, S., Aggarwal, S.G., Malherbe, J., Barre, J.P.G., Berail, S., Gupta, P.K. and Donard, O.F.X. Tracing dust transport from Middle-East over Delhi in March 2012 using metal and lead isotope composition. Atmospheric Environment 132 (2016): 179-187.

Lee, J.-M., Boyle, E.A., Suci Nurhati, I., Pfeiffer, M., Meltzner, A.J. and Suwargadi, B. Coral-based history of lead and lead isotopes of the surface Indian Ocean since the mid-20th century. Earth and Planetary Science Letters 398 (2014): 37-47.

Levy, R.C., Matto, S., Munchak, L.A., Remer, L.A., Sayer, A.M., Patadia, F. and Hsu, N.C. The Collection 6 MODIS aerosol products over land and ocean. Atmospheric Measurement Techniques 6(11) (2013): 2989-3034.

Li, T., Shen, H., Yuan, Q., Zhang, X. and Zhang, L. Estimating Ground-Level $PM_{2.5}$ by Fusing Satellite and Station Observations: A Geo-Intelligent Deep Learning Approach. Geophysical Research Letters 44(23) (2017): 11,985-11,993.

Li, T., Shen, H., Zeng, C., Yuan, Q. and Zhang, L. Point-surface fusion of station measurements and satellite observations for mapping $PM_{2.5}$ distribution in China: Methods and assessment. Atmospheric Environment 152 (2017): 477-489.

Liang, Z.W., Wei, G.T., Irwin, R.L., Walton, A.P., Michel, R.G. and Sneddon, J. Determination of subnanogram per cubic meter concentrations of metals in the air of a trace metal clean room by impaction graphite furnace atomic absorption and laser excited atomic fluorescence spectrometry. Analytical Chemistry 62(14) (1990): 1452-7.

Lidsky, T.I. and Schneider, J.S. Lead neurotoxicity in children: basic mechanisms and clinical correlates. Brain 126(Pt 1) (2003): 5-19.

Liss, P., Malin, G. and Turner, S.M. Production of DMS by Marine Phytoplankton. Dimethylsulphide: oceans, atmosphere and climate. Proc. international symposium, Belgirate, 1992 (1993): 1-14.

Liu, Y., Franklin, M., Kahn, R. and Koutrakis, P. Using aerosol optical thickness to predict ground-level $PM_{2.5}$ concentrations in the St. Louis area: A comparison between MISR and MODIS. Remote Sensing of Environment 107(1) (2007): 33-44.

Liu, Y., Park, R.J., Jacob, D.J., Li, Q., Kilaru, V. and Sarnat, J.A. Mapping annual mean ground-level $PM_{2.5}$ concentrations using Multiangle Imaging Spectroradiometer aerosol optical thickness over the contiguous United States. Journal of Geophysical Research: Atmospheres 109(D22206) (2004).

Liu, Y., Sarnat, J.A., Kilaru, V., Jacob, D.J. and Koutrakis, P. Estimating Ground-Level $PM_{2.5}$ in the Eastern United States Using Satellite Remote Sensing. Environmental Science & Technology 39(9) (2005): 3269-3278.

Lohan, M.C. and Tagliabue, A. Oceanic Micronutrients: Trace Metals that are Essential for Marine Life. Elements 14(6) (2018): 385-390.

Lormphongs, S., Miyashita, K., Morioka, I., Chaikittiporn, C., Miyai, N. and Yamamoto, H. Lead exposure and blood lead level of workers in a battery manufacturing plant in Thailand. Industrial Health 41(4) (2003): 348-53.

Magesh, N.S., Botsa, S.M., Dessai, S., Mestry, M., Leitao, T.D.L. and Tiwari, A. Hydrogeochemistry of the deglaciated lacustrine systems in Antarctica: Potential impact of marine aerosols and rock-water interactions. Science of The Total Environment 706 (2020): 135822.

Mahowald, N.M., Engelstaedter, S., Luo, C., Sealy, A., Artaxo, P., Benitez-Nelson, C., Bonnet, S., Chen, Y., Chuang, P.Y., Cohen, D.D., Dulac, F., Herut, B., Johansen, A.M., Kubilay, N., Losno, R., Maenhaut, W., Paytan, A., Prospero, J.M., Shank, L.M. and Siefert, R.L. Atmospheric Iron Deposition: Global Distribution, Variability, and Human Perturbations. Annual Review of Marine Science 1(1) (2008): 245-278.

Mahowald, N.M., Hamilton, D.S., Mackey, K.R.M., Moore, J.K., Baker, A.R., Scanza, R.A. and Zhang, Y. Aerosol trace metal leaching and impacts on marine microorganisms. Nature Communications 9(1) (2018): 2614.

Majumdar, A., Satpathy, J., Kayee, J. and Das, R. Trace metal composition of rainwater and aerosol from Kolkata, a megacity in eastern India. SN Applied Sciences 2(12) (2020): 2122.

Millot, R., Allègre, C.-J., Gaillardet, J. and Roy, S. Lead isotopic systematics of major river sediments: a new estimate of the Pb isotopic composition of the Upper Continental Crust. Chemical Geology 203(1) (2004): 75-90.

Morton-Bermea, O., Rodríguez-Salazar, M.T., Hernández-Alvarez, E., García-Arreola, M.E. and Lozano-Santacruz, R. Lead isotopes as tracers of anthropogenic pollution in urban topsoils of Mexico City. Geochemistry 71(2) (2011): 189-195.

Mukai, H., Furuta, N., Fujii, T., Ambe, Y., Sakamoto, K. and Hashimoto, Y. Characterization of sources of lead in the urban air of Asia using ratios of stable lead isotopes. Environmental Science & Technology 27(7) (1993): 1347-1356.

Nriagu, J.O. The rise and fall of leaded gasoline. Science of The Total Environment 92 (1990): 13-28.

Nriagu, J.O. and Pacyna, J.M. Quantitative assessment of worldwide contamination of air, water and soils by trace metals. Nature 333(6169) (1988): 134-139.

Ooki, A., Uematsu, M., Miura, K. and Nakae, S. Sources of sodium in atmospheric fine particles. Atmospheric Environment 36(27) (2002): 4367-4374.

Oravisjärvi, K., Timonen, K.L., Wiikinkoski, T., Ruuskanen, A.R., Heinänen, K. and Ruuskanen, J. Source contributions to $PM_{2.5}$ particles in the urban air of a town situated close to a steel works. Atmospheric Environment 37(8) (2003): 1013-1022.

Pacyna, J.M. and Pacyna, E.G. An assessment of global and regional emissions of trace metals to the atmosphere from anthropogenic sources worldwide. Environmental Reviews 9 (2011): 269-298.

Pacyna, J.M., Pacyna, E.G. and Aas, W. Changes of emissions and atmospheric deposition of mercury, lead, and cadmium. Atmospheric Environment 43(1) (2009): 117-127.

Pan, Y., Wang, Y., Sun, Y., Tian, S. and Cheng, M. Size-resolved aerosol trace elements at a rural mountainous site in Northern China: Importance of regional transport. Science of The Total Environment 461-462 (2013): 761-771.

Pani, S., Lee, C.-T., Chou, C., Shimada, K., Hatakeyama, S., Takami, A., Wang, S.-H. and Lin, N.-H. Chemical Characterization of Wintertime Aerosols over Islands and Mountains in East Asia: Impacts of the Continental Asian Outflow. Aerosol and Air Quality Research 17 (2017): 3006–3036.

Pasukphun, N. Environmental health burden of open burning in northern Thailand: a review. PSRU Journal of Science and Technology 3 (2018): 11-28.

Pekney, N.J. and Davidson, C.I. Determination of trace elements in ambient aerosol samples. Analytica Chimica Acta 540(2) (2005): 269-277.

Pelletier, B., Santer, R. and Vidot, J. Retrieving of particulate matter from optical measurements: A semiparametric approach. Journal of Geophysical Research: Atmospheres 112(D6) (2007): D06208.

Phayungwiwatthanakoon, C., Suwanwaree, P. and Dasananda, S. Application of new MODIS-based aerosol index for air pollution severity assessment and mapping in upper Northern Thailand. EnvironmentAsia 7(2) (2014): 133-141.

Pimonsree, S. and Vongruang, P. Impact of biomass burning and its control on particulate matter over a city in mainland Southeast Asia during a smog episode. Atmospheric Environment 195 (2018): 196-209.

Pongpiachan, S. Enhanced PM_{10} bounded PAHs from shipping emissions. Atmospheric Environment (1967) 108 (2015): 13-19.

Pongpiachan, S. Impacts of agricultural waste burning on the enhancement of $PM_{2.5}$-bound polycyclic aromatic hydrocarbons in northern Thailand. WIT Transactions on Ecology and the Environment 198 (2015): 3-14.

Pongpiachan, S. Incremental Lifetime Cancer Risk of $PM_{2.5}$ Bound Polycyclic Aromatic Hydrocarbons (PAHs) before and after the Wildland Fire Episode. Aerosol and Air Quality Research 16(11) (2016): 2907-2919.

Pongpiachan, S., Choochuay, C., Chalachol, J., Kanchai, P., Phonpiboon, T., Wongsuesat, S., Chomkhae, K., Kittikoon, I., Hiranyatrakul, P., Cao, J. and Thamrongthayawong, S. Chemical characterisation of organic functional group compositions in $PM_{2.5}$ collected at nine administrative provinces in northern Thailand during the Haze Episode in 2013. Asian Pacific Journal of Cancer Prevention 14(6) (2013): 3653-3661.

Pongpiachan, S., Hattayanon, M., Suttinun, O., Khumsup, C., Kittikoon, I., Hirunyatrakul, P. and Cao, J. Assessing human exposure to PM_{10} -bound polycyclic aromatic hydrocarbons during fireworks displays. Atmospheric Pollution Research 8 (2017).

Pongpiachan, S., Hattayanone, M. and Cao, J. Effect of agricultural waste burning season on $PM_{2.5}$-bound polycyclic aromatic hydrocarbon (PAH) levels in Northern Thailand. Atmospheric Pollution Research 8(6) (2017): 1069-1080.

Pongpiachan, S. and Iijima, A. Assessment of selected metals in the ambient air PM_{10} in urban sites of Bangkok (Thailand). Environmental Science and Pollution Research 23(3) (2016): 2948-2961.

Pongpiachan, S., Kositanont, C., Palakun, J., Liu, S., Ho, K.F., Cao, J. and Barcelo, D. Effects of day-of-week trends and vehicle types on PM$_{2.5}$ -bounded carbonaceous compositions. Science of The Total Environment 532 (2015): 484-494.

Pongpiachan, S., Liu, S., Huang, R.-J., Zhao, Z., Palakun, J., Kositanont, C. and Cao, J. Variation in Day-of-Week and Seasonal Concentrations of Atmospheric PM$_{2.5}$-Bound Metals and Associated Health Risks in Bangkok, Thailand. Archives of Environmental Contamination and Toxicology 72 (2017): 1-16.

Pósfai, M., Anderson, J.R., Buseck, P.R. and Sievering, H. Compositional variations of sea-salt-mode aerosol particles from the North Atlantic. Journal of Geophysical Research: Atmospheres 100(D11) (1995): 23063-23074.

Pósfai, M., Simonics, R., Li, J., Hobbs, P.V. and Buseck, P.R. Individual aerosol particles from biomass burning in southern Africa: 1. Compositions and size distributions of carbonaceous particles. Journal of Geophysical Research: Atmospheres 108(D13) (2003).

Prospero, J.M., Charlson, R.J., Mohnen, V., Jaenicke, R., Delany, A.C., Moyers, J., Zoller, W. and Rahn, K. The atmospheric aerosol system: An overview. Reviews of Geophysics 21(7) (1983): 1607-1629.

Punsompong, P. and Chantara, S. Pattern of Biomass Burning in Chiang Mai, Thailand and Transportation of Air Pollutants in Dry Season. The 3rd EnvironmentAsia International Conference (2015): 84-91.

Punsompong, P. and Chantara, S. Identification of potential sources of PM$_{10}$ pollution from biomass burning in northern Thailand using statistical analysis of trajectories. Atmospheric Pollution Research 9(6) (2018): 1038-1051.

Qi, L., Chen, M., ge, X., Zhang, Y. and Guo, B. Seasonal Variations and Sources of 17 Aerosol Metal Elements in Suburban Nanjing, China. Atmosphere 7 (2016): 153.

Quirantes, A., Guerrero-Rascado, J.L., Pérez-Ramírez, D., Foyo-Moreno, I., Oritz-Amezcua, P., Benavent-Oltra, J.A., Lyamani, H., Titos, G., Bravo-Aranda, J.A., Cazorla, A., Valenzuela, A., Casquero-Vera, J.A., Bedoya-Velásquez, A.E., Alados-Arboledas, L. and Olmo, F.J. Extinction-related Angström exponent characterization of submicrometric volume fraction in atmospheric aerosol particles. Atmospheric Research 228 (2019): 270-280.

Reimann, C. and Caritat, P.d. <u>Chemical Elements in the Environment</u>. Springer, Berlin, Heidelberg, 1998.

Remer, L.A., Kaufman, Y.J., Holben, B.N., Thompson, A.M. and McNamara, D. Biomass burning aerosol size distribution and modeled optical properties. <u>Journal of Geophysical Research: Atmospheres</u> 103(D24) (1998): 31879-31891.

Reuer, M.K., Boyle, E.A. and Grant, B.C. Lead isotope analysis of marine carbonates and seawater by multiple collector ICP-MS. <u>Chemical Geology</u> 200(1) (2003): 137-153.

Ruangkanchanasetr, S. and Suepiantham, J. Risk factors of high lead level in Bangkok children. <u>Journal of the Medical Association of Thailand</u> 85 Suppl 4 (2002): S1049-58.

Rudnick, R.L. and Gao, S. Composition of the Continental Crust. in Holland, H.D. and Turekian, K.K. (eds.), <u>Treatise on Geochemistry</u>. 1-64. Oxford: Pergamon, 2003.

Rungratanaubon, T., Wangwongwatana, S. and Panich, N. Characterization and Source Identification of Trace Metals in Airborne Particulates of Bangkok, Thailand. <u>Annals of the New York Academy of Sciences</u> 1140(1) (2008): 297-307.

Ryu, S.Y., Kim, J.E., Zhuanshi, H., Kim, Y.J. and Kang, G.U. Chemical Composition of Post-Harvest Biomass Burning Aerosols in Gwangju, Korea. <u>Journal of the Air & Waste Management Association</u> 54(9) (2004): 1124-1137.

Saengsupavanich, C., Coowanitwong, N., Gallardo, W.G. and Lertsuchatavanich, C. Environmental performance evaluation of an industrial port and estate: ISO14001, port state control-derived indicators. <u>Journal of Cleaner Production</u> 17(2) (2009): 154-161.

Saltzman, E.S. Marine Aerosols. in <u>Surface Ocean–Lower Atmosphere Processes</u>. 17-35, 2009.

Sangster, D.F., Outridge, P.M. and Davis, W.J. Stable lead isotope characteristics of lead ore deposits of environmental significance. <u>Environmental Reviews</u> 8(2) (2000): 115-147.

Šaulienė, I. and Šukiene, L. Application of backward air mass trajectory analysis in evaluating airborne pollen dispersion. <u>Journal of Environmental Engineering and Landscape Management</u> 14 (2006): 113-120.

Sayeg, P. Successful Conversion to Unleaded Gasoline in Thailand. World Bank Technical Papers. The World Bank, 1998.

Sayer, A.M., Hsu, N.C., Hsiao, T.-C., Pantina, P., Kuo, F., Ou-Yang, C.-F., Holben, B.N., Janjai, S., Chantara, S., Wang, S.-H., Loftus, A.M., Lin, N.-H. and Tsay, S.-C. In-Situ and Remotely-Sensed Observations of Biomass Burning Aerosols at Doi Ang Khang, Thailand during 7-SEAS/BASELInE 2015. Aerosol and Air Quality Research 16(11) (2016): 2786-2801.

Schlosser, J.S., Braun, R.A., Bradley, T., Dadashazar, H., MacDonal, A.B., Aldhaif, A.A., Aghdam, M.A., Mardi, A.H., Xian, P. and Sorooshian, A. Analysis of aerosol composition data for western United States wildfires between 2005 and 2015: Dust emissions, chloride depletion, and most enhanced aerosol constituents. Journal of Geophysical Research: Atmospheres 122(16) (2017): 8951-8966.

See, S.W., Balasubramanian, R., Rianawati, E., Karthikeyan, S. and Streets, D.G. Characterization and Source Apportionment of Particulate Matter ≤ 2.5 µm in Sumatra, Indonesia, during a Recent Peat Fire Episode. Environmental Science & Technology 41(10) (2007): 3488-3494.

See, S.W., Balasubramanian, R. and Wang, W. A study of the physical, chemical, and optical properties of ambient aerosol particles in Southeast Asia during hazy and nonhazy days. Journal of Geophysical Research: Atmospheres 111 (2006): D10S08.

See, S.W., Wang, Y.H. and Balasubramanian, R. Contrasting reactive oxygen species and transition metal concentrations in combustion aerosols. Environmental Research 103(3) (2007): 317-324.

Sen, I.S., Bizimis, M., Tripathi, S.N. and Paul, D. Lead isotopic fingerprinting of aerosols to characterize the sources of atmospheric lead in an industrial city of India. Atmospheric Environment 129 (2016): 27-33.

Sen, I.S. and Peucker-Ehrenbrink, B. Anthropogenic Disturbance of Element Cycles at the Earth's Surface. Environmental Science & Technology 46(16) (2012): 8601-8609.

Shenoy, D.M., Paul, J.T., Gauns, M., Ramaiah, N. and Kumar, M.D. Spatial variations of DMS, DMSP and phytoplankton in the Bay of Bengal during the summer monsoon 2001. Marine Environmental Research 62(2) (2006): 83-97.

Shridhar, V., Khillare, P.S., Agarwal, T. and Ray, S. Metallic species in ambient particulate matter at rural and urban location of Delhi. Journal of Hazardous Materials 175 (2009): 600-607.

Sirimongkonlertkul, N. and Phonekeo, V. Remote Sensing and GIS Application Analysis of Active Fire, Aerosol Optical Thickness and Estimated PM_{10} In The North of Thailand and Chiang Rai Province. APCBEE Procedia 1 (2012): 304-308.

Sirimongkonlertkul, N., Upayokhin, P. and Phonekeo, V. Multi-temporal analysis of haze problem in northern Thailand: A case study in Chiang Rai province. Kasetsart Journal - Natural Science 47 (2013): 768-780.

Speeckaert, G., Borges, A.V., Champenois, W., Royer, C. and Gypens, N. Annual cycle of dimethylsulfoniopropionate (DMSP) and dimethylsulfoxide (DMSO) related to phytoplankton succession in the Southern North Sea. Science of The Total Environment 622-623 (2018): 362-372.

Srinivasa Gowd, S., Ramakrishna Reddy, M. and Govil, P.K. Assessment of heavy metal contamination in soils at Jajmau (Kanpur) and Unnao industrial areas of the Ganga Plain, Uttar Pradesh, India. Journal of Hazardous Materials 174(1) (2010): 113-121.

Steding, D.J. and Flegal, A. Mercury concentrations in coastal California precipitation: Evidence of local and trans-Pacific fluxes of mercury to North America. Journal of Geophysical Research: Atmospheres 107 (2002): ACH 11-1—ACH 11-7.

Stein, A.F., Draxler, R.R., Rolph, G.D., Stunder, B.J.B., Cohen, M.D. and Ngan, F. NOAA's HYSPLIT Atmospheric Transport and Dispersion Modeling System. Bulletin of the American Meteorological Society 96(12) (2015): 2059-2077.

Sturges, W.T. and Barrie, L.A. Lead 206/207 isotope ratios in the atmosphere of North America as tracers of US and Canadian emissions. Nature 329(6135) (1987): 144-146.

Sudheer, A.K. and Rengarajan, R. Atmospheric Mineral Dust and Trace Metals over Urban Environment in Western India during Winter. Aerosol and Air Quality Research 12 (2012): 923–933.

Sugimoto, N., Shimizu, A., Nishizawa, T., Matsui, I., Jin, Y., Khatri, P., Irie, H., Takamura, T., Aoki, K. and Thana, B. Aerosol characteristics in Phimai, Thailand determined by

continuous observation with a polarization sensitive Mie-Raman lidar and a sky radiometer. Environmental Research Letters 10 (2015): 065003.

Sukitpaneenit, M. and Kim Oanh, N.T. Satellite monitoring for carbon monoxide and particulate matter during forest fire episodes in Northern Thailand. Environmental Monitoring and Assessment 186(4) (2014): 2495-2504.

Sukitpaneenit, M. and Oanh, N.T. Satellite monitoring for carbon monoxide and particulate matter during forest fire episodes in Northern Thailand. Environmental Monitoring and Assessment 186 (2013).

Suwanprasit, C., Charoenpanyanet, A., Pardthaisong, L. and Sin-ampol, P. Spatial and Temporal Variations of Satellite-Derived PM_{10} of Chiang Mai: An Exploratory Analysis. Procedia Engineering 212 (2018): 141-148.

Takemura, T., Nozawa, T., Emori, S., Nakajima, T.Y. and Nakajima, T. Simulation of climate response to aerosol direct and indirect effects with aerosol transport-radiation model. Journal of Geophysical Research: Atmospheres. 110(D2) (2005): D02202.

Thorpe, A. and Harrison, R.M. Sources and properties of non-exhaust particulate matter from road traffic: A review. Science of The Total Environment 400(1) (2008): 270-282.

Tippayawong, N., Pengchai, P. and A, L. Characterization of ambient aerosols in Northern Thailand and their probable sources. International Journal of Environmental Science and Technology 3 (2006).

Trang, N. and Tripathi, N. Spatial Correlation Analysis between Particulate Matter 10 (PM_{10}) Hazard and Respiratory Diseases in Chiang Mai Province, Thailand. ISPRS - International Archives of the Photogrammetry, Remote Sensing and Spatial Information Sciences XL-8 (2014): 185-191.

Vadrevu, K.P., Lasko, K., Giglio, L. and Justice, C. Vegetation fires, absorbing aerosols and smoke plume characteristics in diverse biomass burning regions of Asia. Environmental Research Letters 10(10) (2015): 105003.

Vadrevu, K.P., Lasko, K., Giglio, L., Schroeder, W., Biswas, S. and Justice, C. Trends in Vegetation fires in South and Southeast Asian Countries. Scientific Reports 9(1) (2019): 7422.

Vejpongsa, I., Suvachittanont, S., Klinklan, N., Thongyen, T., Veres, M. and Szymanski, W.J.P. Deliberation between PM_1 and $PM_{2.5}$ as air quality indicators based on comprehensive characterization of urban aerosols in Bangkok, Thailand. Particuology 35 (2017): 1-9.

Wagner, R., Jähn, M. and Schepanski, K. Wildfires as a source of airborne mineral dust – revisiting a conceptual model using large-eddy simulation (LES). Atmospheric Chemistry and Physics 18(16) (2018): 11863-11884.

Wang, J., Hu, Z., Chen, Y., Chen, Z. and Xu, S. Contamination characteristics and possible sources of PM10 and PM2.5 in different functional areas of Shanghai, China. Atmospheric Environment 68 (2013): 221-229.

White, W.M., Albarède, F. and Télouk, P. High-precision analysis of Pb isotope ratios by multi-collector ICP-MS. Chemical Geology 167(3) (2000): 257-270.

Wilkniss, P.E. and Bressan, D.J. Fractionation of the elements F, Cl, Na, and K at the sea-air interface. Journal of Geophysical Research (1896-1977) 77(27) (1972): 5307-5315.

Wimolwattanapun, W., Hopke, P.K. and Pongkiatkul, P. Source apportionment and potential source locations of $PM_{2.5}$ and $PM_{2.5-10}$ at residential sites in metropolitan Bangkok. Atmospheric Pollution Research 2(2) (2011): 172-181.

Wiriya, W., Prapamontol, T. and Chantara, S. PM_{10}-bound polycyclic aromatic hydrocarbons in Chiang Mai (Thailand): Seasonal variations, source identification, health risk assessment and their relationship to air-mass movement. Atmospheric Research 124 (2013): 109-122.

Wiwatanadate, P. Acute Air Pollution-Related Symptoms Among Residents in Chiang Mai, Thailand. Journal of environmental health 76 (2014): 76-84.

Wu, S.-P., Dai, L.-H., Zhu, H., Zhang, N., Yan, J.-P., Schwab, J.J. and Yuan, C.-S. The impact of sea-salt aerosols on particulate inorganic nitrogen deposition in the western Taiwan Strait region, China. Atmospheric Research 228 (2019): 68-76.

Xiao, H.-W., Xiao, H.-Y., Shen, C.-Y., Zhang, Z.-Y. and Long, A.-M. Chemical Composition and Sources of Marine Aerosol over the Western North Pacific Ocean in Winter. Atmosphere 9 (2018): 298.

Yamsrual, S., Sasaki, N., Tsusaka, T.W. and Winijkul, E. Assessment of local perception on eco-industrial estate performances after 17 years of implementation in Thailand. <u>Environmental Development</u> 32 (2019): 100457.

Yao, L., Yang, L, Yuan, Q., Yan, C., Dong, C., Meng, C., Sui, X., Yang, F., Lu, Y. and Wang, W. Sources apportionment of $PM_{2.5}$ in a background site in the North China Plain. <u>Science of The Total Environment</u> 541 (2016): 590-598.

Yao, P.-H., Shyu, G.-S., Chang, Y.-F., Chou, Y.-C., Shen, C.-C., Chou, C.-S. and Chang, T.-K. Lead isotope characterization of petroleum fuels in Taipei, Taiwan. <u>International journal of environmental research and public health</u> 12(5) (2015): 4602-4616.

Yin, L., Niu, Z., Chen, X., Chen, J., Xu, L. and Zhang, F. Chemical compositions of $PM_{2.5}$ aerosol during haze periods in the mountainous city of Yong'an, China. <u>Journal of Environmental Sciences</u> 24(7) (2012): 1225-1233.

Yin, S., Wang, X., Zhang, X., Guo, M., Miura, M. and Xiao, Y. Influence of biomass burning on local air pollution in mainland Southeast Asia from 2001 to 2016. <u>Environmental Pollution</u> 254(Part A) (2019): 112949.

Zang, L., Mao, F., Guo, J., Wang, W., Pan, Z., Shen, H., Zhu, B. and Wang, Z. Estimation of spatiotemporal PM1.0 distributions in China by combining $PM_{2.5}$ observations with satellite aerosol optical depth. <u>Science of The Total Environment</u> 658 (2019): 1256-1264.

Zhang, H. and Tripathi, N. Geospatial hot spot analysis of lung cancer patients correlated to fine particulate matter ($PM_{2.5}$) and industrial wind in Eastern Thailand. <u>Journal of Cleaner Production</u> 170 (2018): 407-424.

Zhao, R., Han, B., Lu, B., Zhang, N., Zhu, L. and Bai, Z. Element composition and source apportionment of atmospheric aerosols over the China Sea. <u>Atmospheric Pollution Research</u> 6(2) (2015): 191-201.

Zhao, Z.-Q., Zhang, W., Li, X.-D., Yang, Z., Zheng, H.-Y., Ding, H., Wang, Q.-L., Xiao, J. and Fu, P.-Q. Atmospheric lead in urban Guiyang, Southwest China: Isotopic source signatures. <u>Atmospheric Environment</u> 115 (2015): 163-169.

Zhou, C., Liu, G., Fang, T., Lam, P.K.S. and Lam, J.C.W. Atmospheric emissions of toxic elements (As, Cd, Hg, and Pb) from brick making plants in China. <u>RSC Advances</u> 5(19) (2015): 14497-14505.

Zhu, B.Q., Chen, Y.W. and Chang, X.Y. Application of Pb isotopic mapping to environment evaluation in China. 2002.

Žibret, G., Van Tonder, D. and Žibret, L. Metal content in street dust as a reflection of atmospheric dust emissions from coal power plants, metal smelters, and traffic. Environmental Science and Pollution Research 20(7) (2013): 4455-4468.

จุฬาลงกรณ์มหาวิทยาลัย

CHULALONGKORN UNIVERSITY

APPENDICES

APPENDIX A

Sources of atmospheric lead (Pb) after quarter century of phasing out of leaded gasoline in Bangkok, Thailand

Table A-1 Metal concentrations in ng/m^3 and PM$_{2.5}$ in µg/m^3 (Bangkok)

	Date	Al	As	Ba	Ca	Cd	Cr	Cu	Fe	Mg	Mn	Na	Ni	Pb	Sr	V	Zn	PM$_{2.5}$
Bangkok																		
BKK1	07/06/2018	59	0.89	3.0	1613	0.07	8.6	3.5	131	290	26	100	4.7	10	3.4	0.50	494	60
BKK2	21/06/2018	212	1.2	5.7	1684	0.39	2.4	4.8	286	468	31	538	1.4	11	6.5	1.6	517	78
BKK3	05/07/2018	50	0.92	3.6	55	0.22	9.8	5.8	151	43	7.4	188	0.84	7.1	0.71	0.81	126	52
BKK4	12/07/2018	313	1.5	8.6	382	0.10	41	32	407	212	12	201	9.1	3.5	N.D.	6.3	77	56
BKK5	19/07/2018	110	0.42	2.6	66	0.04	1.0	2.9	148	84	6.2	316	1.1	3.2	1.0	0.73	30	55
BKK6	26/07/2018	225	0.77	6.4	117	0.12	1.2	6.0	291	157	13	504	1.2	7.3	2.7	1.4	65	76
BKK7	02/08/2018	140	1.6	6.4	137	0.26	1.9	6.5	255	126	12	399	1.9	9.9	2.5	1.5	100	69
BKK8	09/08/2018	110	1.0	4.2	91	0.12	1.3	5.1	181	93	9.2	219	1.5	6.9	1.3	1.3	62	77
BKK9	16/08/2018	88	1.5	4.6	85	0.27	1.6	4.7	153	83	8.0	326	1.5	11	1.3	1.3	99	54
BKK10	23/08/2018	163	1.5	4.9	95	0.26	2.2	5.4	219	115	9.0	432	1.6	10	2.0	2.7	153	74
BKK11	06/09/2018	98	1.7	3.6	82	0.11	1.5	5.6	165	100	6.9	427	1.0	9.7	1.7	1.4	66	56
BKK12	13/09/2018	94	0.28	2.2	86	0.06	1.8	10	122	60	4.3	85	0.86	3.4	0.83	0.91	29	71
BKK13	08/11/2018	19	0.23	1.6	54	0.05	5.4	2.2	61	25	5.1	115	0.87	1.1	0.25	0.44	4.8	95
BKK14	15/11/2018	33	0.53	2.1	48	0.08	0.73	3.6	65	29	3.6	143	0.80	5.1	0.27	1.0	22	126
BKK15	22/11/2018	63	2.1	9.4	102	0.33	1.7	8.4	136	48	8.4	228	2.7	21	1.5	2.0	74	111
BKK16	29/11/2018	54	1.4	7.4	96	0.45	1.2	8.2	149	39	9.7	127	0.94	13	0.58	0.82	38	80
BKK17	13/12/2018	48	0.41	5.0	103	0.23	3.0	6.2	106	30	4.0	125	1.1	4.9	0.46	0.51	16	84
BKK18	20/12/2018	72	4.0	10	123	0.73	2.3	18	271	43	17	331	2.7	29	0.88	2.9	129	137
BKK19	22/12/2018	42	0.83	4.9	62	0.28	0.81	6.9	103	30	5.2	104	0.78	8.7	0.45	0.57	39	169
BKK20	23/12/2018	53	0.64	4.0	77	0.26	1.1	5.6	98	34	3.8	167	0.64	11	0.49	0.68	20	143
BKK21	27/12/2018	46	0.74	7.2	77	0.39	7.1	6.7	140	33	5.6	120	12	12	0.54	0.32	23	160
BKK22	03/01/2019	37	0.58	7.0	84	0.41	1.8	5.4	103	24	4.3	145	0.69	10	0.47	0.57	23	88
BKK23	10/01/2019	74	4.7	9.9	118	0.67	3.4	14	260	83	19	682	4.2	46	1.3	5.5	153	92
BKK24	17/01/2019	59	0.48	4.7	75	0.18	3.1	5.3	159	43	5.9	186	2.7	6.2	0.55	0.95	18	124
BKK25	25/01/2019	60	2.1	6.8	93	0.41	2.0	10	208	36	12	197	1.9	11	0.63	3.0	55	136
BKK26	30/01/2019	46	1.2	4.4	67	0.26	5.2	6.0	138	47	8.2	211	1.4	14	0.56	1.8	49	165
BKK27	31/01/2019	40	0.94	2.5	48	0.22	0.98	3.7	92	52	6.0	286	1.5	6.3	0.44	2.0	29	177
BKK28	29/01/2019	103	3.8	17	173	0.82	2.5	14	274	58	15	353	2.1	43	1.5	2.4	61	157
BKK29	05/02/2019	30	0.53	2.3	98	0.11	1.6	2.3	83	56	6.0	389	1.4	2.2	0.53	2.6	11	99
BKK30	12/02/2019	51	1.0	6.7	90	0.28	1.9	7.0	168	42	12	302	2.2	15	0.76	4.0	79	87
BKK31	19/02/2019	15	0.33	1.4	35	0.03	0.90	1.5	79	35	2.9	234	0.80	1.5	0.30	2.1	9.1	66
BKK32	05/03/2019	38	1.0	2.0	86	0.10	0.89	2.9	76	39	3.7	226	1.0	5.4	0.69	1.8	26	80
BKK33	12/03/2019	113	1.4	4.4	122	0.28	1.6	6.0	195	74	13	255	1.7	12	1.7	2.5	66	75
BKK34	19/03/2019	39	0.80	1.8	49	0.17	0.64	2.2	79	67	4.6	454	1.3	5.2	0.72	2.6	26	109
BKK35	26/03/2019	19	0.56	1.9	41	0.06	5.3	2.6	99	38	7.2	247	1.4	2.3	0.52	2.2	14	83
BKK36	02/04/2019	75	1.4	2.5	54	0.11	1.2	3.4	107	39	4.5	196	3.1	7.2	0.49	3.7	25	79
BKK37	09/04/2019	26	1.3	1.9	42	0.07	1.1	2.6	71	37	3.7	232	1.1	3.2	0.34	2.4	19	75

Table A-2 Metal concentrations in ng/m^3 and PM$_{2.5}$ in µg/m^3 (Chonburi)

	Date	Al	As	Ba	Ca	Cd	Cr	Cu	Fe	Mg	Mn	Na	Ni	Pb	Sr	V	Zn	PM$_{2.5}$
Chonburi																		
A1	22/01/2018	103	2.6	4.1	129	0.57	1.6	7.7	214	69	16	520	2.7	15	0.69	5.8	770	162
A2	24/01/2018	176	2.7	6.3	390	0.15	1.8	8.8	402	93	20	547	2.5	15	1.3	6.2	91	140
A3	25/01/2018	366	4.5	18	1350	0.21	4.8	21	827	263	34	1092	3.7	18	3.6	9.3	515	135
A4	15/03/2018	103	0.83	1.3	171	0.08	2.5	6.8	131	81	6.3	546	1.7	7.7	0.71	3.5	174	-
A5	21/03/2018	61	0.45	0.81	89	0.29	0.53	1.9	38	50	2.3	60	0.97	2.2	0.14	1.1	23	-
A6	28/03/2018	44	0.58	0.52	51	0.09	0.59	1.6	82	31	3.8	153	2.2	6.7	0.08	1.3	113	88
A7	04/04/2018	125	0.85	0.55	44	0.17	0.45	2.8	34	30	1.6	37	1.3	4.0	0.01	2.4	10	86
A8	11/04/2018	76	1.6	1.9	78	0.01	0.93	16	205	96	7.9	802	3.2	5.2	0.47	8.5	118	107
A9	18/04/2018	37	0.51	1.7	53	0.01	1.6	17	94	51	6.3	130	4.1	13	0.31	4.8	76	56
A10	24/04/2018	195	0.68	9.5	503	0.06	2.0	245	621	220	13	806	119	8.8	1.7	6.3	181	61
A11	03/05/2018	51	0.30	1.3	77	0.43	1.7	6.3	103	59	1.8	397	2.4	0.29	0.66	0.27	4.8	45
A12	10/05/2018	23	0.08	0.60	42	0.01	0.90	1.7	31	28	0.60	148	1.1	0.33	0.30	1.5	3.4	52
A13	17/05/2018	86	0.68	2.4	1116	0.07	1.1	7.0	100	207	18	415	2.0	3.7	3.0	2.7	340	67
A14	24/05/2018	224	1.3	8.1	690	0.02	2.7	29	385	536	7.2	5485	13	19	6.7	0.70	347	68
A15	31/05/2018	33	0.10	1.1	42	0.04	0.56	2.1	33	31	0.78	187	1.6	0.35	0.25	1.1	3.0	61
A16	07/06/2018	82	0.68	3.0	160	0.15	3.7	6.2	96	90	2.6	598	5.5	2.0	0.83	1.2	11	47
A17	21/06/2018	30	1.3	1.1	56	0.04	0.94	2.7	36	31	1.0	203	1.3	0.49	0.37	1.5	4.2	52
A18	05/07/2018	46	0.10	1.5	114	0.23	0.93	5.3	55	51	1.2	290	1.5	1.7	0.85	1.3	7.7	41
A19	12/07/2018	187	0.68	4.0	316	0.17	3.0	17	172	218	4.4	2746	13	4.6	2.3	3.3	63	41
A20	18/07/2018	66	0.33	1.2	82	0.86	1.2	3.5	88	76	1.6	467	1.8	2.4	0.73	2.9	6.2	44
A21	26/07/2018	153	0.35	6.0	403	0.61	2.1	23	255	359	5.7	3948	26	5.9	2.7	0.41	130	61
A22	02/08/2018	169	1.5	4.0	382	0.06	3.0	35	261	354	4.3	-	24	2.2	5.6	1.9	110	56
A23	09/08/2018	422	0.26	10	632	0.10	3.4	40	377	496	12	6436	25	15	6.4	7.4	332	69
A24	16/08/2018	436	3.4	12	904	0.93	7.7	100	540	1875	16	-	21	14	8.4	6.8	109	53
A25	23/08/2018	93	2.9	3.5	185	0.12	2.1	11	106	128	2.7	797	3.4	2.0	1.4	2.1	16	68
A26	30/08/2018	61	3.2	2.5	123	0.66	1.7	16	127	64	4.8	362	17	3.3	0.74	1.9	48	58
A27	13/09/2018	228	4.3	9.7	577	0.59	7.3	62	511	309	15	3324	25	16	3.5	8.2	197	54
A28	27/09/2018	85	0.52	4.3	146	0.51	1.2	18	176	87	2.1	592	12	3.1	0.81	1.7	17	49
A31	18/10/2018	148	2.9	12	300	0.71	3.7	14	236	125	15	3793	39	15	1.7	4.3	71	60
A32	25/10/2018	95	4.3	6.0	309	0.30	1.5	11	185	107	9.2	624	7.3	12	1.4	6.7	68	69
A33	01/11/2018	73	1.4	5.3	100	0.21	1.0	11	121	76	7.3	422	2.0	7.3	0.82	1.5	21	83
A34	08/11/2018	248	1.0	9.2	200	1.3	7.3	17	465	136	34	353	5.7	39	2.5	1.6	72	68
A35	15/11/2018	93	1.1	6.9	243	1.6	3.5	8.4	332	73	22	332	3.6	21	7.7	4.4	63	119
A37	24/11/2018	79	0.57	6.8	145	1.1	5.0	10	155	53	8.8	1897	2.4	40	1.8	1.1	87	56
A38	29/11/2018	124	3.8	7.7	612	0.75	6.7	25	319	74	28	544	4.2	33	18	1.1	90	66
A39	06/12/2018	119	1.5	11	154	0.91	22	18	263	91	15	506	7.6	20	1.1	12	62	80
A40	13/12/2018	180	1.5	129	232	0.31	2.3	8.5	199	77	12	428	3.5	24	1.4	0.74	120	67
A41	20/12/2018	115	2.9	9.6	110	1.6	4.6	56	424	71	39	476	8.5	46	1.2	15	245	97
A42	27/12/2018	123	1.4	9.6	139	1.1	2.5	16	258	76	14	343	2.6	36	1.2	3.0	116	144

Table A-3 Pb isotopic composition of PM$_{2.5}$ (in Bangkok)

Sample	^{206}Pb/^{204}Pb	2se	^{207}Pb/^{204}Pb	2se	^{208}Pb/^{204}Pb	2se	^{206}Pb/^{207}Pb	2se	^{208}Pb/^{207}Pb	2se	Pb conc. (ng/m^3)
Bangkok											
BKK1	17.9330	0.0007	15.5758	0.0008	37.8606	0.0025	1.1513	0.00002	2.4308	0.00006	10
BKK2	17.8371	0.0009	15.5600	0.0009	37.7201	0.0024	1.1464	0.00002	2.4242	0.00004	11
BKK3	17.8420	0.0010	15.5743	0.0012	37.7044	0.0030	1.1456	0.00002	2.4211	0.00006	7.1
BKK4	18.0565	0.0092	15.6458	0.0081	38.0096	0.0198	1.1505	0.00002	2.4292	0.00006	3.5
BKK5	17.6990	0.0010	15.5496	0.0010	37.5337	0.0029	1.1382	0.00002	2.4138	0.00006	3.2
BKK6	17.7773	0.0010	15.5528	0.0012	37.6112	0.0029	1.1430	0.00002	2.4184	0.00006	7.3
BKK7	17.7989	0.0008	15.5672	0.0008	37.6449	0.0020	1.1434	0.00002	2.4183	0.00004	10
BKK8	17.9955	0.0016	15.5761	0.0016	37.7812	0.0038	1.1553	0.00001	2.4257	0.00005	6.9
BKK9	17.8549	0.0007	15.5701	0.0007	37.6842	0.0021	1.1467	0.00002	2.4202	0.00006	11
BKK10	17.8489	0.0007	15.5768	0.0007	37.7079	0.0019	1.1459	0.00002	2.4207	0.00004	10
BKK11	17.9249	0.0011	15.5748	0.0011	37.7394	0.0032	1.1508	0.00002	2.4229	0.00006	9.7
BKK12	17.9616	0.0014	15.5992	0.0014	37.7991	0.0034	1.1515	0.00004	2.4233	0.00005	3.4
BKK13	18.0080	0.0024	15.5954	0.0026	37.8618	0.0085	1.1544	0.00005	2.4296	0.00023	1.1
BKK14	17.8852	0.0016	15.5838	0.0017	37.7694	0.0061	1.1474	0.00003	2.4255	0.00013	5.1
BKK15	17.8766	0.0020	15.5837	0.0024	37.7691	0.0081	1.1470	0.00006	2.4260	0.00025	21
BKK16	18.0850	0.0027	15.6055	0.0033	38.0235	0.0113	1.1585	0.00007	2.4383	0.00031	13
BKK17	18.0484	0.0022	15.6003	0.0025	37.9248	0.0080	1.1566	0.00005	2.4331	0.00018	4.9
BKK18	17.8966	0.0021	15.5864	0.0025	37.7963	0.0086	1.1479	0.00006	2.4267	0.00025	29
BKK19	17.9291	0.0016	15.5862	0.0020	37.8216	0.0069	1.1501	0.00004	2.4284	0.00019	8.7
BKK20	17.8730	0.0016	15.5769	0.0019	37.7613	0.0055	1.1471	0.00003	2.4260	0.00014	11
BKK21	17.8886	0.0019	15.5866	0.0023	37.7567	0.0090	1.1474	0.00006	2.4244	0.00025	12
BKK22	17.8573	0.0017	15.5760	0.0020	37.7371	0.0062	1.1462	0.00005	2.4246	0.00017	10
BKK23	17.9230	0.0027	15.5857	0.0032	37.7677	0.0110	1.1498	0.00007	2.4254	0.00031	46
BKK24	18.0420	0.0015	15.6071	0.0016	37.9204	0.0061	1.1557	0.00004	2.4315	0.00018	6.2
BKK25	17.9741	0.0019	15.5929	0.0022	37.8981	0.0076	1.1524	0.00004	2.4324	0.00020	11
BKK26	17.9478	0.0050	15.5883	0.0060	37.8423	0.0209	1.1509	0.00012	2.4296	0.00054	14
BKK27	18.0018	0.0015	15.5941	0.0018	37.9139	0.0056	1.1541	0.00004	2.4332	0.00015	6.3
BKK28	17.9800	0.0033	15.6013	0.0044	37.9077	0.0149	1.1522	0.00010	2.4319	0.00041	43
BKK29	18.2626	0.0018	15.6254	0.0022	38.1744	0.0077	1.1685	0.00005	2.4450	0.00023	2.2
BKK30	17.8754	0.0018	15.5758	0.0022	37.7331	0.0075	1.1473	0.00005	2.4245	0.00021	15
BKK31	17.8993	0.0043	15.5842	0.0048	37.8153	0.0157	1.1484	0.00009	2.4285	0.00041	1.5
BKK32	17.8964	0.0023	15.5924	0.0028	37.7893	0.0097	1.1474	0.00006	2.4256	0.00028	5.4
BKK33	17.8990	0.0018	15.5925	0.0021	37.7910	0.0073	1.1476	0.00005	2.4258	0.00020	12
BKK34	17.9914	0.0018	15.6025	0.0021	37.9378	0.0072	1.1529	0.00004	2.4337	0.00020	5.2
BKK35	17.9641	0.0019	15.5940	0.0023	37.8689	0.0077	1.1517	0.00006	2.4305	0.00023	2.3
BKK36	17.8279	0.0019	15.5759	0.0024	37.7055	0.0081	1.1443	0.00005	2.4228	0.00023	7.2
BKK37	17.6562	0.0029	15.5617	0.0034	37.5332	0.0111	1.1343	0.00007	2.4138	0.00028	3.2
	^{206}Pb/^{204}Pb	**2SD**	^{207}Pb/^{204}Pb	**2SD**	^{208}Pb/^{204}Pb	**2SD**	^{206}Pb/^{207}Pb	**2SD**	^{208}Pb/^{207}Pb	**2SD**	
NBS 981 (True Value)	16.93736						1.0933	0.0004	2.3704	0.0012	
NIST 981 (n=22)	16.92599	0.0022	15.47794	0.0027	36.6591	0.0086	1.0935	0.0001	2.3684	0.0002	
Blank (n=3)	18.93946	0.3205	17.17653	0.2892	40.4743	0.6835	1.1051	0.0030	2.3632	0.0023	

Table A-4 Pb isotopic composition of PM$_{2.5}$ (in Chonburi)

Sample	^{206}Pb/^{204}Pb	2se	^{207}Pb/^{204}Pb	2se	^{208}Pb/^{204}Pb	2se	^{206}Pb/^{207}Pb	2se	^{208}Pb/^{207}Pb	2se	Pb conc. (ng/m^3)
Chonburi											
A1	17.8306	0.0007	15.5592	0.0008	37.7025	0.0022	1.1460	0.00002	2.4232	0.00005	15
A2	17.8857	0.0012	15.5580	0.0011	37.7373	0.0030	1.1496	0.00002	2.4256	0.00005	15
A3	17.8205	0.0024	15.5313	0.0022	37.6507	0.0057	1.1474	0.00002	2.4244	0.00008	18
A4	17.9172	0.0014	15.5590	0.0012	37.7440	0.0033	1.1516	0.00001	2.4258	0.00005	7.7
A5	17.9005	0.0038	15.5286	0.0035	37.6678	0.0086	1.1527	0.00003	2.4258	0.00006	2.2
A6	17.9198	0.0027	15.5368	0.0023	37.6848	0.0053	1.1533	0.00002	2.4256	0.00007	6.7
A7	17.8471	0.0037	15.5575	0.0033	37.7147	0.0083	1.1472	0.00003	2.4243	0.00010	4.0
A8	17.9156	0.0025	15.5443	0.0023	37.7123	0.0061	1.1526	0.00002	2.4261	0.00010	5.2
A9	17.7461	0.0017	15.5933	0.0019	37.7144	0.0062	1.1377	0.00004	2.4204	0.00016	13
A10	17.8592	0.0024	15.5757	0.0025	37.7807	0.0071	1.1463	0.00004	2.4276	0.00016	8.8
A11	18.0273	0.0035	15.5796	0.0031	37.8604	0.0075	1.1572	0.00003	2.4301	0.00005	0.29
A12	17.9035	0.0024	15.5609	0.0020	37.7121	0.0053	1.1506	0.00002	2.4234	0.00006	0.33
A13	17.9240	0.0008	15.5630	0.0009	37.8001	0.0022	1.1517	0.00001	2.4288	0.00005	3.7
A14	17.9313	0.0003	15.5784	0.0003	37.7820	0.0008	1.1510	0.00001	2.4253	0.00002	19
A15	18.0186	0.0031	15.5851	0.0026	37.9101	0.0066	1.1562	0.00002	2.4325	0.00006	0.35
A16	17.9035	0.0011	15.5528	0.0012	37.7611	0.0036	1.1512	0.00002	2.4279	0.00009	2.0
A17	18.0728	0.0016	15.5930	0.0014	37.9680	0.0037	1.1590	0.00002	2.4350	0.00006	0.49
A18	17.9682	0.0012	15.5806	0.0010	37.9299	0.0026	1.1532	0.00002	2.4345	0.00005	1.7
A19	17.9596	0.0010	15.5802	0.0010	37.8346	0.0025	1.1527	0.00002	2.4284	0.00004	4.6
A20	17.9540	0.0015	15.5776	0.0014	37.9320	0.0034	1.1526	0.00002	2.4350	0.00006	2.4
A21	17.8101	0.0007	15.5580	0.0007	37.6469	0.0019	1.1448	0.00002	2.4199	0.00005	5.9
A22	18.0273	0.0008	15.6058	0.0007	37.9622	0.0021	1.1552	0.00002	2.4325	0.00005	2.2
A23	17.8929	0.0006	15.5800	0.0007	37.7468	0.0019	1.1485	0.00002	2.4228	0.00005	15
A24	17.9356	0.0005	15.5835	0.0007	37.8579	0.0017	1.1509	0.00002	2.4294	0.00004	14
A25	18.0886	0.0010	15.6011	0.0010	37.9137	0.0026	1.1594	0.00003	2.4302	0.00005	2.0
A26	17.8952	0.0008	15.5684	0.0006	37.7294	0.0025	1.1495	0.00002	2.4234	0.00005	3.3
A27	17.9392	0.0006	15.5875	0.0007	37.8095	0.0019	1.1509	0.00002	2.4256	0.00005	16
A28	18.0265	0.0007	15.6038	0.0007	37.9975	0.0018	1.1553	0.00002	2.4352	0.00004	3.1
A31	17.8718	0.0043	15.5967	0.0049	37.8108	0.0168	1.1455	0.00010	2.4261	0.00045	15
A32	17.9039	0.0016	15.5952	0.0019	37.8058	0.0062	1.1477	0.00004	2.4260	0.00017	12
A33	17.8458	0.0021	15.5784	0.0025	37.7358	0.0088	1.1453	0.00006	2.4245	0.00024	7.3
A34	18.1328	0.0033	15.6258	0.0038	38.1640	0.0130	1.1603	0.00008	2.4445	0.00036	39
A35	17.7469	0.0024	15.5713	0.0030	37.6354	0.0103	1.1394	0.00007	2.4188	0.00030	21
A37	17.9678	0.0025	15.5940	0.0030	37.8554	0.0114	1.1521	0.00007	2.4300	0.00031	40
A38	17.9966	0.0024	15.5978	0.0028	37.9440	0.0097	1.1536	0.00006	2.4348	0.00027	33
A39	17.9095	0.0038	15.5823	0.0045	37.7939	0.0155	1.1489	0.00009	2.4272	0.00043	20
A40	17.6847	0.0023	15.5571	0.0028	37.5455	0.0095	1.1364	0.00007	2.4153	0.00029	24
A41	17.9365	0.0028	15.5926	0.0032	37.8441	0.0111	1.1501	0.00007	2.4294	0.00029	46
A42	17.9168	0.0031	15.5877	0.0031	37.7966	0.0102	1.1493	0.00006	2.4269	0.00025	36
	^{206}Pb/^{204}Pb	2SD	^{207}Pb/^{204}Pb	2SD	^{208}Pb/^{204}Pb	2SD	^{206}Pb/^{207}Pb	2SD	^{208}Pb/^{207}Pb	2SD	
NBS 981 (True Value)	16.93736						1.0933	0.0004	2.3704	0.0012	
NIST 981 (n=22)	16.92599	0.0022	15.47794	0.0027	36.6591	0.0086	1.0935	0.0001	2.3684	0.0002	
Blank (n=3)	18.93946	0.3205	17.17653	0.2892	40.4743	0.6835	1.1051	0.0030	2.3632	0.0023	

Table A-5 Trace metal correlation matrix for NE monsoon winds in Bangkok.

	Pb	Al	Ca	Cu	Cr	Co	Fe	Mg	Mn	Ni	V	Zn	Na	As	Cd
Pb	1.00														
Al	0.86	1.00													
Ca	0.78	0.84	1.00												
Cu	0.87	0.85	0.77	1.00											
Cr	0.06	-0.07	-0.03	-0.01	1.00										
Co	0.85	0.64	0.54	0.77	0.44	1.00									
Fe	0.86	0.89	0.79	0.94	0.09	0.78	1.00								
Mg	0.70	0.54	0.50	0.46	-0.01	0.65	0.57	1.00							
Mn	0.86	0.75	0.71	0.89	0.03	0.82	0.93	0.69	1.00						
Ni	0.22	0.16	0.09	0.19	0.66	0.51	0.25	0.13	0.14	1.00					
V	0.65	0.48	0.46	0.56	-0.11	0.64	0.66	0.80	0.83	0.04	1.00				
Zn	0.83	0.64	0.53	0.85	-0.04	0.83	0.80	0.65	0.90	0.15	0.82	1.00			
Na	0.72	0.48	0.52	0.52	-0.04	0.67	0.60	0.93	0.75	0.09	0.90	0.74	1.00		
As	0.94	0.82	0.74	0.93	-0.02	0.85	0.90	0.70	0.94	0.15	0.73	0.90	0.74	1.00	
Cd	0.89	0.86	0.82	0.93	0.02	0.71	0.90	0.46	0.82	0.24	0.47	0.72	0.50	0.88	1.00

Table A-6 Trace metal correlation matrix for NE monsoon winds in Chonburi.

	Pb	Al	Ca	Cu	Cr	Co	Fe	Mg	Mn	Ni	V	Zn	As	Cd	Na
Pb	1.00														
Al	0.01	1.00													
Ca	-0.17	0.78	1.00												
Cu	0.59	0.07	0.06	1.00											
Cr	0.15	0.05	-0.02	0.18	1.00										
Co	0.16	0.24	0.07	0.44	0.13	1.00									
Fe	0.15	0.87	0.80	0.36	0.09	0.40	1.00								
Mg	-0.22	0.90	0.85	0.05	0.05	0.19	0.83	1.00							
Mn	0.49	0.57	0.43	0.70	0.13	0.56	0.80	0.43	1.00						
Ni	-0.16	0.01	-0.03	0.09	0.05	-0.01	-0.09	0.16	-0.04	1.00					
V	0.03	0.13	0.14	0.63	0.40	0.59	0.41	0.25	0.43	0.09	1.00				
Zn	-0.11	0.31	0.33	0.07	-0.18	0.80	0.36	0.31	0.26	-0.16	0.30	1.00			
As	0.58	0.49	0.36	0.66	-0.01	0.60	0.73	0.37	0.82	-0.21	0.43	0.41	1.00		
Cd	0.72	-0.11	-0.27	0.45	0.24	0.29	0.19	-0.21	0.51	-0.01	0.23	-0.10	0.47	1.00	
Na	-0.12	0.04	0.10	-0.09	-0.05	-0.14	-0.08	0.20	-0.19	0.86	-0.09	-0.08	-0.25	-0.09	1.00

Table A-7 Trace metal correlation matrix for SW monsoon winds in Bangkok.

	Pb	*Al*	*Ca*	*Cu*	*Cr*	*Co*	*Fe*	*Mg*	*Mn*	*Ni*	*V*	*Zn*	*Na*	*As*	*Cd*
Pb	1.00														
Al	-0.18	1.00													
Ca	0.42	0.11	1.00												
Cu	-0.50	0.69	-0.07	1.00											
Cr	-0.39	0.58	0.10	0.93	1.00										
Co	-0.36	0.76	0.11	0.94	0.96	1.00									
Fe	-0.08	0.96	0.12	0.70	0.64	0.79	1.00								
Mg	0.39	0.44	0.92	0.08	0.18	0.28	0.44	1.00							
Mn	0.52	0.24	0.96	-0.10	0.06	0.11	0.28	0.96	1.00						
Ni	-0.24	0.57	0.29	0.84	0.93	0.93	0.61	0.32	0.24	1.00					
V	-0.26	0.81	-0.05	0.91	0.86	0.93	0.82	0.17	-0.02	0.80	1.00				
Zn	0.58	-0.01	0.97	-0.22	-0.02	-0.02	0.04	0.87	0.94	0.15	-0.14	1.00			
Na	0.49	0.40	0.02	-0.27	-0.35	-0.15	0.39	0.31	0.23	-0.34	0.02	0.09	1.00		
As	0.59	0.26	-0.02	0.22	0.23	0.30	0.40	0.12	0.08	0.26	0.45	0.05	0.42	1.00	
Cd	0.70	0.15	0.26	-0.20	-0.18	-0.12	0.25	0.40	0.40	-0.23	0.03	0.41	0.58	0.50	1.00

Table A-8 Trace metal correlation matrix for SW monsoon winds in Chonburi.

	Pb	*Al*	*Ca*	*Cu*	*Cr*	*Co*	*Fe*	*Mg*	*Mn*	*Ni*	*V*	*Zn*	*As*	*Cd*	*Na*
Pb	1.00														
Al	0.81	1.00													
Ca	0.65	0.65	1.00												
Cu	0.72	0.86	0.59	1.00											
Cr	0.68	0.75	0.50	0.90	1.00										
Co	0.80	0.92	0.69	0.92	0.92	1.00									
Fe	0.90	0.88	0.64	0.93	0.86	0.92	1.00								
Mg	0.60	0.81	0.63	0.89	0.73	0.79	0.76	1.00							
Mn	0.65	0.65	0.93	0.66	0.61	0.78	0.68	0.59	1.00						
Ni	0.61	0.70	0.38	0.70	0.62	0.68	0.79	0.48	0.44	1.00					
V	0.63	0.75	0.49	0.74	0.76	0.87	0.71	0.52	0.69	0.49	1.00				
Zn	0.74	0.56	0.84	0.34	0.26	0.52	0.56	0.30	0.76	0.41	0.38	1.00			
As	0.63	0.73	0.47	0.84	0.77	0.80	0.85	0.62	0.59	0.94	0.64	0.36	1.00		
Cd	0.90	0.85	0.55	0.79	0.79	0.89	0.91	0.55	0.67	0.73	0.85	0.60	0.77	1.00	
Na	0.75	0.56	0.35	0.23	0.23	0.41	0.53	0.11	0.30	0.53	0.31	0.69	0.37	0.66	1.00

Table A-9 Correlation coefficients (r^2) of Pb isotope ($^{206}Pb/^{207}Pb$) with Pb concentrations and trace metal ratios

Bangkok		Chonburi	
NE Monsoon	$^{206}Pb/^{207}Pb$	*NE Monsoon*	$^{206}Pb/^{207}Pb$
$^{206}Pb/^{207}Pb$	1.00	$^{206}Pb/^{207}Pb$	1.00
Pb	-0.32	Pb	0.50
Al/Pb	0.63	Al/Pb	-0.17
V/Pb	0.74	V/Pb	-0.11
SW Monsoon	$^{206}Pb/^{207}Pb$	*SW Monsoon*	$^{206}Pb/^{207}Pb$
$^{206}Pb/^{207}Pb$	1.00	$^{206}Pb/^{207}Pb$	1.00
Pb	0.04	Pb	-0.50
Al/Pb	0.01	Al/Pb	0.61
V/Pb	0.19	V/Pb	0.67
Inter monsoon	$^{206}Pb/^{207}Pb$	*Inter monsoon*	$^{206}Pb/^{207}Pb$
$^{206}Pb/^{207}Pb$	1.00	$^{206}Pb/^{207}Pb$	1.00
Pb	0.05	Pb	-0.75
Al/Pb	-0.10	Al/Pb	0.53
V/Pb	0.01	V/Pb	0.13

APPENDIX B

Metal Concentrations and Source Apportionment of $PM_{2.5}$ in Chiang Rai and Bangkok, Thailand during a Biomass Burning Season

Table B-1 Pb isotope ratios of Singapore clear day (SIN A12) and hazy day (SIN A13) aerosol samples ($PM_{2.5}$) samples collected in 2015 extracted with dilute (50% v/v) and concentrated acid mixture.

Sample	Reagent	$^{206}Pb/^{204}Pb$	2se	$^{207}Pb/^{204}Pb$	2se	$^{208}Pb/^{204}Pb$	2se	$^{206}Pb/^{207}Pb$	2se	$^{208}Pb/^{207}Pb$	2se
SIN A12	50% 3:1 HNO₃:HF	17.7199	0.0012	15.5401	0.0014	37.4776	0.0047	1.14027	0.00002	2.41167	0.00023
SIN A12	3:1 HNO₃:HF	17.7181	0.0022	15.5384	0.0027	37.4671	0.0090	1.14028	0.00004	2.41126	0.00021
SIN A13	50% 3:1 HNO₃:HF	18.1383	0.0014	15.5280	0.0018	38.0346	0.0065	1.15830	0.00003	2.42576	0.00028
SIN A13	3:1 HNO₃:HF	18.1337	0.0016	15.5230	0.0019	38.0169	0.0064	1.15842	0.00003	2.42586	0.00024

Table B-2 Metal correlation in Chiang Rai

	Al	Ba	Ca	Cu	Cr	Fe	Mg	Mn	Ni	Pb	Sr	V	Zn	Na	As
Al	1														
Ba	0.777	1													
Ca	0.821	0.682	1												
Cu	-0.070	0.013	0.497	1											
Cr	-0.173	-0.086	-0.162	0.049	1										
Fe	0.639	0.709	0.699	0.285	0.425	1									
Mg	0.919	0.619	0.911	0.215	-0.273	0.599	1								
Mn	0.431	0.506	0.439	0.123	0.717	0.808	0.311	1							
Ni	-0.151	-0.048	-0.111	0.077	0.986	0.479	-0.247	0.772	1						
Pb	0.665	0.720	0.833	0.354	-0.285	0.629	0.734	0.401	-0.176	1					
Sr	0.891	0.681	0.877	0.119	-0.232	0.631	0.919	0.443	-0.160	0.879	1				
V	0.655	0.507	0.412	-0.345	-0.032	0.223	0.492	0.449	-0.009	0.422	0.651	1			
Zn	0.560	0.593	0.886	0.643	-0.298	0.502	0.712	0.315	-0.219	0.901	0.759	0.331	1		
Na	-0.167	-0.120	0.360	0.889	0.026	0.115	0.133	-0.015	0.017	0.238	0.061	-0.259	0.516	1	
As	0.269	0.372	0.109	-0.351	-0.370	-0.047	0.117	0.004	-0.291	0.353	0.326	0.559	0.194	-0.393	1

Table B-3 Metal correlation in Bangkok

	Al	Ba	Ca	Cu	Cr	Fe	Mg	Mn	Ni	Pb	Sr	V	Zn	Na	As
Al	1														
Ba	0.650	1													
Ca	0.764	0.845	1												
Cu	0.732	0.989	0.865	1											
Cr	-0.044	0.202	0.070	0.205	1										
Fe	0.830	0.921	0.863	0.958	0.249	1									
Mg	0.610	0.294	0.556	0.332	-0.129	0.453	1								
Mn	0.767	0.812	0.831	0.866	0.362	0.950	0.532	1							
Ni	0.625	0.409	0.318	0.458	0.075	0.493	0.068	0.436	1						
Pb	0.716	0.991	0.848	0.989	0.149	0.928	0.341	0.804	0.432	1					
Sr	0.888	0.664	0.837	0.738	0.100	0.848	0.759	0.861	0.281	0.714	1				
V	0.271	0.143	0.020	0.182	-0.083	0.218	-0.046	0.256	0.819	0.128	-0.018	1			
Zn	0.731	0.663	0.677	0.745	0.020	0.815	0.419	0.863	0.496	0.676	0.755	0.478	1		
Na	0.012	0.259	0.292	0.193	-0.090	0.145	0.638	0.215	-0.120	0.238	0.210	0.007	0.106	1	
As	0.718	0.919	0.777	0.922	0.084	0.831	0.287	0.668	0.428	0.946	0.650	0.052	0.535	0.120	1

Table B-4 Principal Component Analysis for metals composition in PM$_{2.5}$ at Chiang Rai and Bangkok

Metals	Chiang Rai				Bangkok			
	Factor 1	Factor 2	Factor 3	Communality	Factor 1	Factor 2	Factor 3	Communality
Al	0.897	0.039	-0.265	0.876	0.753	0.401	0.298	0.817
Ba	0.816	0.136	-0.209	0.727	0.951	0.068	-0.018	0.909
Ca	0.939	0.022	0.282	0.961	0.889	0.019	0.281	0.870
Cu	0.242	0.041	0.937	0.939	0.973	0.134	-0.002	0.964
Cr	-0.219	0.966	0.057	0.985	0.323	-0.223	-0.510	0.415
Fe	0.696	0.617	0.127	0.881	0.964	0.200	0.078	0.975
Mg	0.906	-0.088	0.053	0.832	0.396	-0.029	0.864	0.905
Mn	0.482	0.852	-0.060	0.962	0.898	0.200	0.159	0.871
Ni	-0.152	0.974	0.054	0.974	0.367	0.855	-0.122	0.881
Pb	0.910	-0.074	0.144	0.855	0.956	0.088	0.025	0.922
Sr	0.959	-0.022	-0.080	0.927	0.818	0.054	0.428	0.856
V	0.608	0.073	-0.555	0.683	0.027	0.947	-0.024	0.899
Zn	0.848	-0.143	0.424	0.919	0.704	0.475	0.224	0.772
Na	0.129	-0.037	0.914	0.853	0.152	-0.182	0.700	0.546
As	0.344	-0.302	-0.580	0.547	0.895	0.061	-0.031	0.806
Eigenvalues	7.02	3.18	2.72		8.942	1.957	1.511	
% of Variance	46.59	20.96	18.59		54.97	14.78	12.98	
Cumulative %	46.59	67.55	86.14		54.97	69.75	82.73	

VITA

NAME	Jariya Kayee
DATE OF BIRTH	26 February 1991
PLACE OF BIRTH	Chanthaburi
INSTITUTIONS ATTENDED	B.Sc. in Chemistry with second class honors from Faculty of Science, Srinakharinwirot University in 2013
	M.Sc. in Chemistry from Faculty of Science, Chulalongkorn University in 2016
HOME ADDRESS	55/80-81 Moo. 6 Phlapphla subdistrict, Mueang Chanthaburi district, Chanthaburi province, 22000
PUBLICATION	Metal Concentrations and Source Apportionment of PM2.5 in Chiang Rai and Bangkok, Thailand during a Biomass Burning Season
	Sources of atmospheric lead (Pb) after quarter century of phasing out of leaded gasoline in Bangkok, Thailand
AWARD RECEIVED	The Science Achievement Scholarship of Thailand, SAST
	ASEAN-India Research and Training Fellowship Scheme